Tampere University

Modelling epileptic seizures *in vitro*: The effects of IL-6 on the characteristics and functionality of hPSC-derived cortical neuronal networks

Master's Thesis
Johanna Lotila
Faculty of Medicine and Health Technology
Tampere University
April 2020

PRO GRADU-TUTKIELMA

Paikka: Tampereen yliopisto, Lääketieteen ja terveysteknologian tiedekunta
Tekijä: Johanna Lotila
Otsikko: Epileptisten kohtausten *in vitro* mallinnus: IL-6:n vaikutukset ihmisen monikykyisistä kantasoluista erilaistettujen aivokuoren hermosoluverkostojen ominaisuuksiin ja toiminnallisuuteen
Sivumäärä: 92
Ohjaajat: Dosentti Susanna Narkilahti, FT Sanna Hagman ja FM Ropafadzo Mzezewa
Tarkastajat: Dosentti Susanna Narkilahti ja Professori Heli Skottman
Päiväys: 28.4.2020

TIIVISTELMÄ

Tutkimuksen tausta ja tavoitteet: Epilepsia on yleinen neurologinen sairaus, jolle on ominaista toistuvat epileptiset kohtaukset. Neuroinflammaatio ja tulehduksellisten sytokiinien epänormaalit pitoisuudet on havaittu olevan yhteydessä epilepsiaan. Eläinkokeet ja kliiniset tutkimukset ovat osoittaneet, että interleukiini (IL)-6 -sytokiinin pitoisuudet voivat kohota kohtausten jälkeen. Tieto IL-6:n vaikutuksista epilepsiakohtauksiin ja ihmisen hermosoluihin on kuitenkin vähäistä. Tämän työn tarkoituksena oli tutkia IL-6:n ja Hyper-IL-6 -fuusioproteiinin vaikutuksia ihmisen monikykyisistä kantasoluista erilaistettuihin aivokuoren hermosoluihin yhdessä kainaattihappokäsittelyn kanssa ja ilman sitä. Käsittelyn tarkoituksena oli aiheuttaa kohtaustyyppistä hermosoluaktiivisuutta. Työssä tutkittiin käsittelyiden vaikutuksia IL-6 reseptorien ilmentymiseen, hermosolujen elinkykyyn ja hermosoluverkostojen toiminnallisuuteen.

Menetelmät: Ihmisen monikykyisistä kantasoluista erilaistettuja aivokuoren hermosoluja viljeltiin viisi viikkoa, minkä aikana niiden aktiivisuutta seurattiin mikroelektrodihila-levyillä *(engl. microelectrode array, MEA)*. Tämän jälkeen toiminnallisesti kypsyneet hermosolut käsiteltiin IL-6:lla tai Hyper-IL-6:lla. Myöhemmin osa viljelmistä altistettiin kainaattihappokäsittelylle. IL-6 reseptorien, IL-6R ja glykoproteiini 130 (gp130), ilmentyminen geeni- ja proteiinitasoilla määritettiin ennen käsittelyitä ja niiden jälkeen käyttämällä kvantitatiivista PCR-menetelmää ja immunosytokemiallisia värjäyksiä. Näillä värjäyksillä tutkittiin myös hermosoluille, astrosyyteille ja hermosolujen synapseille tyypillisten proteiinien ilmentymistä viljelmissä. Solujen elinkykyä käsittelyiden jälkeen tutkittiin elävät/kuolleet-värjäyksellä. Käsittelyiden vaikutusta hermosoluverkostojen aktiivisuuteen tutkittiin MEA-mittauksilla.

Tulokset: Molemmat IL-6 reseptorit ilmentyivät ihmisen hermosoluviljelmissä geeni- ja proteiinitasoilla. Käsittelyiden seurauksena IL-6 reseptorien ilmentyminen geenitasolla muuttui hieman. Käsittelyt eivät olleet sytotoksisia soluille. Sytokiinikäsittelyt eivät vaikuttaneet suuresti tutkittuihin hermosoluverkostojen aktiivisuuden ominaisuuksiin. Kainaattihappokäsittely kuitenkin häiritsi hermosoluverkostojen aktiivisuutta ja samanlaisia vaikutuksia havaittiin myös viljelmissä, jotka oli käsitelty sytokiineilla ja kainaattihapolla yhdessä.

Johtopäätökset: Työssä osoitettiin, että ihmisen aivokuoren hermosolut ilmentävät IL-6 reseptoreita, joten niillä on mahdollisuus reagoida IL-6 signalointiin. Lisää tutkimustietoa tarvitaan IL-6:n vaikutuksista ihmisen hermosoluverkostoihin, jotta voidaan syvällisemmin mallintaa sen roolia epilepsiassa ja epilepsiakohtauksissa.

MASTER'S THESIS

Place: Tampere University, Faculty of Medicine and Health Technology
Author: Johanna Lotila
Title: Modelling epileptic seizures *in vitro*: The effects of IL-6 on the characteristics and functionality of hPSC-derived cortical neuronal networks
Pages: 92
Supervisors: Adjunct Professor Susanna Narkilahti, PhD Sanna Hagman and MSc Ropafadzo Mzezewa
Reviewers: Adjunct Professor Susanna Narkilahti and Professor Heli Skottman
Date: 28.4.2020

ABSTRACT

Background and aims: Epilepsy is a common neurological disorder characterized by repetitive epileptic seizures. Neuroinflammation and abnormal inflammatory cytokine levels have been associated to epilepsy. Animal and clinical studies have revealed that the levels of interleukin-6 (IL-6) cytokine can be elevated after seizures. However, the knowledge of the roles of IL-6 in seizures and its functions on human neurons is minimal. The aim of this work was to study the effects of IL-6 and Hyper-IL-6 fusion protein to human pluripotent stem cell (hPSC)-derived cortical neural cultures alone and in combination with kainic acid (KA) treatment. KA was used to induced seizure-like activity. The effects of these treatments on the expression levels of IL-6 receptors, cell viability and functionality of the neuronal networks were investigated.

Methods: hPSC-derived cortical neurons were cultured for five weeks and the functional activity development of neuronal networks was followed with microelectrode arrays (MEAs). Then, functionally maturated neuronal networks were treated with IL-6 or Hyper-IL-6 and subsequently a part of cultures was exposed to KA. The gene and protein expression levels of IL-6 receptors, IL-6R and glycoprotein 130 (gp130), were determined before and after treatments with quantitative PCR and immunocytochemistry (ICC), respectively. ICC was used to determine the protein expression of neuronal, astrocytic and synaptic markers after treatments. Cell viability was studied after treatments with LIVE/DEAD assay. The effects of treatments on the activity of neuronal networks were investigated with MEA measurements.

Results: Human neural cultures expressed both IL-6 receptors at the gene and protein level. Treatments slightly modulated the expression of IL-6 receptors. Treatments were not cytotoxic to the cells. Cytokine treatments did not cause major effects to the functionality of neuronal networks, when few activity features were studied. However, KA treatment disrupted the activity of neuronal networks and similar effects was seen when cultures were treated together with cytokines and KA.

Conclusion: This study indicated that human cortical neurons express both IL-6 receptors thus they can respond to IL-6. More research is needed about the effects of IL-6 on the human neuronal networks for better modelling of its role in the human epilepsy and epileptic seizures.

Acknowledgements

This master's thesis was conducted in the Neuro Group, Faculty of Medicine and Health Technology, Tampere University, Finland. I am sincerely grateful to the leader of Neuro Group, Adjunct Professor Susanna Narkilahti, for supervising this study and for this opportunity to work in your group with this exciting project. I would also like to express my gratitude to my excellent supervisors PhD Sanna Hagman and PhD student, MSc Ropafadzo Mzezewa. Thank you for the supervising, guidance, help and all the advice and long discussions during this work. I highly appreciate that I got to be a part of this project and perform experiments together with Ropafadzo. Thank you all for everything.

I am also grateful to Hanna Mäkelä, Eija Hannuksela and Juha Heikkilä for their guidance in the lab and all the help during this project. Thank you to all the inspiring people in the Neuro Group, you made this into an unforgettable journey. I have learned a lot and enjoyed working with you, as well as with the extremely beautiful and fascinating neurons.

I want to thank my family and all my friends. Your support, help, joy and love have been vital during my life, studies and this project. Thank you to my parents, for always supporting, encouraging and believing in me. Thank you, my dear friend Laura, for your help and comments. Finally, I would like to thank my love Joel. Thank you for your understanding, patience and all the help that you have given me during my studies and through all these years.

28.4.2020 Tampere

Johanna Lotila

Table of Contents

Abbreviations

AMPA	α-amino-3hydroxy-5-methyl-4-isoxazolepropionate
ASD	Anti-seizure drug
BBB	Blood brain barrier
BSA	Bovine serum albumin
β-Tub	Beta-tubulin 3
cDNA	Complementary DNA
CLC	Cardiotrophin-like cytokine
CNS	Central nervous system
CNTF	Ciliary neurotrophic factor
CSF	Cerebrospinal fluid
CT-1	Cardiotrophin-1
Ct value	Threshold cycle value
DAPI	4′,6-diamidino-2-phenylindole
DPBS	Dubecco's phosphate-buffer saline
EB	Embryoid body
FGF	Fibroblast growth factor
GABA	Gamma-aminobutyric acid
GFAP	Glial fibrillary acidic protein
gp130	Glycoprotein 130
GUSB	Glucuronidase beta
hESC	Human embryonic stem cell
hiPSC	Human induced pluripotent stem cell
hPSC	Human pluripotent stem cell
HTP	High-throughput
Hyper-IL-6	Hyper-Interleukin-6
ICC	Immunocytochemistry
IgG	Immunoglobulin G
IgY	Immunoglobulin Y
IL-1β	Interleukin-1 beta
IL-6	Interleukin-6
IL-6R	Interleukin-6 receptor α subunit
IL-6ST	Interleukin-6 signal transducer (same as gp130)
ILAE	International League Against Epilepsy
JAK	Janus kinase
KA	Kainic acid
KO	Knockout
LIF	Leukemia inhibitory factor
LN	Laminin
MAP2	Microtubule-associated protein 2
MAPK	Mitogen-activated protein kinase
MEA	Microelectrode array
NF-κB	Nuclear factor kappa-light-chain-enhancer of activated B cells
NDS	Normal donkey serum
NMM	Neural maturation medium

NMDA	N-methyl-d-aspartate
NPC	Neural progenitor cell
NSC	Neural stem cell
Oct3/4	Octamer-binding protein 3/4
OSM	Oncostatin M
PB	Phosphate buffer
PBS	Phosphate-buffered saline
PFA	Paraformaldehyde
PI3K	Phosphoinositol-3 kinase
PLO	Poly-L-ornithine
PSD95	Postsynaptic density protein 95
RQ-value	Relative quantification value
RT	Room temperature
RT-qPCR	Quantitative reverse transcription polymerase chain reaction
sgp130	Soluble glycoprotein 130
sIL-6R	Soluble interleukin-6 receptor
Sox2	Sex determining region Y-box 2
STAT3	Signal transducer and activator of transcription 3
TNF-α	Tumour necrosis factor alpha
VEGF	Vascular endothelial growth factor
WB	Western blot

1 Introduction

The complexity of the human brain reflects to the complexity of its diseases. The brain together with the spinal cord form the central nervous system (CNS), which main cell types are neurons and glial cells: astrocytes, oligodendrocytes and microglia (Budday et al. 2015). The human brain consists of approximately one hundred billion neurons, and each neuron can communicate electrochemically with thousands of other neurons and form neuronal networks (Budday et al. 2015). Abnormalities in the activity of neuronal networks can cause neurological disorders (Faingold & Blumenfeld 2014). One of such disorders is epilepsy which is caused by abnormal brain activity that leads to spontaneous epileptic seizures and often to other comorbidities (Devisky et al. 2018). Involvement of neuroinflammation and inflammatory cytokines in the pathophysiology of epilepsy is recognized, but their specific roles in epilepsy and seizure generation are still unclear (Vezzani et al. 2008, Vezzani et al. 2019). Neuroinflammation is a complex inflammatory response of the CNS that results from different insults, and it is mediated by several inflammatory factors such as inflammatory cytokines (DiSabato et al. 2016, Vezzani et al. 2019). Cytokines are an extensive group of small soluble proteins which can mediate cell communication via autocrine, paracrine and endocrine signaling, for example they are crucial for development, tissue homeostasis and immunity (Becher et al. 2017, Rose-John 2018). In general, all cytokines need to bind their specific extracellular receptors to mediate signals into the cells (Rose-John 2018). Additionally, cytokines are pleiotropic proteins, which refers that one cytokine can have several different target cells and mediate multiple actions (Becher et al. 2017). Interleukin-6 (IL-6) is one of those cytokines which is associated with epilepsy. Clinical and experimental studies of epilepsy have reported elevated IL-6 levels after epileptic seizures (Li et al. 2011, Liimatainen et al. 2009). However, its role in epilepsy and epileptic seizures and its effects to the human CNS are unclear. Majority of the data about cytokines in neuroinflammation is from animal models of human diseases (Becher et al. 2017). However, the human brain differs a lot from the animal brain, especially from the rodent brain, which is the most commonly used animal model (Avior et al. 2016, Shi et al. 2012). For better disease modelling, it is essential to study human diseases with human cells (Avior et al. 2016). Human pluripotent stem cells (hPSCs) provide unlimited human-based cell source for *in vitro* disease modelling since they can differentiate into all cell types in the human body including CNS cells (Avior et al. 2016). Advantages of *in vitro*

research with hPSCs are patient-specific cells, human-specific cell responses, cost-effectiveness, scalability and reduced number of ethical issues in comparison to animal models, to name a few (Avior et al. 2016, Tukker et al. 2020).

The effects of IL-6 on neurons *in vitro* have been studied previously, but mainly with rodent neurons. Due this reason, it is essential to research its functions to neurons with human-based models. The aim of this work was to investigate the effects of IL-6 and Hyper-IL-6 on the characteristics and functionality in hPSC-derived cortical neuronal networks. Hyper-IL-6 is a fusion protein complex, which can be used to study the functions of IL-6 (Rose-John 2017). Moreover, in a part of networks seizure-like activity was induced with kainic acid (KA), and its effects after cytokine exposure were studied. Additionally, the gene and protein expression levels of IL-6 receptors in human neural cultures were determined in this study. Moreover, the cell viability was studied after treatments. In general, the effects of IL-6 on the functionality of human neuronal networks is less known. Therefore, the effects of IL-6, Hyper-IL-6 and KA treatments on the activity of hPSC-derived cortical neuronal networks were investigated with microelectrode arrays (MEAs), which enable repeatable and long-term measuring of the activity of neuronal networks (Ylä-Outinen et al. 2019).

2 Literature review

2.1 Epilepsy

2.1.1 Epilepsy and epileptic seizures

Epilepsy is one of the most common neurological diseases affecting about 65 million people globally (Devinsky et al. 2018). It is characterized by an abiding predisposition for generation of unpredictable and unprovoked epileptic seizures caused by abnormally excessive or synchronous activity of neurons in the brain (Fisher et al. 2014). Main reason for abnormal activity of neurons is the imbalance between inhibitory and excitatory neurotransmission (Patel et al. 2019). An epileptic seizure is a temporary alteration of behaviour and it appears in multiple forms, durations, frequencies and severity levels (Devinsky et al. 2018). Symptoms can vary a lot: loss of consciousness, jerking, inability to move, absence, déjà vu or sensory changes. At worst, seizures can cause accidents such as drowning, or changes of autonomic functions leading to death. (Devinsky et al. 2018)

Multiple epileptic seizure types as well as epilepsies are recognized and they have been classified in different ways (Fisher et al. 2017). Current classification of seizure types and epilepsies is based on The International League Against Epilepsy (ILAE) 2017 classification (Figure 1). Epileptic seizures can be classified into three main groups based on the seizure origin: focal, generalized and unknown onset. A focal seizure originates within networks in one hemisphere of the brain whereas a generalized seizure originates from both hemispheres. If the origin of a seizure in the brain is not identified, it can be classified as unknown onset. All seizure types can be divided into more specific subcategories according to the patient's awareness and movements during a seizure. Focal onset can be classified into seizures with awareness or impaired awareness. All three main seizure onsets can be classified as motor or nonmotor seizures depending on movements during a seizure. In addition, focal seizures can be classified as a focal to bilateral tonic-clonic -seizure type according to its' propagation pattern from one hemisphere to another. (Fisher et al. 2017) Tonic-clonic seizure proceeds in two phases during a seizure: a tonic phase with muscle contractions, which usually leads to falling, and a clonic phase with rhythmic jerking movements (Devinsky et al. 2018). Moreover, some seizures are divided into unclassified seizures due to deficient knowledge or inability to classify them to other categories (Fisher et al. 2017). Based on epileptic seizure types,

epilepsies are classified into generalized, combined generalized and focal as well as unknown epilepsies (Scheffer et al. 2017).

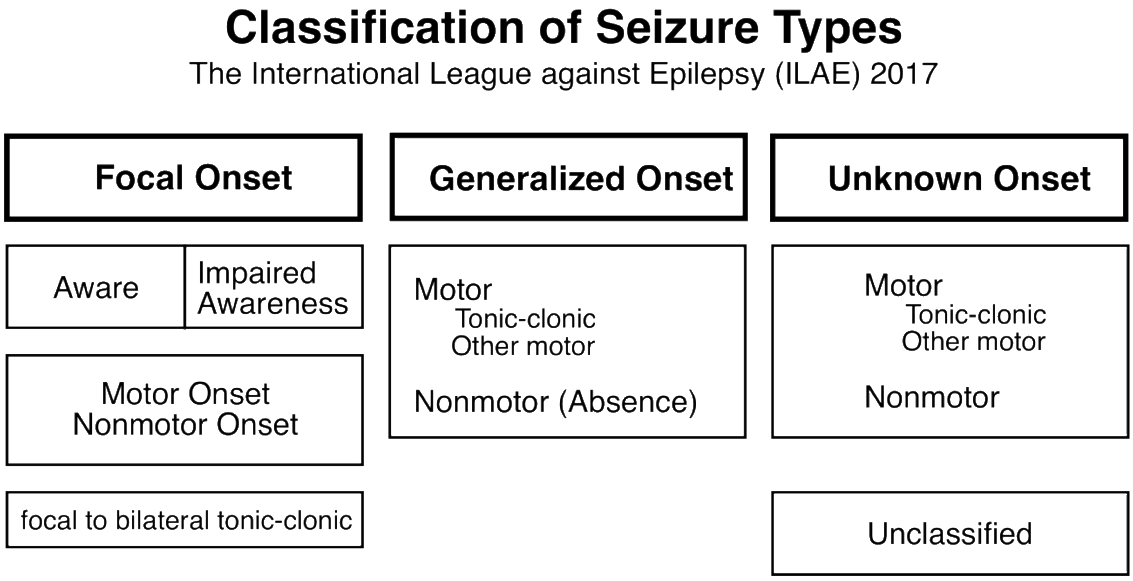

Figure 1. Basic version of ILAE 2017 classification of seizure types. Figure is redrawn and modified from Fisher et al. (2017).

Epilepsy is diagnosed based on unprovoked epileptic seizures (Devinsky et al. 2018). However, one seizure without other factors, such as known structural lesion, is not enough for epilepsy diagnosis. Diagnosis relies on a medical history, physical and neurological examination, electroencephalogram (EEG) and neuroimaging. Currently, there are many treatments available for epilepsy. The most common treatment is anti-seizure drugs (ASDs) which can control epileptic seizures, but they are not curative. Several different ASDs are available such as Carbamazepine, Valproic acid, Topiramate and Lamotrigine. (Devinsky et al. 2018) However, still almost 30% of patients have drug-resistant epilepsy. Patients with drug-resistant epilepsy do not respond to ASD treatments and they suffer from uncontrollable epileptic seizures which can impair the quality of their everyday life (Devinsky et al. 2018, Vezzani et al. 2011). In addition to ASDs, other treatment possibilities are epilepsy surgery, neurostimulation devices and different dietary therapies. However, epilepsy surgery is often not suitable for drug-resistant epilepsy patients. (Devinsky et al. 2018)

Epilepsy is present in all age groups and it can be caused by multiple factors (Scheffer et al. 2017). It can have structural, genetic, metabolic, infectious, immune as well as unknown etiology. For example, acute brain injury, stroke, gene mutations, viral infection or autoimmune-mediated CNS inflammation can cause epilepsy. (Scheffer et al. 2017, Vezzani et al. 2016) Evidence suggests, that there is a close and complex connection between the immune system and epilepsy (Li et al. 2011, Vezzani et al. 2016). Despite enormous amount of epilepsy research, the pathophysiological mechanisms of epilepsy and epileptic seizures are still unclear and more research is needed (Devinsky et al. 2018, Vezzani et al. 2019). However, animal models have revealed various alterations on genetic, epigenetic, molecular, cellular as well as on functional level (Devinsky et al. 2018). These alterations occur in neuronal and non-neuronal cell types in the brain during epileptogenesis, which can also contribute to seizure generation. Epileptogenesis refers to the chronic process in which a healthy brain networks convert into a seizure generating networks. Alterations can be aberrant neurogenesis, ion channel dysfunction, reactive gliosis and blood-brain barrier (BBB) dysfunction, to name a few. (Devinsky et al. 2018) Moreover, one of these pathophysiological mechanisms is neuroinflammation, which is known to have an important role in epilepsy (Devinsky et al. 2018, Vezzani et al. 2019).

2.1.2 Neuroinflammation and cytokines in epilepsy

Neuroinflammation is a common phenomenon in many neurological disorders including epilepsy (Becher et al. 2016, Vezzani et al. 2019). It refers to broad and complex inflammatory responses within the CNS that results from tissue damage, autoimmune responses, infections, seizures or other insults (DiSabato et al. 2016, Vezzani et al. 2019). Multiple factors can mediate neuroinflammation such as pro-inflammatory cytokines, chemokines, growth factors, secondary messengers and reactive oxygen species (Figure 2) (DiSabato et al. 2016, Patel et al. 2019). These inflammatory mediators are secreted in the brain by activated microglia and astrocytes, which are resident CNS glia cells, and by neurons, endothelial cells and infiltrated peripheral immune cells (DiSabato et al. 2016, Vezzani et al., 2011). Secretion of inflammatory mediators is a normal response of the brain to an insult and an attempt to maintain homeostasis and prevent further damage within the brain (Patel et al. 2019, Vezzani et al. 2019). However, excessive and prolonged neuroinflammation is detrimental and causes abnormal cellular functions since inflammatory mediators affect transcriptional and post-transcriptional mechanisms (DiSabato et al. 2016, Patel

et al. 2019, Vezzani et al. 2019). For example, alterations associated to neuroinflammation are activation of astrocytes and microglia, increased production of cytokines and chemokines, BBB dysfunction such as leakage, and infiltration of peripheral immune cells into the brain (DiSabato et al. 2016).

Studies indicate that multiple inflammatory pathways can be activated in the epileptic brain (Vezzani et al. 2019). Neuroinflammation can be a result of seizures, but studies have also suggested that it has a role in the seizure induction. For example, animal models have indicated that neuroinflammation can cause the threshold decrease for seizures, and therefore promote seizure generation and recurrence. (Vezzani et al. 2019) Experimental and clinical studies have reported that the activation of inflammatory cytokines and their abnormal levels are related to epilepsy and seizures (Li et al. 2011, Liimatainen et al. 2009). Several cytokines, such as interleukin-1β (IL-1β), tumour necrosis factor alpha (TNF-α) and IL-6, have shown to be associated with the pathology of epilepsy (Li et al. 2011). Clinical studies of epilepsy have shown increased IL-6 levels in the cerebrospinal fluid (CSF) and blood after seizures (Alapirtti et al. 2009, Lehtimäki et al. 2011, Liimatainen et al. 2009, Peltola et al. 2000). Additionally, it has been reported that IL-6 levels in the blood correlate with the levels in the CSF, and thus it has been suggested that the increased blood IL-6 originates from CNS (Alapirtti et al. 2009). For example, elevated IL-6 levels both in CSF and plasma after tonic-clonic seizures are reported but concentration and increase of IL-6 were greater in the CSF compared to plasma (Peltola et al. 2000). In addition, increased seizure frequency and severe intellectual disabilities were associated with higher serum IL-6 level in epilepsy patients (Lehtimäki et al. 2011). It is also found that epilepsy type affects cytokine levels e.g. studies have shown significant increase in serum level of IL-6 in temporal lobe epilepsy (TLE) patients compared to extra-TLE patients (Alapirtti et al. 2009, Liimatainen et al. 2009). However, more detailed knowledge of the neuroinflammation and IL-6 functions in the CNS and their role in seizure generation and epilepsy is needed.

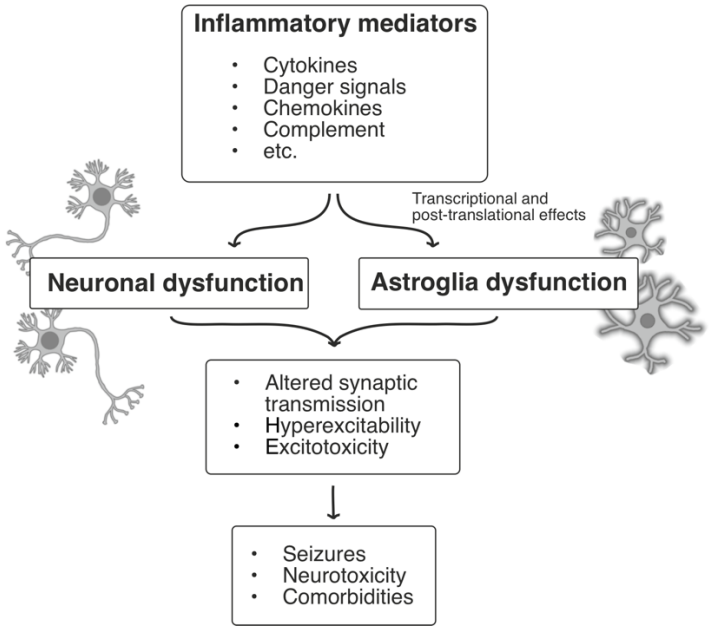

Figure 2. Effects of neuroinflammation on neuropathology. Inflammatory mediators are produced by CNS cells or by infiltrated peripheral immune cells after epileptogenic events. These factors can cause several transcriptional and post-translational effects leading to dysfunction of neurons and glial cells. Furthermore, dysfunctional cells can cause detrimental pathological effects. Figure is redrawn and modified from Vezzani et al. (2019).

2.2 Interleukin-6 (IL-6)

2.2.1 Interleukin-6 family of cytokines

Interleukin-6 family of cytokines include IL-6, IL-11, IL-27, ciliary neurotrophic factor (CNTF), cardiotrophin 1 (CT-1), cardiotrophin-like cytokine (CLC), oncostatin M (OSM) and leukemia inhibitory factor (LIF) (Rose-John 2018). These cytokines belong to the same family since they mediate their effects through a common signaling receptor, glycoprotein 130 (gp130). However, cytokines cannot activate gp130 alone since activation of gp130 requires cytokine specific receptors which are listed in the Table 1. Certain IL-6 family cytokines bind first to specific binding receptors and then they can activate signaling receptors. Contrary, some of IL-6 family cytokines can directly activate their two signaling receptors without specific ligand-binding receptor. IL-6 family cytokines have also structural similarities in their four-helix bundle structure with up-up–down-down topology. In addition, they have many common as well as distinct biological functions. For example, they are involved in the regulation of lymphocyte functions, in metabolic regulation and in several neural functions. (Rose-John 2018)

Table 1. IL-6 family of cytokines and their receptors, which are required for cytokine signaling (Rose-John 2018).

Cytokine	**Ligand-binding receptors**	**Signaling receptors**
IL-6	IL-6R	gp130
IL-11	IL-11R	gp130
IL-27		gp130, WSX-1
CNTF	CNTF-R	gp130, LIF-R
CT-1	CT-1R? (possibly)	gp130, LIF-R
CLC	CNTF-R	gp130, LIF-R
OSM		gp130, LIF-R/gp130, OSM-R
LIF		gp130, LIF-R

Abbreviations: IL=interleukin, gp130=glycoprotein 130, R=receptor, CNTF=ciliary neurotrophic factor, CT-1=cardiotrophin 1, CLC=cardiotrophin-like cytokine, OSM=oncostatin M, LIF=leukemia inhibitory factor.

2.2.2 Interleukin-6 cytokine

Initially, IL-6 was known with diverse names as B-cell stimulatory factor 2 (BSF-2), hepatocyte-stimulating factor (HSF-2), hybridoma-plasmacytoma growth factor, interferon β2 (INFβ-2) or 26 kDa protein (Rose-John 2018). Researchers found similarities as well as differences in biological functions between these proteins. Molecular cloning of the cDNA for these proteins confirmed that these are actually the same identical glycoprotein, and thus was renamed as IL-6 in the late 80's. (Rothaug et al. 2016, Rose-John 2018) IL-6 is a small (21-30 kDa) pleiotropic cytokine which has many target cells and multiple actions around the body (Gruol 2015). For example, it is involved in inflammation, tissue regeneration, immune defence and many pathological processes (Rothaug et al. 2016). It has also functions in neural tissue, for example, its involvement in neurodevelopment, neuronal physiology, neuroprotection, neurotoxicity and neuropathology has been reported (Gruol 2015). However, its specific roles and molecular mechanisms in the CNS are not clear (Gruol 2015). Moreover, both pro- and anti-inflammatory properties have been reported for this multifunctional cytokine depending on the target cell type and signaling pathway (Scheller et al. 2011), which are described more detail in the chapter 2.2.3.

Under normal conditions IL-6 levels are low in the CNS, whereas during pathological events its levels are often elevated (Erta et al. 2012, Gruol 2015). In addition to previously mentioned epilepsy, increased IL-6 levels in the brain or CSF have been reported e.g. in Alzheimer disease,

Parkinson's disease, Huntington's disease, major depression and autism (Erta et al. 2012). IL-6 is secreted by immune cells, such as B-cells, T-cells and microglia, but also by non-immune cells, such as neurons, astrocytes and endothelial cells (Erta et al. 2012, Rothaug et al. 2016). Main sources of IL-6 in the CNS are astrocytes and microglia (Gruol 2015). Neurons can also secrete it under specific conditions such as during robust neuronal activity, CNS injury or disease. Production of IL-6 by neurons is less studied than that by astrocytes, but it is known that IL-1β can induce IL-6 production in both cell types. (Gruol 2015) Also, several different cytokines, inflammatory mediators and other factors can induce production of IL-6 such as TNFα, lipopolysacharide (LPS), interferon gamma (IFN-γ), vascular endothelial growth factor (VEGF), granulocyte macrophage colony-stimulating factor (GM-CSF), OSM, mechanical injury, oxidative stress and hypoxia (Erta et al. 2012, Hodge et al. 2005, Hyvärinen et al. 2019a). Secreted IL-6 can affect various cell types which express specific extracellular receptors for its binding. These receptors and IL-6 signaling pathways are presented in the next chapter.

2.2.3 Interleukin-6 receptors and signaling pathways

IL-6 can transmit its biological actions through its receptors IL-6R and gp130 (Figure 3) (Rothaug et al. 2016). IL-6R (α-receptor, CD126) is a small ligand-binding glycoprotein (80kDa) which exists in membrane-bound (IL-6R) and soluble forms (sIL-6R, 50 kDa) (Kaur et al. 2020, Rose-John 2017). Soluble IL-6R is produced by alternative splicing of IL-6R mRNA, or extracellularly by limited proteolysis of the membrane-bound IL-6R by metalloproteases ADAM10 and ADAM 17 (Chalaris et al. 2011). Gp130 (β-receptor, CD130) is a transmembrane protein (130 kDa) which mediates signals from all IL-6 family cytokines (Table 1) (Kaur et al. 2020).

Expression of membrane-bound IL-6R is considered to be more limited to specific cell types compared to gp130, which is ubiquitously expressed (Luo & Zheng et al. 2016, Rothaug et al. 2016, Scheller & Rose-John 2006). Membrane-bound IL-6R is reported to be expressed predominantly on hepatocytes and leukocytes, but also on epithelial cells, microglia and some neuronal cells, but not on oligodendrocytes (Kaur et al. 2020, Rose-John 2017, Rothaug et al. 2016). Contradictory results about IL-6R expression on astrocytes and neurons have been also reported (Erta et al. 2012, Gruol 2015, Rothaug et al. 2016). However, expression of IL-6R and gp130 on neurons and glial cells in many regions of rodent (Erta et al. 2012, Gruol 2015) and

human brain (Hampel et al. 2005) have been reported. Expression of IL-6 receptors on neurons have been determined in several rodent studies on mRNA and protein level (Ali et al. 2000, D'Arcangelo et al. 2000, Hattori et al. 2020, Nelson et al. 2002, Pieraut et al. 2011, Ropelle et al. 2010, Vereyken et al. 2007, Vollenweider et al. 2003), but also in few studies with human neural stem cells (Sulistio et al. 2018), human embryonic stem cell (hESC)-derived neural progenitor cells (Hagman et al. 2019), human induced pluripotent stem cell (hiPSC)-derived neurons (Como et al. 2018) and human brain autopsies (Hampel et al. 2005). Taken together, expression of IL-6 receptors on neurons and glia have been reported. However, most of the studies have used rodent cells and expression of IL-6 receptors on hPSC-derived neurons is less studied.

IL-6 can signal through classic- and trans-signaling pathways (Figure 3) (Rothaug et al. 2016). In classic signaling pathway, IL-6 binds to membrane-bound IL-6R, causing the dimerization and activation of membrane-bound gp130, which activates intracellular signaling. IL-6R is not ubiquitously expressed, but still cells which do not express membrane-bound IL-6R can respond to IL-6 via trans-signaling. In trans-signaling pathway, IL-6 forms a complex with sIL-6R. This protein complex can activate distant cells by binding to gp130, resulting in the dimerization and activation of gp130 and thereafter, downstream signaling. (Rothaug et al. 2016) Moreover, gp130 can exist on soluble form, soluble gp130 (sgp130), which can inhibit trans-signaling by binding to IL-6/sIL-6R complex (Rose-John 2017). It is suggested that sIL-6R and sgp130 can act as a buffer for IL-6 in the circulation (Rose-John 2017).

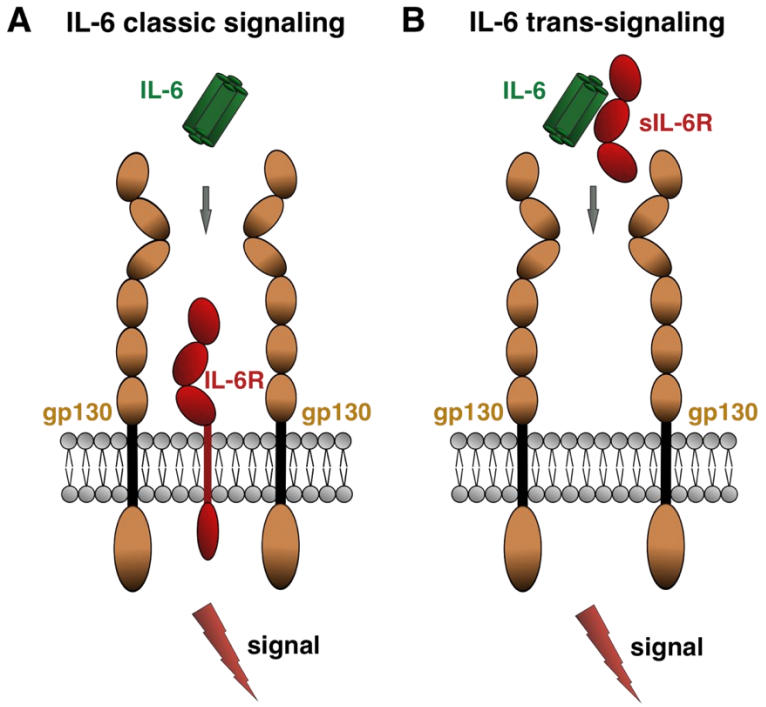

Figure 3. IL-6 receptors and signaling pathways. A) IL-6 classic signaling. At first, IL-6 binds to membrane-bound IL-6R. This complex can activate gp130 signaling receptors, which leads to activation of intracellular signaling. B) IL-6 trans-signaling. IL-6 forms a complex with sIL-6R, which can activate gp130 receptors, leading to activation of intracellular signaling. Figure is redrawn and modified from Rose-John (2017). Abbreviations: IL-6=interleukin-6, IL-6R=interleukin-6 receptor, gp130=glycoprotein 130, sIL-6R=soluble IL-6R.

As mentioned, IL-6 can activate intracellular downstream signaling pathways through classic- or trans-signaling, in which gp130 mediate extracellular signal to the intracellular proteins. Activated intracellular tyrosin-kinases, such as Janus kinase (JAK), can activate three downstream signaling pathways: signal transducer and activator of transcription 3 (STAT3) pathway, RAS-RAF-(mitogen-activated protein kinase) MAPK pathway or phosphoinositol-3 kinase (PI3K)/Akt pathway which can activate nuclear factor-κB (NF-κB) (Erta et al. 2012, Kaur et al. 2020). Transcription factor NF-κB has an important role in the regulation of several immune and inflammatory responses, and its abnormal function can lead to many pathogenic functions (Liu et al. 2017).

Effects of IL-6 can differ between the target cells and signaling pathways (Rothaug et al. 2016). Classic signaling is considered to induce more anti-inflammatory responses whereas trans-singnaling is thought to induce more pro-inflammatory responses. Regenerative role has been

reported for classic signaling in neural tissue and hypothesized that it can mediate protective effects in rodent CNS. (Rothaug et al. 2016) Contrary, it is reported that in rodent CNS trans-signaling can mediate neuronal degeneration (Rothaug et al. 2016) and its blocking can reduce detrimental effects of IL-6 (Campbell et al. 2014).

2.2.4 Hyper-IL-6

Trans-signaling can be studied *in vitro* and *in vivo* with the designer fusion protein called Hyper-IL-6 (Fisher et al. 1997, Rose-John 2017). Hyper-IL-6 consists of both IL-6 and sIL-6R which have been covalently linked together with a small and flexible peptide chain (Figure 4) (Fisher et al. 1997). Since this fusion protein contains sIL-6R, it can activate directly gp130 expressing cells which do not express membrane-bound IL-6R (Rose-John 2017). Compared to unlinked IL-6 and sIL-6R, Hyper-IL-6 can be 100-1000 times more effective on gp130-expressing cells (Fisher et al. 1997). Interestingly, neuroprotective effects of Hyper-IL-6 on rodent neurons and glial cells have been reported e.g. after mechanical nerve injury (Leibinger et al. 2016, Leibinger et al. 2019, Scheller & Rose-John 2006), although detrimental effects of trans-signaling in the CNS have been reported as mentioned in the previous chapter.

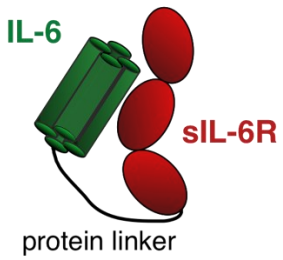

Figure 4. Designer fusion protein Hyper-IL-6. Together IL-6, sIL-6R and a small protein linker form Hyper-IL-6 complex. Figure is redrawn and modified from Rose-John (2017). Abbreviations: IL-6=interleukin-6, sIL-6R=soluble IL-6 receptor.

2.3 Stem cells

2.3.1 Human pluripotent stem cells

hPSCs consists of both hESCs and hiPSCs. hPSCs have unlimited self-renewal capacity, they are expandable and they can differentiate into all three embryonic germ layers: endoderm, mesoderm and ectoderm but not extra-embryonic tissues (Avior et al. 2016). hESCs are obtained from the

undifferentiated inner cell mass of blastocyst stage embryos (Thomson et al. 1998), whilst hiPSCs are generated from somatic cells with iPSC technology. This ground-breaking technology was published by Takahashi & Yamanaka in 2006 when they generated iPSCs from mouse somatic cells. They reprogrammed already differentiated mouse fibroblasts with four transcriptional factors, called OSKM or Yamanaka factors: octamer-binding protein 3/4 (Oct3/4), Sex determining region Y-box 2 (Sox2), Krüppel-like factor 4 (Klf4) and c-Myc (Takahashi & Yamanaka 2006). On the following year, first hiPSCs were generated from human fibroblast using retroviral transduction and Yamanaka factors (Takahashi et al. 2007) as well as using lentiviral transduction and Thomson factors including Oct3/4, Sox2, Nanog and Lin28 (Yu et al. 2007). Morphology, proliferation, telomerase activity as well as gene and protein expression of pluripotent markers were very similar with iPSCs and hESCs, even though they have different origin (Takahashi et al. 2007, Yu et al. 2007). However, differences between hiPSCs and hESCs as well as within these cell lines have been found such as variation in DNA methylation, gene expression and differentiation capacity. Due to these differences, it is worthwhile to use several cell lines for experiments. (Avior et al. 2016, Sandoe & Eggan 2013, Toivonen et al. 2013)

After invention of the iPSC technology, it has been used worldwide and hiPSCs have become common, powerful and promising tool for multiple applications such as disease modelling, drug discovery and regenerative medicine (Takahashi & Yamanaka 2016). Compared to hESCs, hiPSCs have many advantages. Since hiPSCs are generated from somatic cells, such as skin or blood cells, accessibility is much simpler, cell source is unlimited and research raises less ethical concerns compared to hESC which are obtained from surplus in vitro fertilization embryos (Shi et al. 2017). Both cell sources can be used to study human diseases, such as monogenic disorders (Avior et al. 2016). For example, if hPSCs do not carry genetic disorders naturally, mutations can be generated by gene editing. Although the use and potential of hESC is more limited. (Avior et al. 2016) However, hiPSC are patient-specific and combined with modern gene editing technologies, they are advantageous tool for modelling of neurological disorders such as monogenic, neurotoxicity testing, drug discovery, personalized medicine and transplantation therapies (Grainger et al. 2018, Shi et al. 2017).

2.3.2 Cortical neuronal differentiation of human pluripotent stem cells

Neurons of the cerebral cortex include excitatory glutamatergic neurons and inhibitory GABAergic neurons (Shi et al. 2012). Majority of cortical neurons are glutamatergic which develop from cortical stem and progenitor cells in the cortex whereas less prominent GABAergic neurons migrate to the cortex during the development. Rodent models are common and widely used to study the cerebral cortex. (Shi et al. 2012) However, they are not directly comparable with humans since rodent and human brain differ a lot in size, folding, complexity, developmental stage and neuron types, to name a few (Shi et al. 2012, Sun & Hevner 2014). For example, rodent cortex is smooth whereas human cortex is highly folded and thicker in comparison to rodents (Sun & Hevner 2014). Human PSC-derived cortical neurons are crucial for multiple research areas such as for modelling of development and function of human cerebral cortex, since human-based model systems are limited but still diseases associated to cerebral cortex are very common (Shi et al. 2012).

In general, hPSCs can be differentiated into neural stem cells (NSCs) in adherent 2-dimensional (2D) cultures (neural rosettes), and in free-floating 3D cultures (neurospheres) (Hong & Do 2019). Tripotent NSCs can further differentiate into three neuronal lineages: neurons, oligodendrocytes and astrocytes (Hong & Do 2019). First reports of neural differentiation from hPSCs were published almost twenty years ago (Carpenter et al. 2001, Reubinoff et al. 2001, Zhang et al. 2001). In these studies, embryoid bodies (EBs), which are three-dimensional (3D) aggregates of hPSCs, were formed from hESCs, and later plated in 2D adherent culture with neuronal differentiation supporting medium. Cells were differentiated and they formed neural rosettes, which are neural-tube resembling structures of neural precursor cells expressing neuroectodermal markers. Then, neural precursor cells were isolated, cultured and differentiated into neurons and glia cells. (Carpenter et al. 2001, Reubinoff et al. 2001, Zhang et al. 2001) Additionally, neural precursor cells can be obtained from hPSC in 3D culture using neurosphere method, in which hPSC clusters are cultured in neural induction medium (Lappalainen et al. 2010). Neurospheres can be expanded by dissociation and replating, and further differentiate when needed (Lappalainen et al. 2010). In addition to EBs and neurospheres, highly efficient, rapid and widely used neural induction protocol termed dual SMAD inhibition was published by Chambers et al. 2009. This feeder-free adherent culture protocol is based on inhibition of Lefty/Activin/Transforming growth factor beta (TGFβ) and Bone morphogenetic protein (BMP) signaling with combination of small molecules SB-

431542 and Noggin or LDN193189, respectively (Chambers et al. 2009, Hyvärinen et al. 2019b). Moreover, differentiation protocols for complex in vivo mimicking 3D neuronal cultures such as free-floating cerebral organoids and cortical spheroids have been established (Gunhanlar et al. 2018, Hong & Do 2019).

Both hESCs and hiPSCs can be differentiated towards cortical neurons with multiple 2D protocols (Figure 5) (Hyvärinen et al. 2019b, McCaughey-Chapman & Connor 2018, Shi et al. 2012). Differentiation of hPSC towards electrophysiologically functional cortical neurons takes several weeks (Hyvärinen et al. 2019b, Shi et al. 2012). Neuronal induction for hPSCs can be performed with dual SMAD inhibition which directly differentiates cells into neuroectoderm. Generated neural stem and progenitor cells (NPCs) can be efficiently expanded and differentiated e.g. in medium containing fibroblast growth factor (FGF) towards neurons. Thereafter, neuronal maturation can be supported with a cocktail of neurotrophic factors for several weeks to achieve functionally mature neuronal networks. In addition to neurons with functional synapses, cultures can also contain astrocytes which number increase during the maturation of cultures. Astrocytes have an important role in cortical neural cultures since it is known that they can support synaptogenesis, functional maturation of neurons as well as synchronization of networks. (Hyvärinen et al. 2019b)

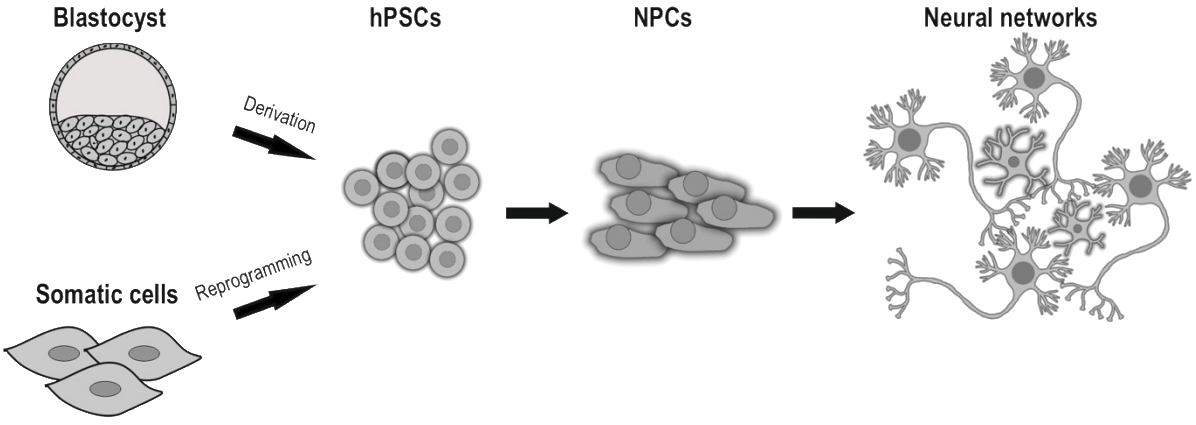

Figure 5. Neuronal differentiation of hPSC. hESCs are obtained from inner cell mass of blastocysts whilst hiPSCs are reprogrammed from somatic cells. hPSCs can be differentiated into NPCs and further differentiated into functionally mature neural networks. Figure is redrawn and modified from Hyvärinen et al. (2019b). Abbreviations: hPSC=human pluripotent stem cell, NPC=neural progenitor cell.

2.4 Functionality of neuronal networks

2.4.1 Introduction to functionality of neurons

Neurons can communicate via electrical signals, called action potentials, and chemical signals (Alberts et al. 2014). Action potential is a rapid change in a membrane potential of a neuron. It can be generated when stimulus depolarizes membrane potential enough to reach threshold value. Then depolarization travels along axon followed by repolarization. Action potential propagates rapidly towards axon terminal, where electrical signal is transmitted via synapses. Neurons can have chemical synapses and less common electrical synapses, which transmit signalling via ions through gap junctions. In chemical synapses, action potential triggers the release of neurotransmitters from synaptic vesicles of presynaptic axon terminal into the synaptic cleft, where they can bind to specific cell surface receptors on the postsynaptic neuron. Binding of excitatory neurotransmitters cause small depolarization of postsynaptic neuron whilst inhibitory neurotransmitters cause small hyperpolarization. Depending on the sum of signals, new action potential can be generated in the postsynaptic neuron. (Alberts et al. 2014) Since electrical signalling is crucial for neuronal functions, functional analysis of neuronal networks is an essential part of neuronal studies (Heikkilä et al. 2009, Ylä-Outinen et al. 2010, Ylä-Outinen et al. 2019). Functionality of neurons can be measured in vitro with different techniques, such as patch clamp, calcium imaging and MEAs (Ylä-Outinen et al. 2019). Patch clamp is a low to high-throughput (HTP) endpoint analysis which can be used to measure ion currents on single cell level with a micropipette (Obien et al. 2015, Ylä-Outinen et al. 2019). Calcium imaging is fluorescence-based endpoint analysis, which can be used to determine cellular calcium signals on single cell or network level (Grienberger & Konnerth 2012, Ylä-Outinen et al. 2019).

2.4.2 Microelectrode arrays (MEAs)

MEAs are useful and widely used tools to characterize the activity of cultured neuronal networks (Heikkilä et al. 2009, Hyvärinen et al. 2019a, Hyvärinen et al. 2019b, Paavilainen et al. 2018, Ylä-Outinen et al. 2010). In addition, MEAs can be used *in vivo* but the focus here is on *in vitro* MEAs, which are cell culture dishes or different kind of microfluidics devices containing embedded microelectrodes on the bottom of the dish (Obien et al. 2015). Number of electrodes can vary a lot

from tens to thousands (Nam & Wheeler 2011). On MEAs, neurons can grow and freely form networks on top of the electrodes (Ylä-Outinen et al. 2019). MEAs can detect the changes in the extracellular ionic current flows at many sites of culture simultaneously, measuring extracellular action potentials (EAPs or spikes) and local field potentials (LFPs) (Nam & Wheeler 2011, Obien et al. 2015).

This technology has many advantages and potential for many applications. Compared to patch clamp or calcium imaging, it is technically easier to perform. It is a non-invasive, label-free and repeatable method which enables the following of neuronal network activity levels from the same cultures in real time for long culture periods (Ylä-Outinen et al. 2019). In addition, with this HTP method multiple different neuronal cultures can be measured simultaneously with multiwell-MEAs (Hyvärinen et al. 2019b). In addition, the morphology of the cells and the organization of networks related to electrodes on MEAs can be followed during a culture period with a microscope if MEAs are transparent (Nam & Wheeler 2011). Figure 6 represents one of the multiwell-MEA measurements system (from Axion BioSystems) which provides visualized data from the activity of neuronal networks during MEA measurements.

MEA measurements provide enormous amount of data about the activity of neuronal networks. With MEAs, it is possible to investigate several parameters such as number of active electrodes, spike rate, burst rate and burst duration, to name a few (Paavilainen et al. 2018, Hyvärinen et al. 2019b). Active electrodes report how many electrodes detect determined number of spikes during the specific time e.g. 10 spikes per minute. Spike rate (also known as mean firing rate) reports detected spikes during the determined time, whilst burst rate describes a number of bursts, groups of very frequent spikes, during the time (Heikkilä et al. 2009, Hyvärinen et al. 2019b). During the maturation of hPSC-derived neurons, random spiking activity can develop to spike trains, bursts and synchronous network bursts, which can be observed during MEA measurements (Heikkilä et al. 2009, Hyvärinen et al. 2019b). Spike trains means several spikes with regular short time between them and synchronous bursts refer to bursts which can be detected simultaneously from several electrodes (Heikkilä et al. 2009).

Many commercial MEA systems are available but also non-commercial MEAs are widely used (Nam & Wheeler 2011, Obien et al. 2015, Ryynänen et al. 2018, Ryynänen et al. 2019). First MEA measurements for cell cultures were performed as early as the 1970's (Thomas et al. 1972). In general, rodent networks have been considered as "golden standards" in the MEA field (Hyvärinen et al. 2019b). However, spontaneous neuronal network activity of hPSC-derived neurons has been detected on MEAs already more than ten years ago (Heikkilä et al. 2009, Ylä-Outinen et al. 2019). Since then, human neurons have been studied on MEAs (Ylä-Outinen et al. 2019). This technology can be used in many neuronal applications. For example, it can provide valuable information about the functionality of hPSC-derived neuronal cultures in vitro for developmental studies, neurotoxicity studies, drug screening as well as disease modelling (Grainger et al. 2018, Ylä-Outinen et al. 2019).

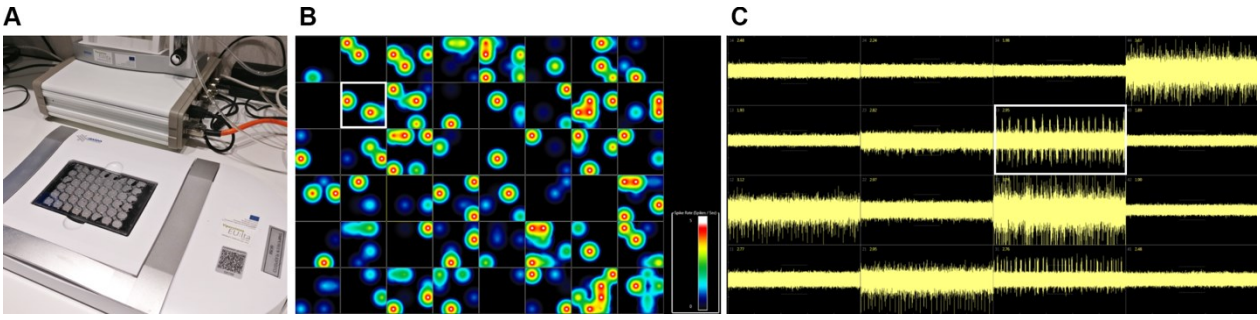

Figure 6. Example images of MEA measurements (Axion BioSystems) A) MEA plate on MEA measurement system. B) Heat map presents activity of neuronal cultures with different colours during MEA measurements. Each box (white box) indicates a single well from MEA 48-well plate. C) Spike detector shows activity patterns of neuronal cultures from one MEA well (16 electrodes). Each box (marked with white) indicates a single electrode.

2.5 Epilepsy research and disease modelling

2.5.1 Introduction to disease modelling

Disease modelling attempts to clarify the pathological cellular and molecular mechanisms observed in the disease (Avior et al. 2016). Moreover, disease modelling includes the investigation of development of the disease, strategies for disease prevention as well as the search for possible treatment options. Diseases can be investigated using *in vivo* and *in vitro* models which are both invaluable tools. Multiple animal models, such as rodents, non-rodent species and non-human primates, with or without gene modifications have been used. (Avior et al. 2016, Xu & Zhong

2013) For *in vitro* disease modelling, different kind of cells, such as primary cells or stem cells, and culturing methods, such as 2D, 3D, co-cultures and PSC-derived organoids, can be used (Avior et al. 2016, Grainger et al. 2018). Rodent tissues and primary cells are widely used in disease modelling. Rodent-based *ex vivo* brain slices resemble *in vivo* conditions and contain functional networks but slice preparation and culturing can be challenging. Primary rodent CNS cultures also contain many *in vivo* cell types and have HTP compared to brain slices. (Grainger et al. 2018) However, these animal models or models with animal cells do not correlate directly with humans since they differ in the genetic, developmental, anatomical and physiological levels (Avior et al. 2016, Xu & Zhong 2013). Due to these differences, human diseases are better to be modelled with human cells (Avior et al. 2016). However, use of human brain tissue is also problematic, since it is a highly limited cell source and usually the obtained brain tissue is unhealthy or post-mortem (Grainger et al. 2018, Xu & Zhong 2013). As mentioned, hPSCs have become very promising and powerful tools to model human diseases-in-a-dish (Avior et al. 2016, Thodeson et al. 2018, Xu & Zhong 2013). Possibly in the future, use of hiPSCs can overcome the challenges of animal studies and reduce the number of animals needed (Avior et al. 2016, Grainger et al. 2018). In addition, disease modelling with hiPSCs raises less ethical questions compared to animal studies or studies with human brain tissue or hESCs-derived neurons (Grainger et al. 2018). For *in vivo* and *in vitro* epilepsy research, all the above-mentioned model systems can be used. The next chapters describe a few in vivo studies related to epilepsy and IL-6. In addition, the effects of IL-6 on neuronal cultures in several *in vitro* studies are discussed.

2.5.2 In vivo studies related to interleukin-6 and epilepsy

Animal models have been used widely in epilepsy and seizure research (Devinsky et al. 2018, Li et al. 2011). Rodents are the most commonly used animals, but also non-rodent species such as rabbits, dogs, cats and zebrafish have been used (Devinsky et al. 2018, Vezzani et al. 2016). Epilepsy models can have epilepsy naturally, but usually it is induced. In rodent models, epilepsy can be caused with multiple methods such as various postnatal or *in utero* brain injuries, infectious agents or genetic modifications (Devinsky et al. 2018). Moreover, epilepsy can be induced with chemoconvulsants such as KA via systemic, intranasal or local administration (Devinsky et al. 2018, Zheng et al. 2011). KA is an analog of glutamate, which is a major excitatory neurotransmitter in the CNS. KA can be used to activate excitatory neurotransmission since it is

an agonist for kainate receptors, which are a type of ionotropic glutamate receptors. (Zheng et al. 2011) It is widely used in epilepsy research since it induces recurrent seizures, but it is also utilized in other neurological and neurodegenerative disease models related to excitotoxicity (Zheng et al. 2011). The findings from a few experimental epilepsy studies related to IL-6 are presented in the next chapters.

In many rodent models, the effect of IL-6 on seizures have been investigated (Table 2). In Lehtimäki et al. (2003) study, increase in gene expression levels of IL-6 and its receptors, IL-6R and gp130, have been reported in the brain after KA-induced seizures in adult rats. The study revealed that the location and timing of the expression of IL-6 and its receptors can vary in the brain after seizures. In controls, IL-6R mRNA was undetectable but gp130 was expressed. To conclude, mRNA levels of IL-6 and its receptors were low in controls but after seizures their expression was increased widely in the brain. (Lehtimäki et al. 2003)

Kalueff et al. (2004) studied the effects of intranasal administrated IL-6 (400 ng) to pentylenetetrazole (PTZ) induced seizures in adult rats. Rats were treated with IL-6 one hour before seizure induction. PTZ was used to induce seizures since it inhibits inhibitory GABA signaling in the CNS. The severity of seizures was dramatically increased in IL-6 treated rats. Moreover, IL-6 levels in the frontal lobe were elevated. Seizure severity was revealed by shorter latency time, longer duration of seizures and higher mortality rate. These results indicated that exogenous IL-6 has proconvulsive effects in the brain. (Kalueff et al. 2004)

Contrary, more anti-convulsive effects of exogenous IL-6 (500 ng and 50 ng) have been reported with developing rats, which seizures were induced by hyperthermia (Fukuda et al. 2007). In this study, IL-6 was administrated intra-nasally one hour before seizure induction. IL-6 treated rats had longer latency time and shorter seizures, especially with higher IL-6 dose. In addition, they treated rats with IL-6 and aminophylline which is an adenosine receptor antagonist. Results from these studies suggested that IL-6 have anti-convulsive effects via the adenosine system in this experimental model. (Fukuda et al. 2007)

In a study with IL-6 knockout (KO) mice, number of KA-induced seizures and mortality rate were higher in IL-6 KO group compared to controls (Penkowa et al. 2001). After seizures, IL-6 was increased in hippocampus of control mice, but in IL-6 KO mice it was undetected as expected. Moreover, hippocampal damage, neuronal death and oxidative stress were increased, and glial responses were reduced after seizures in the brain of IL-6 KO mice. (Penkowa et al. 2001). Another study with IL-6 KO mice, investigated the effects of different chemoconvulsants to seizure susceptibility (De Sarro et al. 2004). The study showed that IL-6 KO mice were more sensitive to seizures which were caused by impairing GABAergic or increasing glutamatergic neurotransmission (e.g. with KA). In addition, same group reported that IL-6 KO mice are more vulnerable to audiogenic seizures and neuroactive amino acid level changes in the brain (De Luca et al. 2004). A study with transgenic mice producing elevated levels of IL-6 from astrocytes showed increased sensitivity to glutamatergic (KA and N-methyl-d-aspartate, NMDA)-induced seizures and higher mortality compared to controls (Samland et al. 2003). Transgenic mice had also increased mean frequency and duration of KA -induced seizures (Samland et al. 2003).

In conclusion, *in vivo* studies indicate that IL-6 has a complex role in seizures since both pro- and anti-convulsive properties have been reported. Diverse and dual effects of IL-6 may depend on the different experimental models and context (Erta et al. 2012, Kalueff et al. 2004). However, the role and mechanisms of IL-6 in seizures and epilepsy are not clear yet.

Table 2. *In vivo* rodent studies related to IL-6 and epilepsy.

Study	**Animals**	**Seizure induction**	**Exogenous IL-6**	**Main findings**
De Sarro et al. 2004	IL-6 knockout mice	several chemo-convulsants e.g. KA	-	IL-6 increased seizure susceptibility to some chemoconvulsants, especially to glutamatergic KA, NMDA and AMPA.
Fukuda et al. 2009	developing rats	hyperthermia	intranasal, 50 ng & 500 ng	Longer latency time and shorter seizures in IL-6 group, indicating more anticonvulsive effects.
Kalueff et al. 2004	adult rats	PTZ	intranasal, 400 ng	Shorter latency time, longer seizures and higher mortality in IL-6 group, indicating more proconvulsive effects.
Lehtimäki et al. 2003	adult rats	KA	-	Gene expression levels of IL-6, IL-6R and gp130 increased in the brain after seizures.
Penkowa et al. 2001	IL-6 knockout mice	KA	-	More seizures, higher mortality and increased neuronal injury in IL-6 KO mice after seizures.
Samland et al. 2003	transgenic GFAP-IL6 mice	KA, NMDA, pilocarpine	-	Enhanced sensitivity to glutamatergic-induced seizures and higher mortality in transgenic mice.

Abbreviations: KA=kainic acid, NMDA=N-methyl-d-aspartate, AMPA=α-amino-3hydroxy-5-methyl-4-isoxazolepropionate, PTZ=pentylenetetrazole.

2.5.3 In vitro studies related to interleukin-6 and neurons

With *in vitro* studies, the investigation of local seizure generating networks is possible whilst *in vivo* studies offer only a limited access to the brain circuitry (Devinsky et al. 2018). However, pharmacology or electrical stimulation is required to induce seizure-like activity in *in vitro* studies (Devinsky et al. 2018). Currently, there are many possible *in vitro* seizure models such as rodent based acute slice assays, organotypic slice cultures and primary CNS cultures, as well as less used but highly potential human-based iPSCs-derived cultures (Grainger et al. 2018). The generation of seizure-like activity has been studied in multiple primary *in vitro* models and brain slice studies, but also in some hiPSC-derived neural cultures, by modulating the ion levels or neurotransmission of heathy cells/tissues inducing seizure generation. The modulation of ion levels, such as potassium, magnesium and calcium levels, can increase neuronal activity and seizure-like activity

since ion gradients control neuronal excitability. In addition, seizure-like activity can be induced pharmacologically by modulating excitatory and inhibitory neurotransmission. (Grainger et al. 2018) For example, excitatory neurotransmission can be potentiated with KA, whilst inhibitory neurotransmission can be reduced with gabazine which is an antagonist of $GABA_A$ receptor (Grainger et al. 2018, Zheng et al. 2011). *In vitro* findings related to the effects of IL-6 on neuronal cultures, their viability and functionality are discussed in the next chapters and listed in the Table 3.

Neuroprotective effects of IL-6 have been reported in a study which used mice cortical neurons mixed with glial cells, as well as near pure mice cortical neuronal cultures containing <5% glial cells (Ali et al. 2000). In this study, IL-6 mRNA level was increased in a time-dependent manner after NMDA and ionomycin treatment, but the expression of IL-6 receptors was unchanged. When cultures were treated with IL-6 (50 ng/ml for 24 h), it protected neurons dose-dependently against NMDA-induced neuronal death, but not against serum deprivation- or staurosporine-induced apoptotic cell death, or α-amino-3hydroxy-5-methyl-4-isoxazolepropionate (AMPA)- or kainate-mediated excitotoxicity. (Ali et al. 2000)

Moreover, a study with rat cortical neurons indicated that IL-6 has neuroprotective properties as it regulates voltage-gated Na^+ channels (Xia et al. 2015). Patch-clamp measurements revealed that IL-6 (0.1, 5, 1 or 10 ng/ml for 24 h) can reduce Na^+ currents dose-dependently, but also time-dependently (IL-6 10 ng/ml, between 2-48 h) through its receptors. Reduction of Na^+ currents was greatest after 24 hours. Additionally, IL-6 treatments did not affect Na^+ channel activation or inactivation. However, IL-6 treatments reduced the amplitude of APs but not the threshold of APs. (Xia et al. 2015)

Another study with rat cerebellar granule neurons (CGNs) reported neuroprotective effects of chronic IL-6 exposure (40 or 120 ng/ml for 8 days) against NMDA-induced apoptosis, when expression levels of anti-apoptotic Bcl-2, pro-apoptic Bax and apoptosis marker caspase-3 were investigated and apoptotic nuclei were counted (Liu et al. 2011). Results also suggested that the protective effects of IL-6 were mediated by JAK/STAT3 and PI3K/Akt pathways (Liu et al. 2011). Later, the same group found that IL-6 (120 ng/ml for 24 h) can decrease calcium influx via NMDA-

receptor, inward current and neuronal death on NMDA-treated CGNs, and the results suggested that the effects of IL-6 were mediated by JAK/calcineurin (CaN) pathways (Ma et al. 2015). Additionally, controversial findings about effects of IL-6 have been published. A study with rat hippocampal neurons reported that IL-6 (5 ng/ml) increases the calcium influx through NMDA-receptor rapidly, which was mediated by the JAK/STAT pathway (Orellana et al. 2005).

Moreover, the effects of IL-6 and Hyper-IL-6 on neural differentiation have been studied. A study with mice NSCs presented that Hyper-IL-6 can enhance neurogenesis and gliogenesis (Islam et al. 2009). Hyper-IL-6 increased the expression of gp130 dose-dependently and increased the expression neuronal and astrocytic markers. It also reduced proliferation of NSCs and expression of stem cell markers but did not cause apoptosis. However, IL-6 did not cause similar effects on cultures, which was explained with undetected IL-6R. The study suggested that the effects of IL-6 are dependent on the expression of sIL-6R. (Islam et al. 2009) Later, the same group studied the effects of IL-6 on differentiation of hiPSC-neural cultures showing that co-stimulation with IL-6 and sIL-6R also enhance the neurogenesis and gliogenesis of hiPSC-derived NSCs (Sulistio et al. 2018). Functionality of the differentiated neurons was determined with patch-clamp (Sulistio et al. 2018).

In a few *in vitro* studies, human neurons have been treated with IL-6. The effects of IL-6 and two other inflammatory cytokines on the hPSC-derived NPCs have been investigated recently (Hagman et al. 2019). Study reported that IL-6 treatment (1, 10 or 100 ng/ml for 12-72 h) did not affect cell viability nor neuronal migration of NPCs, but it induced secretion of inflammatory factors VEGF and IL-10 (Hagman et al. 2019). Moreover, a study with hiPSC-derived neural aggregates showed that IL-6 treatment (100 ng/ml for 24 h) can increase the expression of astrocytes, decrease the expression of early-born neurons and increase the expression of phosphorylated STAT3 (Zuiki et al. 2017). IL-6 did not affect the size of aggregates or expression of apoptotic marker, cleaved-caspase 3 (Zuiki et al. 2017).

A recent study investigated the effects of IL-6 on the functionality of adult mouse dorsal root ganglia (DRG) neurons on MEAs (Black et al. 2018). Study revealed that IL-6 treatment (100 ng/ml for 3, 24 or 48 h) can increase spontaneous and stimulus-evoked (capsaicin or temperature

stimulus) activity of sensory neurons. Moreover, spontaneous hyperexcitability of IL-6 cultures was reduced with cercosporamide, which is a MAPK-interacting kinase 1/2 inhibitor. The study also suggested that the explanation for increased stimulus-evoked activity after IL-6 treatment might be the increased expression of capsaicin and temperature-sensitive cation channel transient receptor potential vanilloid 1 (TRPV1). Additionally, this study stated that the effects of IL-6 on neuronal functionality are still unclear, but MEA technology is promising for several applications even though repeatable long-term functionality studies can be challenging. (Black et al. 2018) Additionally, a study with lesioned mice organotypic hippocampal slice cultures on MEAs reported that IL-6 (150 ng/ml for six days) can potentiate functional recovery after injury and increase the expression of growth associated protein 43 (GAP-43) suggesting a regenerative role of IL-6 in the CNS (Hakkoum et al. 2007).

The effects of chronic exposure of IL-6 on rodent CNS cultures have been investigated in several studies where neurons were treated with IL-6 for 1-14 days with 1-10 ng/ml. These findings are not listed in Table 3. Studies have indicated that IL-6 can alter the electrical properties and calcium signaling (Nelson et al. 2002, Nelson et al. 2004) as well as modulate the expression levels of several proteins on neurons (Gruol et al. 2011) such as synaptic proteins (Vereyken et al. 2007). Moreover, chronic IL-6 can decrease cell viability and cause neuronal loss on developing neurons (Conroy et al. 2004). Interestingly, it has been also reported that chronic IL-6 exposure can have antiviral effects on hiPSC-derived neurons (Como et al. 2018).

Taken together, *in vitro* studies indicate that exogenous IL-6 treatment can cause wide range of effects on neuronal cultures. Clear conclusion about IL-6 effects on neuronal cultures is difficult to state since different cell sources, culture times, experimental designs, and IL-6 concentrations and exposure times have been used. Additionally, it seems that effects of IL-6 on hPSC-derived neuronal cultures have not been studied much and more research is needed.

Table 3. *In vitro* neuronal studies related to IL-6.

Study	**Cells**	**IL-6 stimulation**	**Functionality assays**	**Cell viability assays**	**Main findings**
Ali et al. 2000	mouse cortical neurons and glia	IL-6 (5-50 ng/ml for 24 h)	-	trypan blue dye staining, lactate dehydrogenase release	IL-6 protects against NMDA induced neuronal death, but not AMPA- or kainate mediated excitotoxicity.
Black et al. 2018	adult mouse dorsal root ganglia (DRG) neurons	IL-6 (100 ng/ml for 3, 24 or 48 h)	MEA (Axion BioSystems)	-	IL-6 increases spontaneous and stimulus-evoked activity, and increases TRPV1 expression.
Hagman et al. 2018	hESC-derived neural progenitor cells (NPCs)	IL-6 (1, 10 or 100 ng/ml for 12-72 h)	-	LIVE/DEAD assay, time-lapse imaging	IL-6 does not affect cell viability nor neuronal migration. IL-6 induces secretion of inflammatory molecules.
Hakkoum et al. 2007	mice lesioned organotypic hippocampal slice cultures	IL-6 (150 ng/ml for 6 d)	MEA	-	IL-6 promotes functional recovery.
Liu et al. 2011	rat cerebellar granule neurons (CGNs)	IL-6 (40 or 120 ng/ml for 8 days)	-	RT-qPCR & Western blot (Bcl-2, Bax, and caspase-3), Hoechst 33342 staining	IL-6 protects against NMDA-induced apoptosis, may be mediated by JAK/STAT3 and PI3K/Akt pathways.
Ma et al. 2015	rat cerebellar granule neurons (CGNs)	IL-6 (120 ng/ml for 24 h)	Calcium imaging, patch clamp	TUNEL assay	IL-6 decreases NMDA-receptor mediated Ca^{2+} influx and neuronal death.

Study	Cells	IL-6 stimulation	Functionality assays	Cell viability assays	Main findings
Orellana et al. 2005	rat hippocampal neurons	IL-6 (5 ng/ml)	Calcium imaging	-	IL-6 increases Ca^{2+} influx through NMDA-receptor, may be mediated by JAK/STAT pathway.
Sulistio et al. 2018	hiPSC-derived NSCs	IL-6 and sIL-6R (100 ng/ml)	-	-	IL-6 + sIL-6R enhances neurogenesis and gliogenesis.
Islam et al. 2009	mouse NSCs	IL-6 or Hyper-IL-6 (50-480 ng/ml)	-	CellTiter-Glo Luminescent Cell Viability Assay	Hyper-IL-6, but not IL-6 only, enhances neurogenesis and gliogenesis. Hyper-IL-6 induces gp130 expression.
Zuiki et al. 2017	hiPSC-derived neural aggregates	IL-6 (100 ng/ml for 24 h)	-	Western blot (cleaved-capase-3)	IL-6 increases the area ratio of astrocytes and decrease the area ratio of early-born neurons. IL-6 increase STAT3 levels.
Xia et al. 2015	rat cortical neurons	IL-6 (0.1, 1, 5 and 10 ng/ml for 24 h & 10 ng/ml for 2, 4, 8, 24 and 48 h)	Patch-clamp	-	IL-6 reduces Na^{+} currents dose- and time-dependently through its receptors. IL-6 reduces amplitude of APs, but not threshold.

Abbreviations: NMDA=N-methyl-d-aspartate, AMPA=α-amino-3hydroxy-5-methyl-4-isoxazolepropionate, MEA=microelectrode array, TRPV1=transient receptor potential vanilloid 1, RT-qPCR=quantitative reverse transcription PCR, AP=action potential.

3 Objectives

The aim of this study was to investigate the effects of exogenous IL-6 and Hyper-IL-6 on the characteristics and functionality of hPSC-derived cortical neurons and networks. Moreover, the effect of KA as potentiating factor of seizure-like activity after cytokine treatments was explored.

More specific aims were:

1. To determine the gene and protein expression levels of IL-6 receptors, IL-6R and gp130, in human neural cultures.

2. To investigate the effect of IL-6, Hyper-IL-6 and KA on the cell viability.

3. To explore the effect of IL-6, Hyper-IL-6 and KA on the neuronal network activity using MEAs.

4 Materials and methods

4.1 Experimental design of the study

In this study, effects of IL-6, Hyper-IL-6 and KA on hPSC-derived cortical neurons were investigated (Figure 7). For cell experiments, differentiated neurons were plated on culture plates as well as on MEA plates at day 0 and cultured for five weeks until the treatments with cytokines and KA were initiated. During the five-week culturing, neurons on MEA were followed for the development of spontaneous activity. Thereafter, functionally maturated neuronal networks were pretreated with 100 ng/ml IL-6 (PeproTech, Rocky Hill, NJ, USA) or 100 ng/ml Hyper-IL-6 (a kind gift from Prof. Dr. Stefan Rose-John, Germany). After 24 hours, a part of the cultures was exposed to 5 μM KA (Sigma-Aldrich) for an additional 24 hours without medium change. In total, each experiment has six treatment groups: controls, IL-6 only, IL-6 + KA, Hyper-IL-6 only, Hyper-IL-6 + KA and KA only.

Additionally, the gene and protein expression levels of IL-6 receptors were studied during the maturation phase (days 0 and 7) with quantitative reverse transcription PCR (RT-qPCR) and immunocytochemistry (ICC), respectively. Furthermore, the gene expression levels of IL-6 receptors were studied 24 hours after KA addition (day 37). Protein expression of neuronal, synaptic and astrocytic markers was also investigated with ICC at the same time points. Moreover, the effects of treatments on the cell viability and the neuronal network activity were studied with LIVE/DEAD assay and MEA measurements, respectively. Summary of used methods is presented in Table 4.

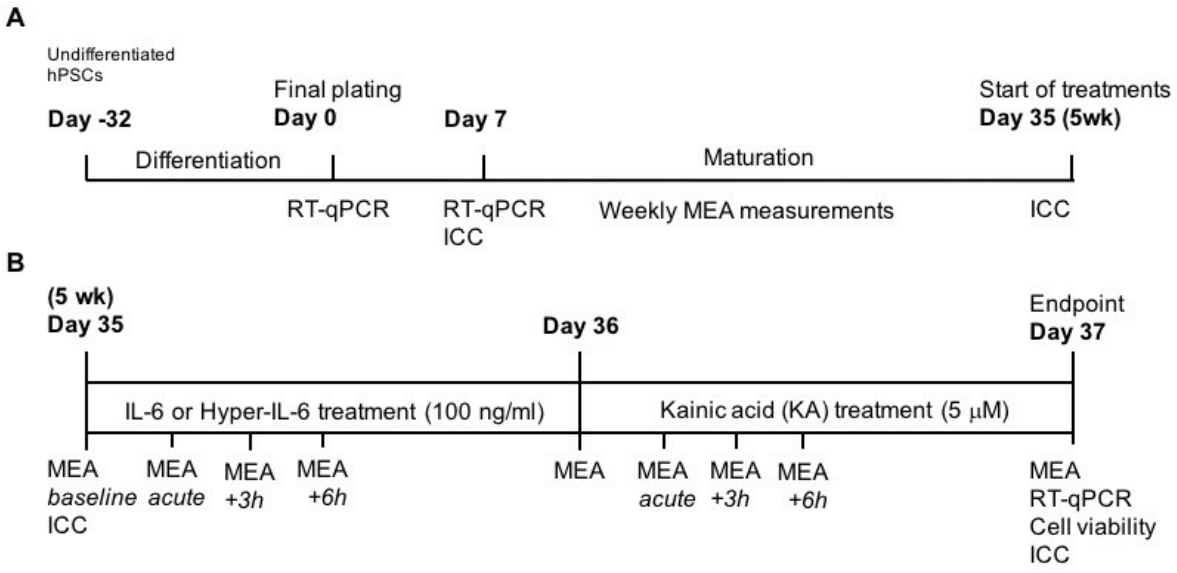

Figure 7. Experimental design of the study. A) hPSC-derived cortical neurons were plated on culture plates as well as on MEA plates at day 0 and cultured for five weeks. Activity of neuronal networks was followed with MEA measurements during the culture. B) At day 35, neurons were treated with IL-6 or Hyper-IL-6 for 24 hours prior to exposure of KA for an additional 24 hours. Effects of the treatments were investigated with several methods at different time points which are marked to the figure. Timeline is not-to-scale. Abbreviations: hPSC=human pluripotent stem cell, MEA=microelectrode array, IL-6=interleukin-6, ICC=immunocytochemistry, RT-qPCR=quantitative reverse transcription PCR.

Table 4. Summary of used methods with hESC (08/023)- and hiPSC (10212.EURCCs)-derived cortical neural cultures.

Method	**Cell line**	**Subject of evaluation**	**Culture time**
ICC	08/023, 10212.EURCCs	Protein expression: neuronal, astrocytic and synaptic markers, and IL-6 receptors	1-7 weeks
RT-qPCR	08/023, 10212.EURCCs	Gene expression: IL-6 receptors	1-5 weeks
LIVE/DEAD assay	08/023, 10212.EURCCs	Cell viability	5 weeks
MEA	10212.EURCCs	Activity of neuronal networks	5 weeks

Abbreviations: ICC=immunocytochemistry, RT-qPCR=quantitative reverse transcription PCR, MEA=microelectrode array.

4.2 Human pluripotent stem cell derived cortical neurons

Both hESC- and hiPSC-derived cortical neurons were used in this study. In-house derived cell lines were 08/023 (hESC) (Skottman 2010) and 10212.EURCCs (hiPSC) (Kiamehr et al. 2019). Both human pluripotent stem cell (hPSC) lines were expanded and cultured in feeder-free and xeno-free culture according to Hongisto et al. (2017). Faculty of Medicine and Health Technology has consent from the Finnish Medicines Agency (FIMEA) for human stem cell research (Dnro 1426/32/300/05) and supportive statements from the regional ethics committee of Pirkanmaa Hospital District to derivate, culture and differentiate hESCs (R05116) and iPSCs (R08070).

4.2.1 Cortical neuronal differentiation and culture

hPSCs were differentiated towards cortical neurons according to protocol of Hyvärinen et al. (2019b). During neural differentiation, the cells were cultured in the neural maintenance medium (N3, Table 5) supplemented with different components depending on the differentiation phase. Cells were cultured on poly-L-ornithine (PLO) and human recombinant laminin LN521 coated cell culture plates. Before each plating, culture plates were coated with 100 μg/ml PLO (Sigma-Aldrich, Saint Louis, Missouri, USA) in 0.1 M borate buffer for one hour at +37 °C, thereafter PLO was washed away three times with sterile water and let it air dried. Then, plates were incubated overnight with 15 μg/ml LN521 (Biolamina, Sundbyberg, Sweden) in 1×Dubecco's phosphate-buffer saline (DPBS) containing calcium and magnesium (Thermo Fisher Scientific, Waltham, Massachusetts, USA) at +4°C.

At the first differentiation phase, neural induction (differentiation days 1-12; here differentiation day 0 refers day -32 in Figure 7), hPSC-medium was replaced with N3 medium supplemented with 100 nM LDN193189 hydrochloride (SML0559, Sigma-Aldrich) and 10 μM SB431542 (S4317, Sigma-Aldrich). At differentiation day 12, the cells were passaged with StemPro Accutase (A1110501, Thermo Fisher Scientific) and cultured in neural induction medium with 10 μM ROCK inhibitor (Y-27632, Stemcell Technologies, Vancouver, Canada). On the following day, neural proliferation phase (differentiation days 13-25) was started with N3 medium supplemented with 20 ng/ml recombinant human fibroblast growth factor-2 (FGF2, 234-FSE, R&D Systems, Minneapolis, Minnesota, USA). Moreover, the cells were passaged and replated at differentiation

days 17, 21 and 25 as described earlier. NPCs were cryopreserved at differentiation day 21 and thawed for experiments when needed. This enables efficient and fast yield of neurons directly from the master NPC banks. In neural maturation phase (from differentiation day 26 to the end of experiments, days 37 or 49), the cells were in neural maturation medium (NMM) containing N3 medium supplemented with 20 ng/ml brain-derived neurotrophic factor (BDNF, 248-BDB, R&D Systems), 10 ng/ml glial-derived neurotrophic factor (GDNF, 212-GD, R&D Systems), 500 μM dibutyryl cyclic adenosine monophosphate (db-cAMP, D0627, Sigma-Aldrich) and 200 μM L-Ascorbic acid (AA, A5960, Sigma-Aldrich).

Final plating for experiments was performed at day 0. Neurons were plated on 24-well and 48-well Thermo Scientific™ Nunc™ Cell-Culture Treated plates (Thermo Fisher Scientific) or glass coverslips at cell density 50 000 cells/cm^2 in NMM with ROCK inhibitor. For glass coverslips LN521 concentration was 50 μg/ml. Plating and culturing on MEA plates is described in chapter 4.6.1. The cells were cultured in the Thermo Scientific™ Forma™ Steri-Cycle™ i160 CO_2 incubator at 37 °C in 5% CO_2 atmosphere. NMM was changed three times per week and cells were imaged weekly with Nikon Eclipse Ti-S inverted microscope equipped with a Nikon digital sight DS-Fi2 camera (both from Nikon, Minato, Tokyo, Japan).

Table 5. Ingredients of the neural maintenance medium (N3).

Ingredients	**Concentration**	**Manufacturer**
D-MEM/F-12 (Dulbecco's Modified Eagle Medium/Nutrient Mixture F-12) with GlutaMAX™	0.5×	Thermo Fisher Scientific, 31331-028
Neurobasal™ Medium	0.5×	Thermo Fisher Scientific, 21103-049
N-2 supplement	0.5%	Thermo Fisher Scientific, 17502-048
B-27™	1%	Thermo Fisher Scientific, 17504-044
GlutaMAX™ Supplement	0.5 mM	Thermo Fisher Scientific, 35050-061
Non-Essential Amino Acids Solution (NEA)	0.5%	Thermo Fisher Scientific, 11140-050
2-mercaptoethanol	50 μM	Thermo Fisher Scientific, 31350-010
Insulin	2.5 μg/ml	Sigma-Aldrich, I9278
Penicillin-Streptomycin antibiotic	0.1%	Lonza, DE-602E

4.3 Gene expression analysis

The gene expression levels of IL-6 receptors, gp130 and IL-6R, and the housekeeping gene glucuronidase beta (GUSB) were investigated during maturation phase (days 0 and 7) and during the cytokine and KA treatment (day 37) (Figure 7) using real-time RT-qPCR. Before gene expression analysis, RNA was isolated from cell samples and it was converted into complementary DNA (cDNA).

4.3.1 RNA isolation

Cortical neuronal cultures were lysed and total RNA was isolated with a NucleoSpin® RNA kit (Macherey-Nagel, Düren, Germany). At the plating day (day 0), cell samples were collected by centrifugation (5 min, 300 × *g*) and lysed with Buffer RA1 with 1% β-mercaptoethanol (Sigma-Aldrich). For plated and cultured cells, two to three wells from 24-well plates were lysed with RA1 with 1% β-mercaptoethanol (Sigma-Aldrich) and then pooled together. All lysed cell samples were stored at -80°C until use. Total RNA was isolated from thawed cell lysates according to the manufacturer's instructions. Briefly, the lysate was cleared by filtrating through a NucleoSpin®

Filter (1 min, 11, 000 × *g*). Then 70% ethanol was added on the lysate to adjust RNA binding conditions and lysates were transferred to NucleoSpin® Colum silica membrane and centrifuged for 30 sec, 11, 000 × *g*. Silica membrane was desalted with membrane desalting buffer (MDB) (1 min, 11, 000 × *g*). DNA was removed from membrane by incubating rDNase reaction mixture for 15 min at RT. Thereafter, membrane was washed with Buffer RAW2 (30 sec, 11, 000 × *g*), Buffer RA3 (30 sec, 11, 000 × *g*) and dried with Buffer RA3 (2 min, 11, 000 × *g*). Finally, RNA was eluted in 60 µl RNase-free water (1 min, 11, 000 × *g*) and the concentration and quality of RNA were measured with a NanoDrop™ 1000 UV-Vis spectrophotometer (Thermo Fisher Scientific). Isolated RNA samples were stored at -80°C.

4.3.2 cDNA synthesis

200 ng of total RNA from each sample was reverse transcribed into cDNA with a High-Capacity cDNA Reverse Transcription kit (Applied Biosystems, Thermo Fisher Scientific) according to the manufacturer's instructions. Briefly, 10 µl Reverse Transcription (RT) Master Mix and 10 µl isolated RNA diluted in nuclease free water were used for each reaction. 10 µl RT Master Mix contained 2 µl 10X RT Buffer, 2 µl 10X RT Random Primers, 0,8 µl 25X dNTP Mix (100 mM), 1 µl MultiScribe® Reverse Transcriptase (50 U/µL), 0,25 µl RiboLock RNase Inhibitor (40 U/µL) and 3,95 µl nuclease free water. Reverse transcription was performed in Eppendorf MasterCycler EP Gradient Thermal Cycler (Eppendorf, Hamburg, Germany) under the following conditions: 25°C for 10 min (primer annealing), 37°C for 120 min (DNA polymerization), 85°C for 5 min (enzyme inactivation) and then samples were chilled to 4°C. cDNA samples were stored at -20°C until use.

4.3.3 TaqMan real-time quantitative reverse transcription-PCR

Gene expression analysis of IL-6R, gp130 and GUSB was performed with TaqMan® gene expression assay (Applied Biosystems), following the manufacturer's instructions. Each 15 µl reaction contained 15 ng thawed cDNA diluted in nuclease free water, 0.75 µl 20×TaqMan Gene Expression Assay primers (Table 6), 7.5 µl 2× TaqMan Gene Expression Master Mix and 3.75 µl nuclease free water on MicroAmp™ Optical 96-Well Reaction Plates (Applied Biosystems). In

addition, no template controls (NTCs) were included in each run. RT-qPCR analysis was carried out on ABI7300 Real-Time PCR System (Applied Biosystems) using following conditions: 50°C for 2 min, DNA denaturation step at 95°C for 10 min, the annealing and extension step repeated 40 times at 95°C for 15 secs and at 60°C for 1 min. Data analysis for the raw data was performed in ABI 7300 Real-Time PCR System Software. Each sample had three technical replicates. Relative gene expression levels were calculated with the comparative deltadelta Ct method ($2^{-\Delta\Delta Ct}$) which indicates the gene expression difference between two genes. These relative quantification (RQ) values (also called fold change) were determined for each sample as following: $RQ=2^{-\Delta\Delta Ct}$, where $\Delta\Delta Ct=\Delta Ct_{sample}-\Delta Ct_{calibrator}$ and $\Delta Ct=Ct_{gene} - Ct_{endogenous\ control}$. Housekeeping gene GUSB was used as an endogenous control.

Table 6. TaqMan Gene Expression Assay primers used in the RT-qPCR.

Gene	**Marker type**	**ID**	**Manufacturer**
GUSB	Housekeeping gene	Hs00939627_m1	Thermo Fisher Scientific
gp130 (IL6ST)	Interleukin-6 signal transducer gene	Hs00174360_m1	Thermo Fisher Scientific
IL-6R	Interleukin-6 receptor gene	Hs01075664_m1	Thermo Fisher Scientific

4.4 Cell viability assay

4.4.1 LIVE/DEAD assay

Effects of IL-6, Hyper-IL-6 and KA treatments on the cell viability were analysed with a fluorescence-based LIVE/DEAD viability/cytotoxicity kit for mammalian cells (Thermo Fisher Scientific) (Hyvärinen et al. 2019a). LIVE/DEAD assay was performed once for treated 08/023 cells after seven-week culture (day 49) and twice for treated 10212.EURCCs cells after five-week culture (day 37). The cells were plated on 48-well plate, cultured and treated as described previously. The culture medium was replaced in every well with 200 µl dye solution containing 0.1 µM calcein-AM and 0.5 µM EthD-1 in culture medium. Live cells were stained green with Calcein-AM and dead cells red with ethidium homodimer-1 (EthD-1) indicating functional intracellular esterase activity and damaged cell membrane, respectively. Dyes were incubated light protected 30 minutes at room temperature (RT) on a shaker. Thereafter, cell viability was determined immediately with Olympus IX51 inverted fluorescence microscope (10× magnification) equipped with an Olympus DP30BW Microscope Digital Camera (Olympus

Corporation, Shinjuku, Tokyo, Japan). Each experiment contained five to six treatment groups, 3-4 wells were included in each group and 3-4 images were taken from each well. CellProfiler (3.1.8) was used for quantification of live and dead cells (Carpenter et al. 2016). Mean area coverage of live and dead cells from the total culture area was calculated and compared between each treatment group (Hyysalo et al. 2017).

4.5 Immunocytochemistry (ICC)

4.5.1 ICC staining

Protein expression of neuronal and astrocytic markers as well as IL-6 receptors were investigated with indirect ICC. Both control and treated samples were stained similarly as previously described (Lappalainen et al. 2010). Samples were fixed with 4% paraformaldehyde (PFA) in phosphate-buffer saline (PBS) for 15 min, washed twice in PBS for five minutes and stored in PBS at +4°C. Nonspecific antigen binding sites were blocked with 10% normal donkey serum (NDS), 0.1% TritonX-100, 1% bovine serum albumin (BSA) in PBS for 45 min at RT and was washed with 1% NDS, 0.1% TritonX-100, 1% BSA in PBS. The primary antibodies (Table 7) were diluted with the same washing solution, added to the cells and incubated overnight at +4°C on a shaker. On the next day, the cells were washed twice in 1% BSA in PBS for five minutes. Secondary antibodies (Table 8), diluted with 1 % BSA in PBS solution, were added to the cells and incubated light protected 1 hour in RT. Then, the cells were washed twice in PSB for five minutes and once in phosphate buffer (PB) for five minutes. The cells were mounted with ProLong™ Gold Antifade Mountant with DAPI (Thermo Fisher Scientific) and covered by a coverslip. 4′,6-diamidino-2-phenylindole (DAPI) binds to DNA and stains nuclei blue. Mounted samples were kept light protected at +4°C. Fluorescence imaging was performed using an Olympus IX51 inverted fluorescence microscope equipped with an Olympus DP30BW Microscope Digital Camera (Olympus Corporation, Shinjuku, Tokyo, Japan**)** and confocal imaging was performed with an LSM780 laser scanning confocal microscope (Carl Zeiss, Oberkochen, Germany).

Table 7. Primary antibodies used in the immunocytochemistry.

Primary antibody	**Expression**	**Dilution**	**Origin**	**Manufacturer & Cat. no.**
anti-MAP2	Neuronal marker	1:400	rabbit	Merck Millipore, AB5622
anti-MAP2	Neuronal marker	1:400	chicken	Novus Biologicals, NB300-213
anti-β-tubulin 3 (β-Tub)	Neuronal marker	1:1000	mouse	Sigma-Aldrich, T8660
anti-β-tubulin 3 (β-Tub)	Neuronal marker	1:200, 1:4000 for synaptic staining	chicken	Abcam, ab41489
anti-GFAP	Astrocyte marker	1:4000	chicken	Abcam, ab4674
anti-Synaptophysin	Presynaptic marker	1:2000	rabbit	Abcam, ab32127
anti-PSD95	Postsynaptic marker	1:50	mouse	Abcam, ab2723
anti-IL-6Rα	Interleukin-6 receptor α subunit	1:100, 1:200, 1:500	rabbit	Abcam, ab128008
anti-IL-6Rα	Interleukin-6 receptor α subunit	1:50, 1:100, 1:200, 1:500	mouse	R&D Systems, MAB2271
anti-gp130 (IL6ST)	Interleukin-6 signal transducer	1:50, 1:200, 1:500	mouse	Santa Cruz, sc-376280

Table 8. Secondary antibodies used in the immunocytochemistry.

Secondary antibody	Dilution	Origin	Manufacturer & Cat. no.
Alexa Fluor® 488 anti-mouse IgG	1:200, 1:400	donkey	Thermo Fisher Scientific, A21202
Alexa Fluor® 488 anti-rabbit IgG	1:200, 1:400	donkey	Thermo Fisher Scientific, A21206
Alexa Fluor® 568 anti-mouse IgG	1:200, 1:400	donkey	Thermo Fisher Scientific, A10037
Alexa Fluor® 568 anti-rabbit IgG	1:200, 1:400	donkey	Thermo Fisher Scientific, A10042
Alexa Fluor® 568 anti-chicken IgY	1:200, 1:400	goat	Thermo Fisher Scientific, A11041
Alexa Fluor® 647 anti-chicken IgY	1:200	goat	Thermo Fisher Scientific, A21449
Alexa Fluor® 647 anti-rabbit IgG	1:200	donkey	Thermo Fisher Scientific, A31573

4.5.2 Antibody optimization and validation

Optimization for antibodies against IL-6 receptors was performed since these antibodies were used for the first time for hPSC-derived cortical cultures. Anti-IL-6R antibody (ab128008, Abcam) and anti-gp130 antibody (sc-376280, Santa Cruz) were tested with 08/023 cell line at 7-day time point using three different staining protocols and several antibody concentrations as well as at five-week time point (day 35) with peptide blocking test. Additionally, peptide blocking test for anti-gp130 was repeated with 10212.EURCCs cell line. Tested staining protocols, concentrations and peptide blocking tests are described in the next chapters. Moreover, to confirm similar staining pattern, another anti-IL-6R antibody from R&D Systems was tested with 10212 EURCCs cell line at two-week time point (day 14) using normal ICC protocol (chapter 4.5.1) and different antibody concentrations (1:50, 1:100, 1:200).

Different ICC conditions and antibody concentrations. Tested ICC protocols for IL-6 receptors were otherwise similar as described in previous chapter (4.5.1) but different permeabilization reagents were used. All three staining conditions are listed in Table 9. Permeabilization reagents were 0.1% TritonX-100 and 1% saponin. Moreover, staining without permeabilization reagent was tested. Tested primary antibody dilutions for anti-IL-6R (Abcam) were 1:100, 1:200 and 1:500, and for anti-gp130 (Santa Cruz) 1:50, 1:100 and 1:200.

Table 9. Tested immunocytochemistry conditions in the antibody optimization.

Condition	**Blocking solution**	**Primary antibody and wash solution**	**Secondary antibody and wash solution**
1 (control)	10% NDS, 0.1% TritonX-100, 1% BSA in PBS	1% NDS, 0.1% TritonX-100, 1% BSA in PBS	1% BSA in PBS
2	10% NDS, 1% saponin, 1% BSA in PBS	1% NDS, 1% saponin, 1% BSA in PBS	1% saponin, 1% BSA in PBS
3	10% NDS, 1% BSA in PBS	1% NDS, 1% BSA in PBS	1% BSA in PBS

Abbreviations: NDS=normal donkey serum, BSA=bovine serum albumin, PBS=phosphate buffer solution.

Peptide blocking test. Specificity of anti-IL-6R (Abcam) and anti-gp130 (Santa Cruz) antibodies was investigated with peptide blocking test. In peptide blocking test, primary antibody is incubated overnight with a blocking peptide before staining. During incubation, antibody will recognize and bind to an epitope of the blocking peptide. After their binding, antibody cannot bind to the proteins of the cells and therefore a signal of the staining is weaker if antibody is specific. Solutions containing 0, 10, 20, 50 µg/ml recombinant human gp130 protein (228-GP, R&D Systems) and 1:50 (4 µg/ml) anti-gp130 antibody (Santa Cruz) or 0, 1, 10, 50 µg/ml recombinant IL-6R protein (ab50082, Abcam) and 1:200 (5 µg/ml) anti-IL-6R antibody (Abcam) in 1% NDS, 0,1% TritonX-100, 1% BSA in PBS were incubated overnight in separate eppendorf tubes at +4°C. Peptide-antibody solutions (150 µl/well) were added to the cells. For both antibodies, two replicates were used for each peptide concentration. As controls, in addition to 0 µg/ml peptide samples, secondary antibody controls without primary antibodies were performed and few wells were stained with anti-IL-6R and -gp130 using standard ICC protocol (chapter 4.5.1). All samples were incubated overnight at +4°C. Thereafter, the samples were washed, stained with 1:400 Alexa Fluor® 488 anti-mouse IgG or Alexa Fluor® 488 anti-rabbit IgG secondary antibody, washed and mounted as described in the chapter 4.5.1. Samples were imaged with an Olympus IX51 inverted fluorescence microscope equipped with an Olympus DP30BW Microscope Digital Camera (Olympus Corporation).

4.6 Microelectrode arrays (MEAs)

4.6.1 Coating, plating and cell maintenance of MEAs

The activity of neuronal networks was studied using MEAs as previously described (Hyvärinen et al. 2019b). At first, CytoView MEA 48 (Axion BioSystems, Atlanta, GA, USA) plates were washed with 70% ethanol, rinsed with sterile water and air dried. Thereafter, MEAs were coated as a 10 µl droplet with 0.1% polyethylenimine (PEI, Sigma-Aldrich) in 0.1 M borate buffer for one hour at +37 °C, PEI was washed three times with sterile water and air dried. Thereafter, 10 µl droplet of 50 µg/ml LN521 (Biolamina) in 1×DPBS was incubated overnight at +4°C. Next day (day 0), the coating solution was removed without rinsing, and neurons were plated as a 10 µl droplet of 80 000 cells in NMM with ROCK inhibitor. After half an hour, 500 µl NMM with ROCK inhibitor was added. MEAs were cultured in the incubator at 37 °C in 5% CO_2 atmosphere, NMM were changed four times per week and cells were imaged weekly with Zeiss Axio Observer A1 equipped with an Axiocam 506 color camera (Carl Zeiss).

4.6.2 MEA measurements

Extracellular neuronal network activity was measured using CytoView MEA 48 plates and an Axion Maestro MEA system integrated with heating system, temperature controller and real-time signal monitoring AxIS software (all from Axion BioSystems) as previously described (Hyvärinen et al. 2019b). CytoView MEA 48 plates have 16 electrodes in each well and total number of electrodes per plate is 768. Development of spontaneous neuronal activity was followed with MEA measurements twice a week for 10 minutes at +37°C, for five weeks. Prior to the recordings, the MEA plates were equilibrated for five minutes in the Maestro system.

At fifth culture week (days 35-37), effects of IL-6, Hyper-IL-6 and KA on the neuronal network activity were investigated (Figure 7). At days 35 and 36, experiment measurements were performed just before IL-6, Hyper-IL-6 or KA treatments (baseline measurement), immediately after (acute effect) as well as three hours and six hours after treatments. At day 37, endpoint measurement was performed 48h after the first treatment. Medium change was not performed during experiments. All experiment recordings were performed similarly at +37°C with 5% CO_2 supplier for 15 minutes. 16 MEA wells per treatment group were measured.

4.6.3 MEA data analysis

For detecting neuronal spikes, the data was analysed with an in-house made script (Hyvärinen et al. 2019b) for MATLAB adapted from Mayer et al. 2018. Electrodes which detected more than 10 spikes per minute were "active electrodes". Burst detection was then analysed using the R-package meaRtools (Gelfman et al. 2018) with the spike timestamps using the log ISI algorithm adapted from Pasquale et al. 2010 with additional modifications (Hyvärinen et al. 2019b). MEA data was analysed by PhD student Mzezewa and detailed data analysis is described in Hyvärinen et al. (2019b).

4.7 Statistical analysis

Gene expression data was analysed with GraphPad Prism 8 (GraphPad Software, San Diego, USA) and cell viability data was analysed with IBM SPSS Statistics, Version 26.0 (IBM, Armonk, New York, USA). Distributions of the data were studied using Shapiro-Wilk test which showed that all the data were not normally distributed. Therefore, the nonparametric Mann-Whitney U test with Bonferroni correction was used for the gene expression data to study statistical significance. Cell viability data was analysed with Mann-Whitney U test. MEA data was analysed with GraphPad Prism 5 and IBM SPSS Statistics, Version 25.0 (IBM, Armonk, New York, USA) by PhD student Mzezewa. Statistical tests for the MEA data were performed with SPSS Statistics using the one-way ANOVA with Bonferroni post hoc test. P-values lower than 0.05 were considered statistically significant. All the graphs were created with GraphPad Prism.

5 Results

5.1 Characterization of hPSC-derived neural cultures

Both hESC- and hiPSC-derived cortical neural cultures were used in this study. Before the cytokine and KA treatments, hESC-derived neurons were cultured for five or seven weeks and hiPSC-derived neurons were cultured for five weeks. Cultures were followed with phase-contrast microscope imaging (Figure 8) and ICC by staining neuronal (MAP-2, β-Tub) and astrocytic (GFAP) markers (Figure 9). All cultures expressed neuronal markers whilst GFAP-positive astrocytes were detected on some culture areas at five- and seven-week time points (days 35 and 49).

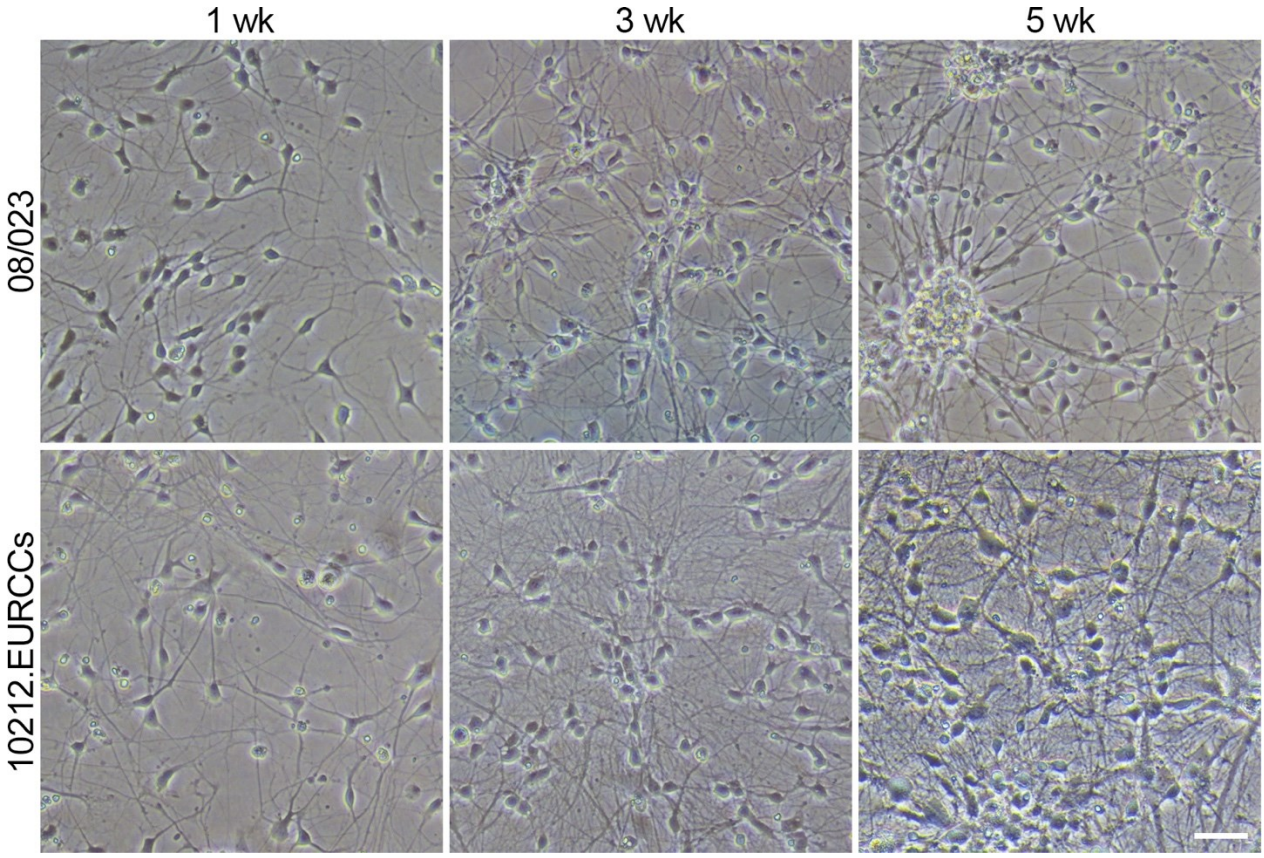

Figure 8. Phase-contrast microscopy images of hESC (08/023)- and hiPSC (10212.EURCCs)-derived cortical neural cultures after one, three and five-week culture before cytokine and KA treatments. The scale bar is 50 μm in all images.

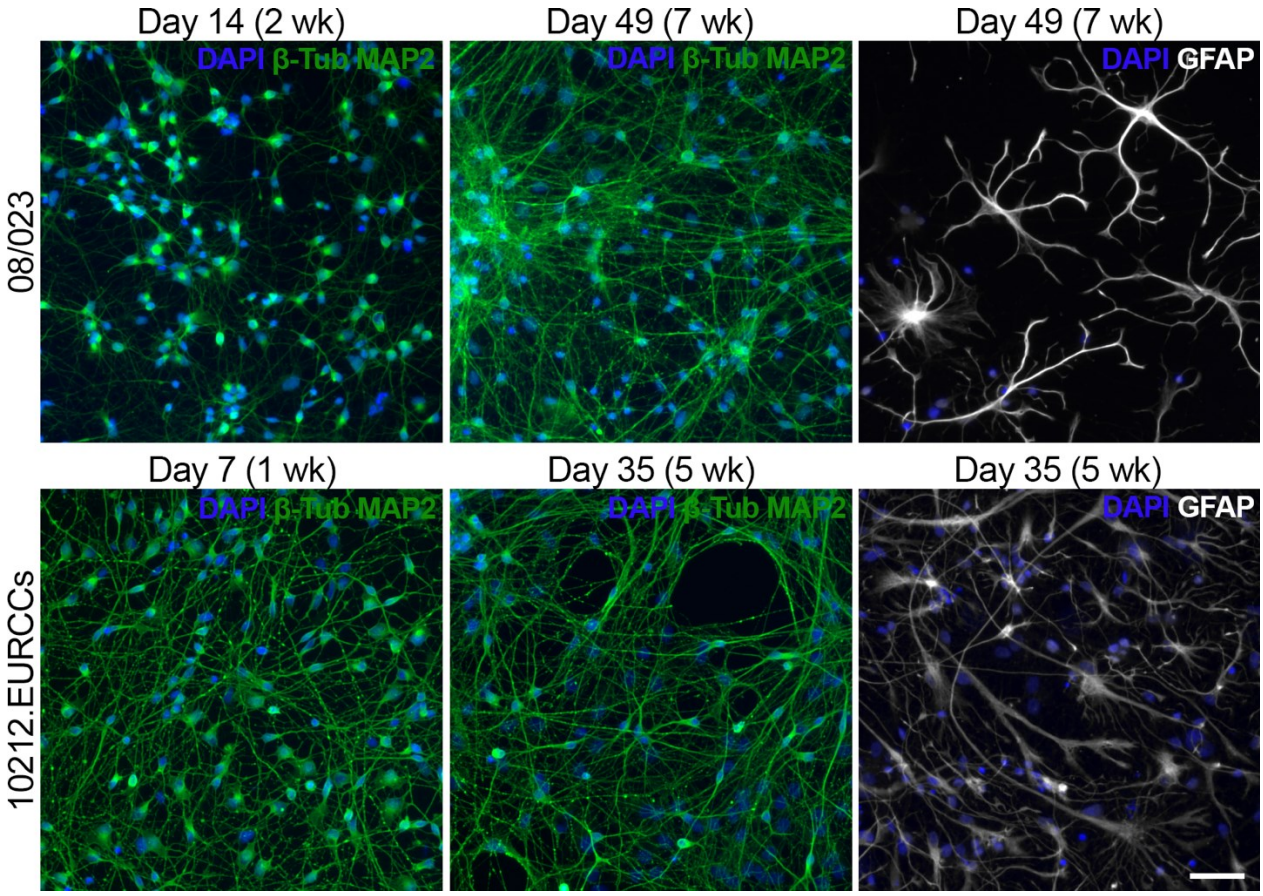

Figure 9. ICC characterization of hESC (08/023)- and hiPSC (10212.EURCCs)-derived cortical neural cultures at different time points before cytokine and KA treatments. Both cell lines expressed neuronal markers MAP-2 and β-Tub after neuronal differentiation. In some culture areas, also GFAP-positive astrocytes were detected at fifth- and seventh culture week. DAPI stained nuclei blue. The scale bar is 50 μm in all images.

5.2 Expression of IL-6 receptors on hPSC-derived neural cultures

5.2.1 hPSC-derived neural cultures express IL-6 receptors at gene level

Gene expression levels of IL-6 receptors, *IL-6R* and *gp130* were determined with RT-qPCR during the maturation phase (days 0, 7 and 37). The expressions of receptors were investigated in both hESC- and hiPSC-derived cortical neural cultures. Representative gene expression data is presented in Figure 10 (n=2 with three technical replicates from one experiment with hiPSC-cultures, statistical tests were not performed due to the low number of replicates). Results indicated that both cell lines express *IL-6R* and *gp130*. Already at day 0, threshold cycle values (Ct values) of *gp130* were lower compared to Ct values of *IL-6R*, indicating that the gene expression level of *gp130* is higher compared to *IL-6R* expression (Figure 10 A). Moreover, the gene expression levels

of both *IL-6R* and *gp130* were elevated during the five-week culture compared to the expression levels of day 0 (Figure 10 B-C). Increase in the expression levels was higher in *IL-6R*. However, *IL-6R* expression was lower compared to the *gp130* expression after five-week culture (day 37). To conclude, both hPSC-derived cortical neural cell lines expressed *IL-6R* and *gp130* at the gene level. The gene expression levels of both IL-6 receptors increased during the neuronal maturation and the expression of *gp130* was higher compared to the expression of *IL-6R*.

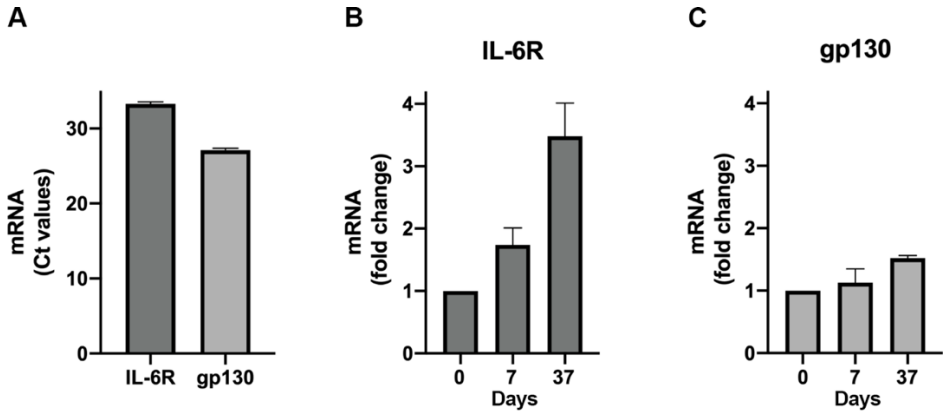

Figure 10. Gene expression levels of IL-6 receptors *IL-6R* and *gp130* on hiPSC-derived cortical neural cultures. A) Both IL-6 receptors were expressed in the beginning of the experiments (day 0). *Gp130* expression is higher in comparison to the expression of *IL-6R* as demonstrated by lower Ct value. B) Gene expression of *IL-6R* increased during the five-week culture. C) Gene expression of *gp130* also increased during the five-week culture. In the B and C, fold changes are calculated from ΔΔCt values by comparing to the day 0 expression. The data is from one experiment and it is presented as the mean ± SD (n=2 with three technical replicates) in all graphs.

5.2.2 Antibody optimization and validation

ICC optimization for antibodies against IL-6 receptors, IL-6R and gp130 was performed as described above (4.5.2), since IL-6 receptors were stained for the first time on hESC (08/023)- and hiPSC (10212.EURCCs)-derived cortical cultures. Two antibodies against IL-6R (from Abcam and Santa Cruz) and one against gp130 (from Santa Cruz) were tested. ICC images from these optimizations are presented in Appendices.

Different permeabilization reagents and antibody concentrations were tested for anti-IL-6R and anti-gp130 antibodies. TritonX-100, saponin and staining without permeabilization reagent were tested (Appendix 1 & 3). Based on the staining results TritonX-100 was chosen for the following IL-6R and gp130 stainings. Staining with saponin or without permeabilization reagent were dim

compared to the staining with TritonX-100. For anti-IL-6R (Abcam) 1:100, 1:200 and 1:500 dilutions were tested. Staining with 1:200 dilution was considered to be most optimal (Appendix 1). 1:200 dilution was also optimal for another anti-IL-6R antibody (R&D Systems), when 1:50, 1:100, 1:200 and 1:500 dilutions were tested (Appendix 2). Staining patterns of both anti-IL-6R antibodies were quite similar. For anti-gp130 (Santa Cruz), 1:50, 1:200 and 1:500 dilutions were tested, from which 1:50 dilution was the most optimal (Appendix 3). Moreover, peptide blocking test was performed to investigate the specificity of anti-IL-6R (Abcam) and anti-gp130 (Santa Cruz) antibodies (Appendix 4 & 5). IL-6R expression seemed to be slightly decreased with the highest blocking peptide concentration (Appendix 4). In addition, very bright fluorescence signal was detected from some neurons only in the cultures without blocking peptide (Appendix 5). In conclusion, after antibody optimization TritonX-100 was used as a permeabilization reagent and antibody dilutions were 1:200 for both anti-IL-6R antibodies and 1:50 for anti-gp130.

5.2.3 IL-6 receptors are expressed on hPSC-derived neurons at protein level

After optimization of IL-6 receptor ICC staining, receptors were co-stained with neuronal MAP-2 and β-Tub and astrocytic GFAP markers to investigate the localization of IL-6 receptors on hPSC-derived cortical neural cultures. As reported above, gene expression analysis already confirmed that IL-6 receptors are expressed in these cultures. However, determination of protein expression was also important because in the later experiments the cultures were treated with cytokines which mediate their effects through IL-6 receptors. ICC results indicated that both hESC- and hiPSC-derived cortical neurons express IL-6R and gp130 after one-week (day 7) and five-week (day 37) cultures. Representative images of IL-6R and gp130 protein expression on hiPSC-derived cultures are presented in Figure 11. In both time points, IL-6R expression seemed to be higher compared to the gp130 expression. Expression of both receptors, particularly IL-6R, was higher on soma part of neurons, around the nuclei, as seen in Figure 10. However, both receptors seemed to be expressed also along axons and dendrites. Moreover, very weak expression of IL-6R (Figure 11) and gp130 on GFAP-positive astrocytes were detected (Figure 14). Taken together, IL-6R and gp130 are expressed on hPSC-derived cortical neuronal cultures, mainly on neurons, before cytokine and KA treatments.

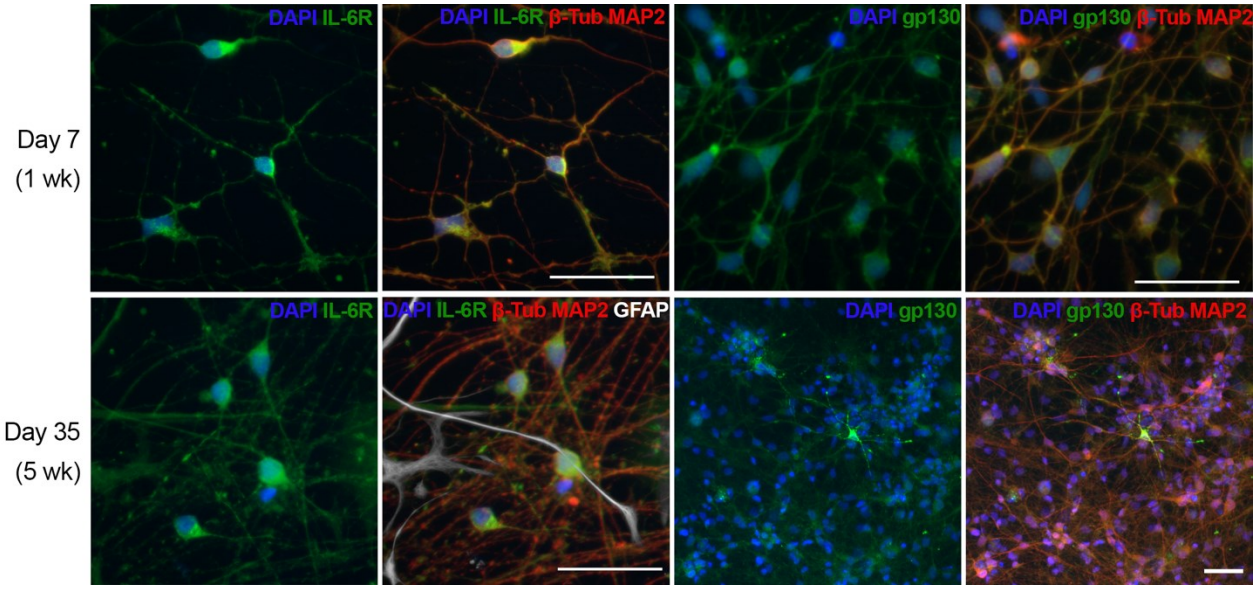

Figure 11. Protein expression of IL-6 receptors, IL-6R and gp130, on hiPSC-derived cortical neuronal cultures. Both IL-6 receptors are expressed with after one- and five-week culture before cytokine and KA treatments. Moreover, cultures are positive for neuronal (MAP-2 and β-Tub) and astrocytic (GFAP) markers. DAPI stained nuclei blue. The scale bar is 50 μm in all images.

5.3 Development of spontaneous neuronal network activity of hPSC-derived neural cultures

Functionality of hiPSC-derived cortical neural cultures was studied with MEA measurements. First, neural cells were cultured for five weeks on MEAs and the development of spontaneous neuronal network activity was followed twice a week. Moreover, networks were followed weekly with phase-contrast microscopy, which indicated how cultures changed from dense to more aggregated cultures (Figure 12 A). MEA data from two separate experiments (Exp1 and Exp2 both consist of two 48-well MEA plates, referred as A-B and C-D) with 10212.EURCCs cell line showed how the activity of neuronal networks increased during the five-week culture (Figure 12 B-E). MEA enables continuous measurement of the activity of neuronal networks in real time. Representative images of heat map of 48-well MEA measurements indicated that the cultures were more active at five-week time point (day 36) in comparison to the one-week point (day 7) (Figure 12 B). Each box in heat map represents a single well (as explained in Figure 6), and activity is represented as a color-coded spike rate (colour scale indicates 0-5 spikes/second). Representative images of spontaneous neuronal network activity from one well of the culture (16 electrodes/well) at one-week (day 7) and five-week time point (day 35) represent how the activity patterns changed during the neuronal network maturation (Figure 12 C). Activity patterns changed from spontaneous

spiking to spike trains, smaller burst and finally synchronous network bursts (Figure 12 C). During the five-week culture the number of active electrodes (>10 spikes/min) per MEA wells increased slightly in Exp1, but in another experiment Exp2 the number of active electrodes stayed quite stable over follow-up (Figure 12 D). The median spike rate per MEA well increased in each plate up to day 21 after which a slight decrease followed by an increase was seen (Figure 12 E). At day 31, spike rate of A-D plates was approximately 5-7 Hz.

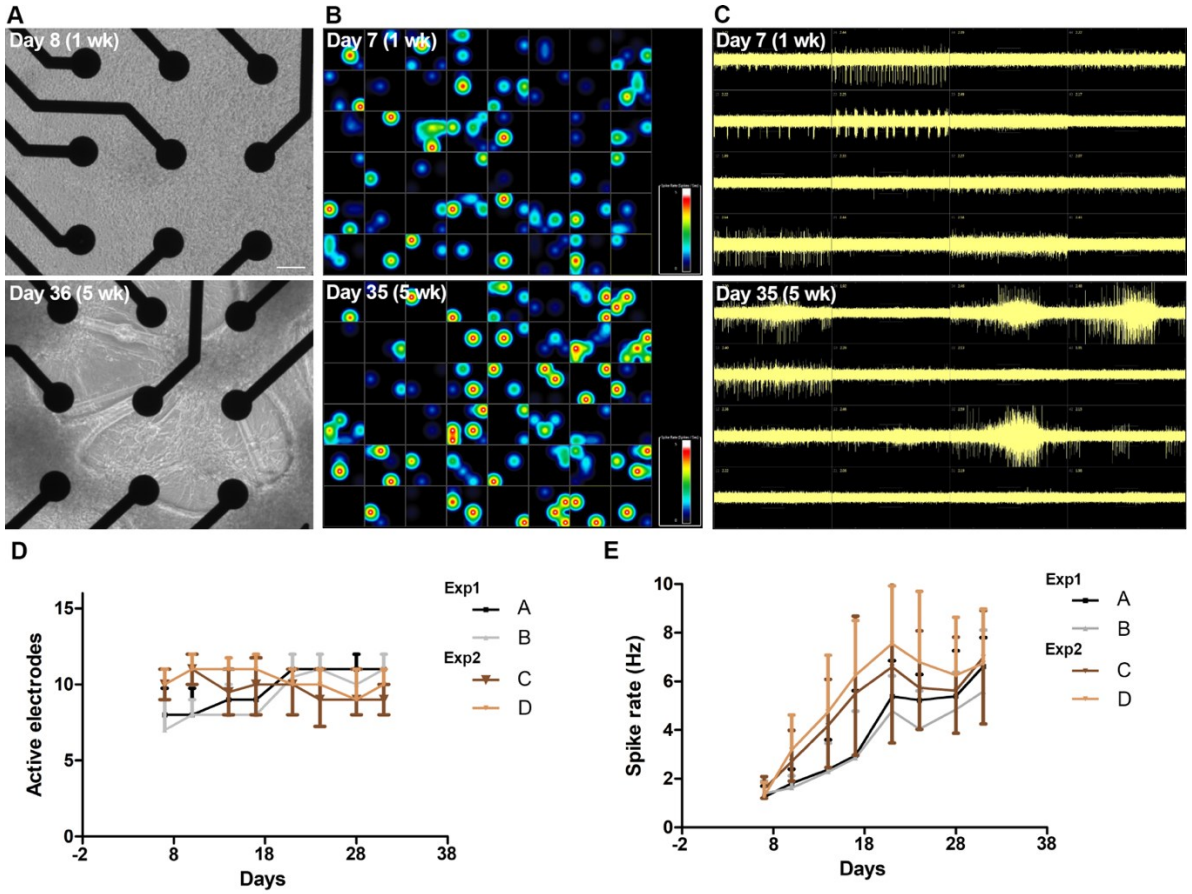

Figure 12. Development of spontaneous neuronal network activity of hiPSC-derived cortical neurons was investigated with MEA measurements during a five-week culture. A) Phase-contrast images of cultures on MEAs after one-week and five-week culture. The scale bar is 50 µm in both images. B) Representative images of heat map of 48-well MEA measurements at day 7 and 35 show a spike rate of neuronal cultures with different colours. Each box indicates a single well in both images. C) Representative images of the activity patterns from one well at day 7 and 35. Each box indicates a single electrode in both images. D) Number of active electrodes on MEA wells during five-week culture. Total number of electrodes in each well is 16. E) Development of the spike rate (Hz) during five-week culture. In both graphs, A-B and C-D values are from two separate experiments Exp1 and Exp2, and A-D represent different 48-well MEA plates. The data is presented as the median and range (n=48 wells/plate).

5.4 Expression of IL-6 receptors on hPSC-derived neural cultures after IL-6, Hyper-IL-6 and KA treatments

Functionally maturated hPSC-derived cortical neural cultures were treated with IL-6 or Hyper-IL6 for 24 hours at five-week time point (day 35). Then, part of the cultures was treated with KA for additional 24 hours to induce seizure-like functionality (Figure 7). Thereafter, the effects of treatments on gene expression levels of IL-6 receptors, *IL-6R* and *gp130*, were investigated with RT-qPCR (day 37). The aim of this study was to investigate whether IL-6, Hyper-IL-6 or KA alone can affect gene expression levels of IL-6 receptors, and if cytokine treatments together with KA exposure can change expression levels. Gene expression levels were investigated once with hESC (08/023) and twice with hiPSC (10212.EURCCs) derived cultures. Results from both cell lines followed the same trend and had statistically significant differences between treatment groups compared to controls (Figure 13). Results are presented in next chapters. Shapiro-Wilk test indicated that all the data is not normally distributed, therefore the nonparametric Mann-Whitney U test was used with Bonferroni correction.

When cultures were treated alone with IL-6 or Hyper-IL-6, the following effects were detected in comparison to untreated controls from the same time point (day 37). After IL-6 treatment, difference in *IL-6R* expression was not detected, but *gp130* expression was increased in 08/023 derived cultures ($p<0.01$) (Figure 13 A-B). In 10212.EURCCs line, IL-6 treatment increased *IL-6R* expression ($p<0.01$), and *gp130* expression increased slightly ($p>0.05$). (Figure 13 C-D). Hyper-IL-6 treatment caused elevated *IL-6R* and *gp130* levels ($p\leq0.0001$ for both) in 08/023 line (Figure 13 A-B.). Moreover, *IL-6R* ($p<0.01$) and *gp130* levels were also upregulated in Hyper-IL-6 treated 10212.EURCCs cultures, but the change in *gp130* expression levels was not statistically significant ($p>0.05$) (Figure 13 C-D).

In KA treated cultures, major changes in gene expression levels in comparison to untreated controls from the same time point (day 37) were not observed. However, the increase of *gp130* expression was statistically significant ($p<0.01$) in KA treated 10212.EURCCs cultures in comparison to controls (Figure 13 D). Additionally, cytokine treatments with KA induction modulated gene expression levels of *IL-6R* and *gp130* compared to controls. *IL-6R* expression was increased

($p<0.01$) and *gp130* levels were unchanged in IL-6+KA treated 08/023 cultures (Figure 13 A-B). In 10212.EURCCs cultures, *IL-6R* and *gp130* levels were slightly increased after IL-6+KA treatments but differences were not statistically significant (Figure 13 C-D). Although, Hyper-IL-6+KA treatment elevated both *IL-6R* and *gp130* levels in 08/023 ($p\leq0.0001$ for both) and 10212.EURCCs cultures (*IL-6R*: $p<0.01$, *gp130*: $p\leq0.0001$). When compared differences between of IL-6 and IL-6+KA treatments and similarly Hyper-IL-6 and Hyper-IL-6 treatments, small difference in expression levels could be seen. However, statistically significant differences in the gene expression levels between these groups were not detect in either cell lines.

Additionally, protein expression of IL-6 receptors with neuronal and astrocytic markers on hiPSC (10212.EURCCs)-derived cortical neural cultures were studied with ICC after treatments at five-week time point (day 37) (Figure 14). Both IL-6R and gp130 positive neurons were detected in all treatment groups. In general, IL-6R protein expression seemed to be higher in each group compared to gp130 protein expression. Major changes in IL-6R or gp130 expression between treatment groups were not detected. However, it seemed that Hyper-IL-6 and Hyper-IL-6+KA treatments could upregulate IL-6R expression, which is also in line with the gene expression data.

In conclusion, results indicate that IL-6, Hyper-IL-6 and KA treatments, especially H-IL-6, can modulate the gene expression levels of IL-6 receptors in both hESC-and hiPSC-derived cortical neural cultures. At protein level both IL-6 receptors were detected after all treatments. Even though there seems to be no great differences between groups, some treated cultures exhibited slightly different expression profiles.

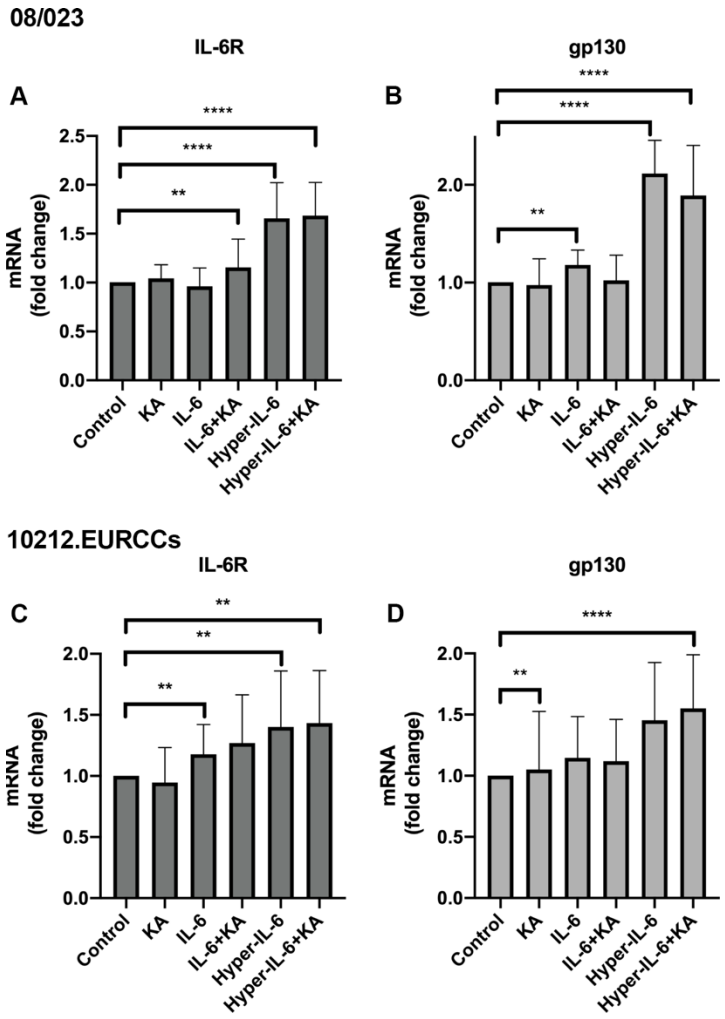

Figure 13. The gene expression levels of IL-6 receptors, *IL-6R* and *gp130*, after IL-6, Hyper-IL-6 and KA treatments at five-week time point (day 37). A-B) Fold change of *IL-6R* and *gp130* mRNA on hESC (08/023)-derived cortical neural cultures compared to control group. The data is from one experiment and it is presented as the mean ± SD (n=3 with three technical replicates in each group). C-D) Fold change of *IL-6R* and *gp130* mRNA on hiPSC (10212.EURCCs)-derived cortical neuronal cultures compared to control group. The data is combined from two experiment and it is presented as the mean ± SD (n=5 with three technical replicates in each group). Mann-Whitney U test with Bonferroni correction was used to determine statistical significance between different groups compared to control group (* $p<0.05$, ** $p<0.01$, *** $p<0.001$ and **** $p\leq0.0001$).

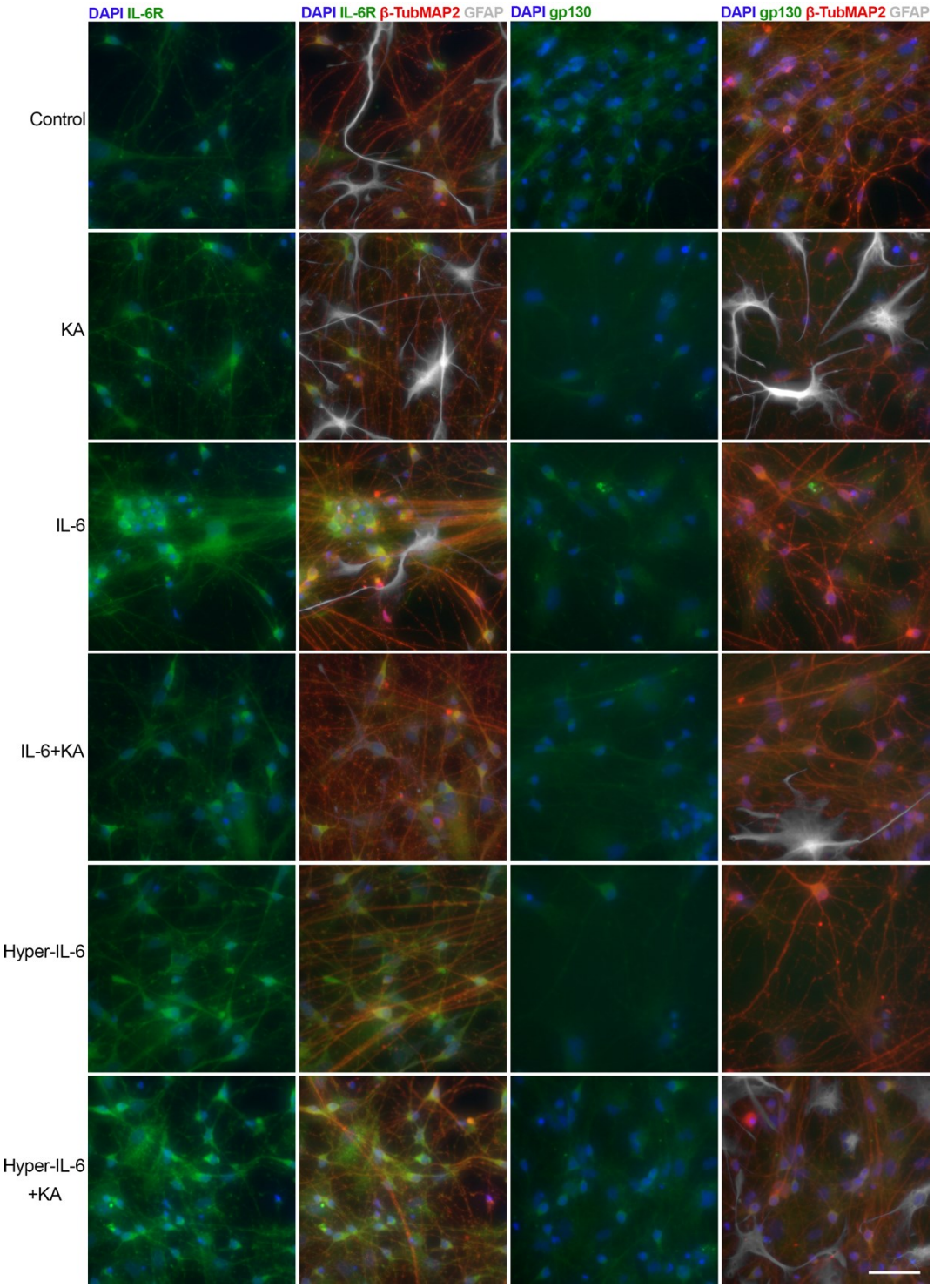

Figure 14. ICC staining of IL-6 receptors, IL-6R and gp130, on hiPSC-derived cortical neuronal cultures after IL-6, Hyper-IL-6 and KA treatments at five-week time point (day 37). Cultures are stained also with neuronal (MAP-2 and β-Tub) and astrocytic (GFAP) markers. DAPI stained nuclei blue. The scale bar is 50 μm in all images.

5.5 Effects of IL-6, Hyper-IL-6 and KA treatments on the cell viability of hPSC-derived neural cultures

Effects of IL-6, Hyper-IL-6 and KA treatments on the neuronal networks were studied with ICC by staining neuronal (MAP-2 and β-Tub) and astrocytic (GFAP) markers after treatments at five-week time point (day 37) (Figure 15). ICC staining shown that both neuronal markers and astrocytic markers, on some culture areas, are expressed in all the cultures and differences in the neuronal networks between control and treatment groups could not be seen.

Moreover, effects of treatments on the cell viability of hPSC-derived cortical neural cultures were analysed with a LIVE/DEAD viability/cytotoxicity assay. Cell viability assay was performed once for hESC (08/023)-derived neurons after seven-week culture (day 51) and twice for hiPSC (10212.EURCCs)-derived neurons after five-week culture (day 37) after IL-6, Hyper-IL-6 and KA treatments. Visible differences between the controls and treated cultures were not detected during the LIVE/DEAD imaging. Representative LIVE/DEAD assay images are presented in Figure 16 A. Most of the cells were viable (stained green) but also dead cells (stained red) were detected in all the cultures in each experiment. Cell viability was quantified by calculating the percentage area coverage of live or dead cells from the total culture area (Figure 16 B-C). In both cell lines, the area coverage of the live cells was higher compared to the dead cells, and the area coverage of the dead cells was very low in controls and all treated cultures. Statistical significance for live and dead cells was calculated with Mann-Whitney U-test, but no significant ($p<0.05$) differences between control and treated groups were detected. Taken together, major differences in the cell viability or neuronal networks were not detected after IL-6, Hyper-IL-6 and KA treatments.

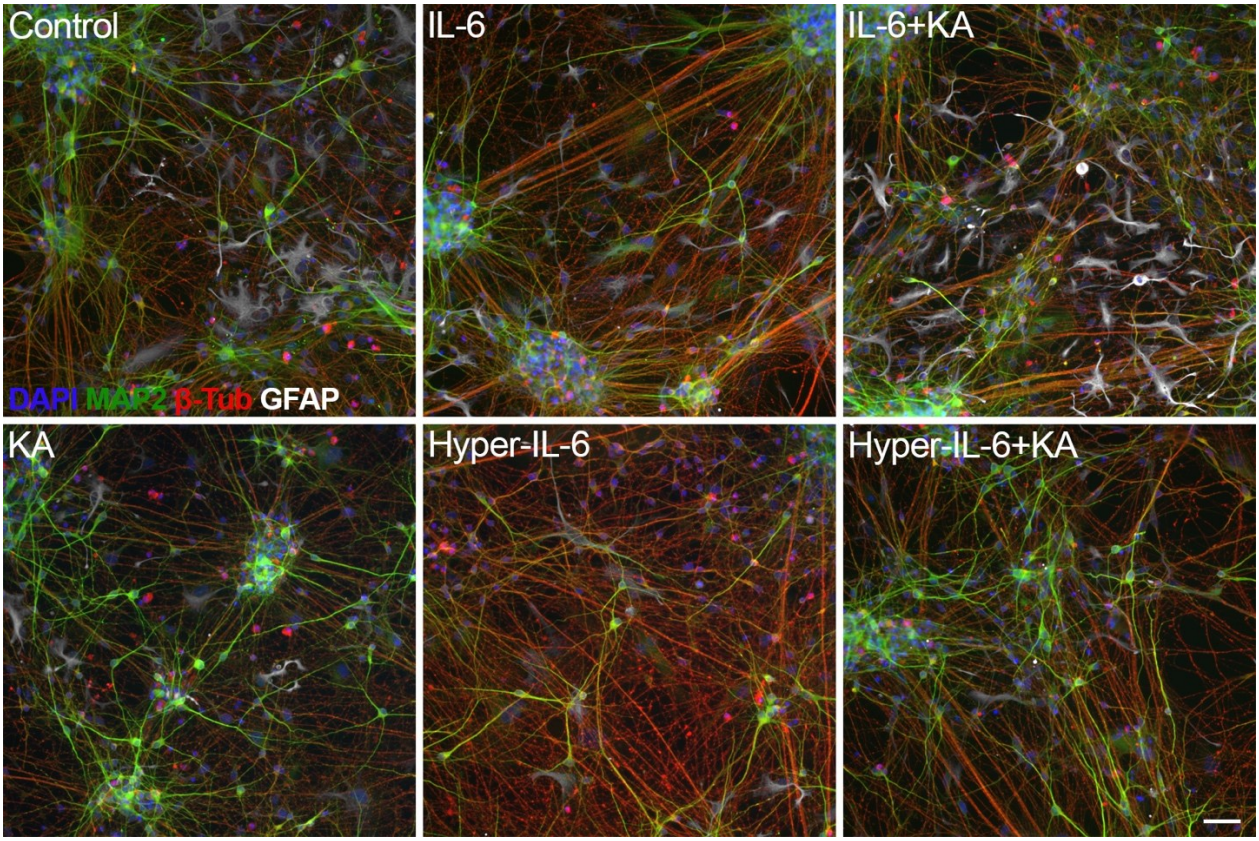

Figure 15. ICC staining of neuronal and astrocytic markers on hiPSC-derived cortical neuronal cultures after IL-6, Hyper-IL-6 and KA treatments at five-week time point (day 37). Neuronal markers MAP-2 and β-Tub and astrocytic marker GFAP were expressed in all treatment groups. DAPI stained nuclei blue. The scale bar is 50 μm in all images.

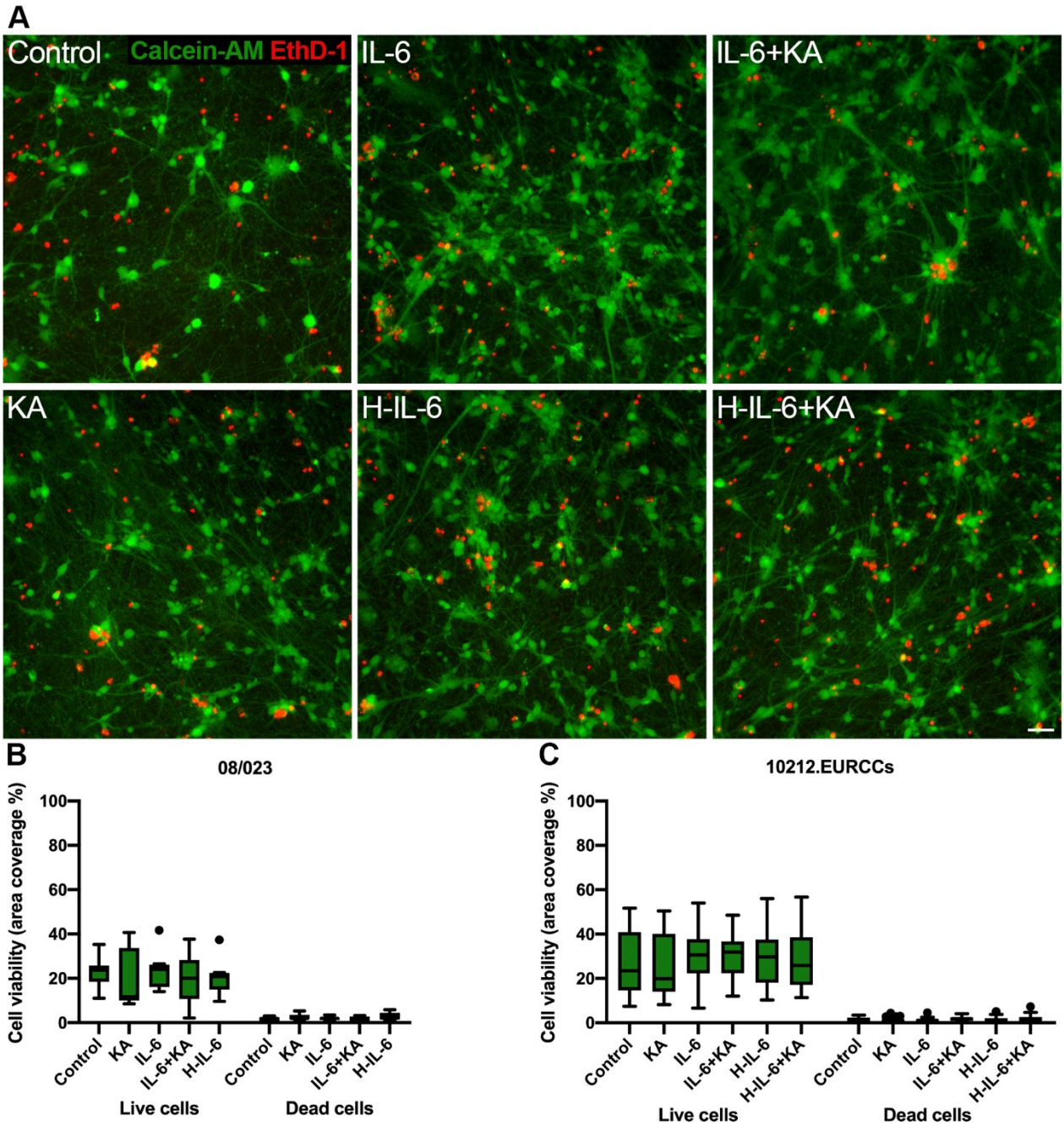

Figure 16. LIVE/DEAD analysis of hPSC-derived cortical neuronal cultures after IL-6, Hyper-IL-6 and KA treatments. A) Representative LIVE/DEAD assay images of hiPSC- derived neurons at five-week time point (day 37). The scale bar is 50 µm in all images. B) Quantification of the cell viability of the hESC (08/023)-derived neurons at the seven-week time point (day 49). The data presented as Tukey boxplots represent live/dead cell area coverage from the total culture area. Two individual points are outliers which have values higher than 75th percentile plus 1.5IQR. The data is from one experiment (n=8-12 images in each group). C) Quantification of the cell viability of the hiPSC (10212.EURCCs)-derived neurons at the five-week time point (day 37). The data is from two experiment (n=26-30 images in each group) and it is presented similarly as B.

5.6 Effects of IL-6, Hyper-IL-6 and KA treatments on the functionality of hiPSC-derived neural cultures

After the five-week culture, functionally maturated neuronal networks were treated with IL-6 or Hyper-IL-6 for 24 hours (pre-treatments at day 35), and on the next day some of the cultures were treated with KA for additional 24 hours (KA induction) to induce seizure-like functionality. The activity of neuronal networks was studied with MEA measurements just before treatments (baseline), immediately (acute), and 3, 6 and 24 hours after treatments (Figure 7). Effects of IL-6 or Hyper-IL-6 pre-treatments on spike and burst rates are presented in Figure 17 A-B. Both normalized spike rate and bursts per minute values are presented as median percentage changes by comparing measured values to the baseline measurements. Statistical analyses for all spike and burst rates were performed using the one-way ANOVA with Bonferroni post hoc test. In pre-treatments, spike and burst rates followed the same trend in IL-6 and Hyper-IL-6 treated cultures as well as in control cultures from baseline to the 24-hour time point (Figure 17 A-B). However, the spike rate of IL-6 treated cultures was higher in comparison to control and Hyper-IL-6 treated cultures at 24-hour time point, but the difference was not statistically significant ($p>0.05$). Moreover, after pre-treatments the burst rate was slightly decreased in Hyper-IL-6 treated cultures in comparison to controls ($p>0.05$) and IL-6 treated ($p<0.05$) cultures at 24-hour time point (Figure 17 B).

Effects of KA treatment on the spike and burst rates during 24 hours are presented in Figures 17 C-D. Moreover, figures show the spike and burst rates of control, IL-6 and Hyper-IL-6 treated cultures during this same 24-hour period. In general, cultures treated only with IL-6 or Hyper-IL-6 followed similar trend with controls, and cultures treated with cytokines and KA followed similar trend with KA only treated cultures.

Spike rate of IL-6, Hyper-IL-6 and control cultures was slightly increased at acute time point, although these cultures were not treated with KA (Figure 17 C). Difference between IL-6 and control cultures at acute time point was statistically significant ($p<0.05$). At other time points, differences between IL-6 and Hyper-IL-6 treated cultures in comparison to controls or each other were not detected. However, in each time points KA treatment caused statistically significant ($p<0.001$) reduction on the spike rates of IL-6+KA, Hyper-IL-6+KA and KA only treated cultures

in comparison on controls. Differences on spike rates were not detected between IL-6+KA and Hyper-IL-6+KA cultures in comparison to KA only treated cultures. Moreover, statistically significant differences on spike rates between IL-6+KA and Hyper-IL-6+KA treated cultures were not detected ($p>0.05$).

Burst rates did not change statistically significantly ($p>0.05$) between treatment groups during KA induction (Figure 17 D). However, it seems that at first KA induction increased the burst rate, especially in cultures which were treated only with KA, and during the time burst rate decreased. After 24-hour KA exposure (endpoint), the burst rate was lower in KA only treated cultures in comparison IL-6+KA and Hyper-IL-6+KA treated cultures (Figure 17 D). Moreover, during the MEA measurements KA addition seemed to disorganize synchronous network bursts back to spike trains. Taken together, the activity of hiPSC-derived cortical neuronal networks developed and increased during the five-week culture on MEAs. The spike and burst rates of IL-6 or Hyper-IL-6 only treated cultures resembled control cultures, and cytokine and KA treated cultures followed similar trend with KA only cultures.

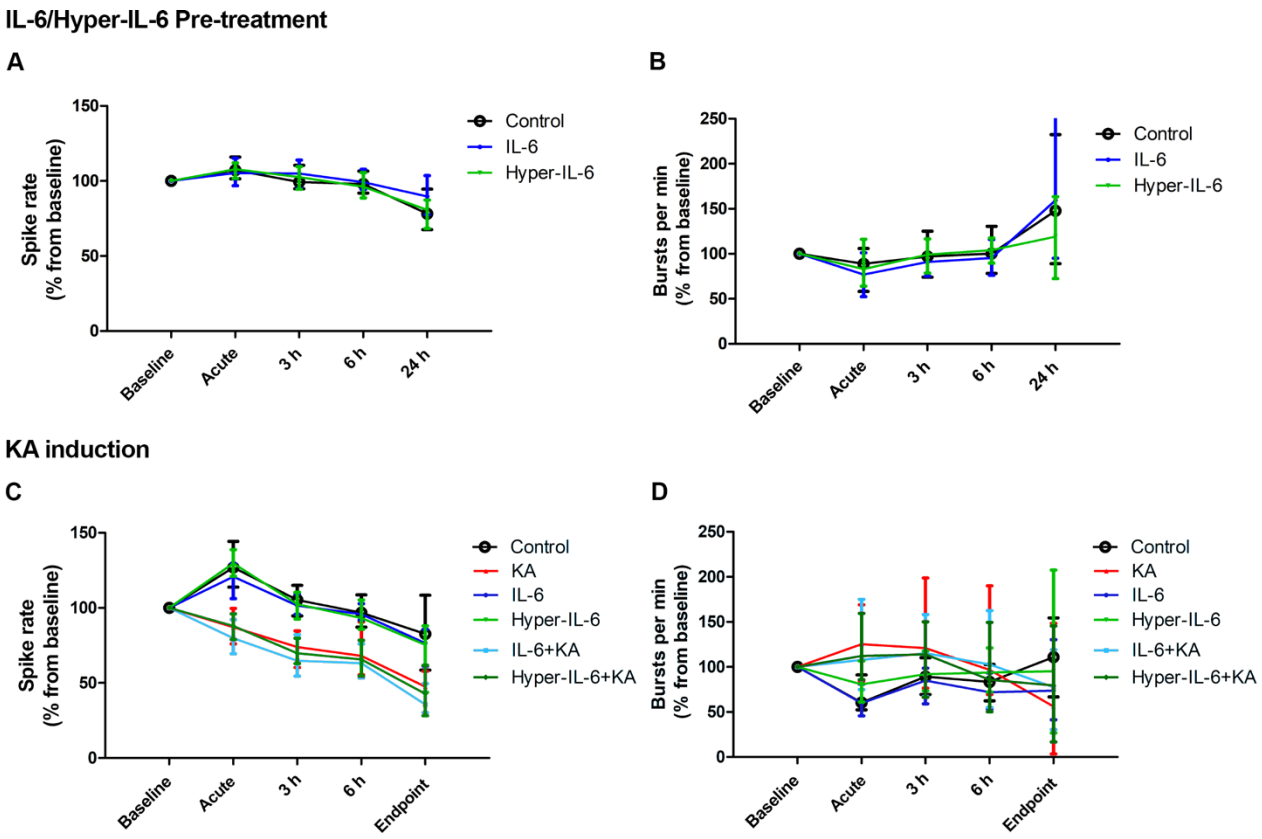

Figure 17. Effects of IL-6, Hyper-IL-6 and KA treatments on functionality of hiPSC-derived cortical neural cultures at five-week time point (days 35-37). A) Spike rate change in percentages compared to baseline after IL-6 or Hyper-IL-6 pre-treatments. Treatments were added just before "acute" MEA measurement. B) Number of bursts per minute change in percentages compared to baseline after IL-6 or Hyper-IL-6 pre-treatments. Treatments were added just before "acute" measurement. C) Spike rate change in percentages compared to baseline measurement after KA induction. KA was added to cultures just before "acute" measurement, but not to IL-6 and Hyper-IL-6 only cultures. D) Number of bursts per minute change in percentages compared to baseline after KA induction. KA was added to the cultures just before "acute" measurement. IL-6 and Hyper-IL-6 only cultures are also measured but they were not treated with KA. In all graphs, the data is presented as the median and range, and it is combined from two separate experiments (n=32 wells in each treatment group).

Additionally, the expression of synaptic proteins on hiPSC-derived cortical neural cultures was investigated since synapses are crucial for neuronal functionality. After IL-6, Hyper-IL-6 and KA treatments, cultures were stained with presynaptic synaptophysin (Syn), postsynaptic density protein 95 (PSD-95) and neuronal marker β-Tub (Figure 18). Expression of both synaptic proteins and their co-localization was detected in control and treated cultures. Moreover, it seemed that there was more synaptic staining in the IL-6 treated cultures.

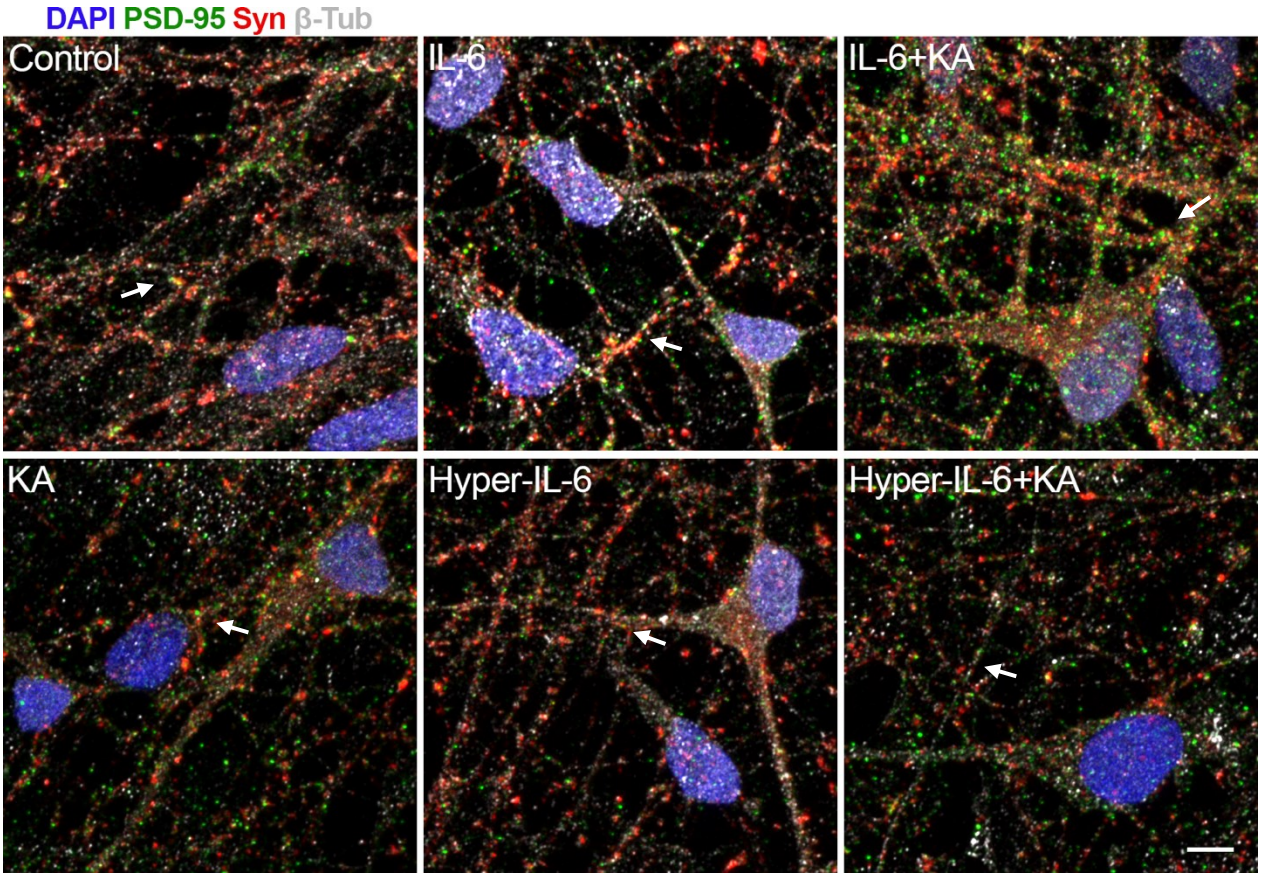

Figure 18. Confocal microscope images of synaptic markers on hiPSC-derived cortical neurons after five-week culture (day 37). Presynaptic synaptophysin (Syn) and postsynaptic density protein 95 (PSD-95) proteins were expressed in all the treatment groups. Arrows indicate co-localization of synaptic proteins. DAPI stained nuclei blue. The scale bar is 10 μm in all images.

6 Discussion

The aim of this work was to study the effects of exogenous IL-6 and Hyper-IL-6 on the characteristics and functionality of hPSC-derived cortical neural cultures after five-week culture. Additionally, part of the cultures was exposed to neuroexcitatory KA after cytokine treatments to induce seizure-like activity. First, the gene and protein expression levels of IL-6 receptors were determined during culturing and after IL-6, Hyper-IL-6 and KA treatments. Moreover, ICC staining of IL-6 receptors was optimized. Secondly, the effects of treatments on the cell viability were investigated. Thirdly, development of neuronal network activity was followed for five weeks with MEA measurements. Thereafter, the effects of treatments on the activity of functionally maturated neuronal networks were investigated.

6.1 Expression of IL-6 receptors on hPSC-derived neural cultures

Multifunctional IL-6 cytokine can mediate its effects via IL-6R and gp130 receptors (Kaur et al. 2020). IL-6 can bind to membrane-bound IL-6R or sIL-6R, and this complex can activate transmembrane signaling receptor gp130 (Kaur et al. 2020). Expression of IL-6 receptors on hPSC-derived neurons is not extensively studied (Como et al. 2018, Hagman et al. 2019, Sulistio et al. 2018). Here, the expression of IL-6R and gp130 on hESC- and hiPSC-derived neural cultures was investigated during maturation phase, before cytokine and KA treatments, at gene and protein expression levels. Moreover, antibody optimization for ICC staining of IL-6 receptors was performed, since the receptors were stained for the first time on these human neural cultures. All results from both cell lines followed a similar trend. In general, hESC- and hiPSC-derived neurons had similar morphology and expression of neuronal and astrocytic markers were quite similar during the culture.

6.1.1 Methodological considerations

ICC stainings for antibodies against IL-6R and gp130 on hESC- and hiPSC-derived neural cultures were optimized, and suitable staining conditions and antibody concentrations were determined. Cell line differences between the staining patterns of receptors were not detected. Staining patterns of both used anti-IL-6R antibodies were quite similar, and stainings were clear and bright, whist gp130 stainings were weaker and had more non-specific background in comparison to both IL-6R

stainings. Testing of another antibody against gp130 would be beneficial to achieve less blurry and dim ICC staining.

Moreover, the specificity of primary antibodies against IL-6 receptors was studied with peptide blocking test. Tests did not show dramatic decrease in IL-6R or gp130 signal even with the highest blocking peptide concentrations. However, it seemed that the expression of both receptors was slightly reduced with the highest blocking peptide concentrations. Although, the use of peptide blocking test and its reliability has been criticized, and other primary antibody controls is recommended to use with this method (Burry 2000, Burry 2011). Other methods to verify the specificity of primary antibody are genetic approaches, such as KO or transfected cells, Western blot (WB) analysis or co-localization staining with an additional label which shows that antibodies bind to the same location (Burry 2011). In fact, we noticed that both tested anti-IL-6R antibodies had quite similar staining patterns but co-staining was not performed. Moreover, the evaluation of IL-6 receptor stainings was challenging because availability of comparative ICC data from studies with hPSC-derived neurons (Como et al. 2018, Sulistio et al. 2018) was limited, as discussed in the next chapters.

6.1.2 IL-6 receptors are expressed on hPSC-derived neural cultures

This study indicated that both hESC- and hiPSC-derived cortical neural cultures expressed *IL-6R* and *gp130* at gene level during five-week culture at days 0, 7 and 37 (results only from hiPSC-derived cultures are presented in Figure 10). Gene expression levels of both receptors increased during the neuronal maturation. Moreover, *gp130* expression was higher in comparison to the *IL-6R* expression in each studied time point. Gene expression results were in line with the literature. Similarly, higher gene expression level of *gp130* compared to *IL-6R* was also reported on hESC-derived NPCs cultures (Hagman et al. 2019). Additionally, a study with mouse cortical neurons showed that cultures expressed both receptors, and the gene expression of *gp130* was slightly higher than the gene expression of *IL-6R* (Ali et al. 2000). They also showed that in mouse astrocyte cultures both IL-6 receptors were expressed at gene and protein level. In our hPSC-derived cortical neural cultures, astrocytes were also detected at some culture areas but neurons were still the major cell type as shown earlier (Hyvärinen et al. 2019b). Presence of astrocytes may still affect gene expression results.

However, according to staining of IL-6 receptors, IL-6 receptors were mainly expressed on neurons in hPSC-derived neural cultures and cell line differences on the staining patterns were not detected. Protein expression of IL-6 receptors was mainly detected on soma part of neurons but also on neuronal processes. Especially, the area near the nucleus was highly positive for IL-6R. Moreover, protein expression of IL-6R was higher in comparison to gp130 expression. Protein expression results were not in line with gene expression results, which showed that the gene expression levels of *gp130* are higher in comparison to the gene expression levels of *IL-6R*. However, it is known that direct comparison of gene and protein expression levels may not be beneficial, although gene and protein levels correlate, the correlation is often not strong (Liu et al. 2016, Vogel & Marcotte 2012). In general, transcriptional, post-transcriptional and translational regulation as well as protein degradation can affect these levels (Liu et al. 2016, Vogel & Marcotte 2012).

In many reviews, it is stated that gp130 is expressed on almost all cell types but the expression of membrane-bound IL-6R is more limited (Kaur et al. 2020, Luo & Zheng 2016, Rothaug et al. 2016). Therefore, it was a quite surprising result that the protein expression of IL-6R was higher than the protein expression of gp130. Although, expression of both receptors on neurons, mainly on rodent studies, are described in the literature (Erta et al. 2012, Gruol 2015). However, few studies have shown protein expression of IL-6 receptors on hPSC-derived neurons with ICC (Como et al. 2018, Sulistio et al. 2018) A study with hiPSC-derived NSCs showed that IL-6R and gp130 are expressed on hiPSC-derived NSCs. Moreover, they used the same anti-gp130 antibody but anti-IL-6R antibody was different than we used (Sulistio et al. 2018). However, staining pattern of IL-6 receptors is difficult to compare to our results since their cells were less mature than neurons that we used. Additionally, protein expression of IL-6R on hiPSC-derived neurons has been shown in a staining with neuronal marker β-Tub, but expression of gp130 was not studied (Como et al. 2018). In this study, protein expression of IL-6R seems quite similar with our results since IL-6R was highly expressed near the nucleus but also neurites were slightly stained.

Although, in rodent studies protein expression of IL-6 receptors has been studied more than human neurons. Ali et al. (2000) showed that mouse cortical neurons and astrocytes express both receptors at protein level. Both receptors were strongly expressed on the soma part of neurons but neurites

were also stained (Ali et al. 2000). Additionally, Nelson et al. (2002) presented that rat Purkinje and granule neurons express both receptors on the soma and dendrites. Contrary to our results, they showed that protein expression of IL-6R is lower than the protein expression of gp130. However, they reported also that the protein expression of IL-6 receptors is low on astrocytes. (Nelson et al. 2002) Moreover, another rodent study also showed similar staining pattern for IL-6 receptors on hippocampal neurons: both receptors were expressed mainly on the soma but also slightly on neurites (Vereyken et al. 2007). Controversial results are also presented in mouse NSC cultures with WB in a study which reported that only gp130 was expressed at low levels and IL-6R was not detectable (Islam et al. 2008).

In conclusion, this study indicated that both IL-6 receptors are expressed on hPSC-derived cortical neural cultures, mainly on neurons. The gene expression of *gp130* was higher in comparison to *IL-6R*, which was in line with the literature. Although, the protein expression of gp130 seemed to be quite weak. Protein expression of IL-6 receptors is essential for IL-6 signaling, thus this needs to be studied further with these cells. It seems that the expression of IL-6 receptors on hPSC-derived neurons is not well described in the literature. However, few studies which have investigated expression of IL-6 receptors on hPSC-derived neurons (Como et al. 2018, Hagman et al. 2019, Sulistio et al. 2018) are in line with our results. Although, more knowledge about the expression of IL-6 receptors on human neurons is needed, and it is essential to determine expression levels of receptors, when the effects of IL-6 are investigated with hPSC-derived neurons.

6.2 Development of spontaneous neuronal network activity of hPSC-derived neural cultures

Functionality of hiPSC-derived neural cultures was followed for five-weeks with multiwell-MEAs which enable repeatable HTP measurements of the activity of neuronal networks. Additionally, the cell morphology and the protein expression of neuronal and astrocytic markers were followed with light microscope and ICC on the cultures from normal culture plates. During neuronal maturation, the length of neurites increased, neurons formed neuronal networks and all cultures expressed neuronal markers. Moreover, after five-week culture neuronal networks expressed synaptic markers and astrocytes were observed at some culture areas as described earlier (Hyvärinen et al. 2019b). MEA results indicated that the spontaneous neuronal network activity developed and

enhanced during the neuronal network maturation, which is in line with the recent work describing the functional development of similarly differentiated human neural cultures (Hyvärinen et al. 2019b). Change in the activity patterns was visually observed during the MEA measurements, when spontaneous spiking developed to spike trains, bursts and synchronous network bursts, similarly as described previously with hPSC-derived neurons on MEAs (Heikkilä et al. 2010, Hyvärinen et al. 2019b, Paavilainen et al. 2018). Major changes in the number of active electrodes per MEA well were not detected, but in the first experiment (Exp1) slight increase was observed. After five-week culture, at least half of the electrodes were active in each plate. Hyvärinen et al. (2019b) reported similar, or slightly higher, percentages of active electrodes for hPSC-derived cortical networks after five-week culture. The spike rate per MEA well followed similar increased trend in each plate but small decreases were also observed. In both experiments the spike rate increased from ~2 Hz to ~5-7 Hz during the five-week maturation. The trend in detected spike rates during the five-week culture is quite similar with hPSC-derived cortical networks presented by Hyvärinen et al. (2019b), but they reported slightly lower spike rate values. Additionally, Odawara et al. 2016 reported that the spike rate increased in hiPSC-derived cortical neurons on MEAs during culturing. However, they reported that the spike rate was ~1 Hz after five-week culture and it reached ~5-7 Hz after 17-23 weeks (Odawara et al. 2016). According to these parameters, it seems that the activity of our neuronal networks was higher after five-week culture.

During experiments, some variation in the activity of neuronal networks was observed between two experiments but also within MEA plates. However, the cell line and the differentiation batch were the same but cells were thawed and plated at different times. Although each experiment was performed similarly, e.g. thawing, coating, plating, MEA plate, medium changes and imaging can affect the activity of neuronal networks. Moreover, the number of astrocytes and the ratio of excitatory and inhibitory neurons in each culture can affect the activity of neuronal networks (Tukker et al. 2020). For example, it is reported that astrocytes can enhance spiking activity, and cultures containing high numbers of excitatory glutamatergic neurons can cause more synchronous bursting in comparison to cultures with low number of these neurons (Tukker et al. 2020). In conclusion, the functionality of hiPSC-derived cortical neuronal cultures maturated during five-week culture. Development of the activity was essential, since the effects of IL-6, Hyper-IL-6 and KA on the functionally mature neuronal networks were investigated in the following experiments.

6.3 Expression of IL-6 receptors on hPSC-derived neural cultures after IL-6, Hyper-IL-6 & KA treatments

The effects of IL-6, Hyper-IL-6 and KA treatments on the gene and protein expression levels of IL-6 receptors IL-6R and gp130 on functionally maturated hPSC-derived neural cultures were investigated with RT-qPCR and ICC, respectively. Comparative studies which have treated hPSC-derived neurons with these cytokines and then determined gene expression levels of IL-6 receptors were not found. Gene expression analysis indicated that treatments, particularly Hyper-IL-6, increased the gene expression levels of IL-6 receptors in both hESC- and hiPSC-derived neural cultures. As mentioned, staining of IL-6 receptors indicated that IL-6 receptors are mainly expressed on neurons, thus it seems that hPSC-derived cortical neurons can respond to IL-6 via classic- and trans-signaling. KA treatment, alone or combined with cytokines, did not cause dramatic effects to the expression of IL-6 receptors and in general, results had similar trend with cultures which were treated only with cytokines. However, IL-6+KA treatment slightly increased the gene expression levels of *IL-6R* on both cell lines in comparison to controls but also IL-6 only treated cultures. Lehtimäki et al. (2003) showed also that the gene expression levels of IL-6 and its receptors were elevated after KA-induced seizures in the rat brain. However, comparison of *in vivo* and *in vitro* results is not straightforward since *in vivo* models are much complicated. Although, they showed that expression of *IL-6* and *IL-6R* was highest after 12 and 6 hours after seizures, respectively. Based on these results, it would be also noteworthy to determine the expression levels of IL-6 and IL-6 receptors sooner than 24 hours after KA induction. To add this, it would be good to have e.g. 24-hour time point after cytokine additions since here we measured levels of IL-6 receptors only 48 hours after IL-6 and Hyper-IL-6 treatments. Ali et al. (2000) investigated gene expression levels of IL-6 and its receptors 0.5, 1 hour and 3 hours after glutamatergic NMDA or AMPA treatments in mouse cortical neurons. However, they did not detect change in gene expression levels of *IL-6R* or *gp130*, but *IL-6* upregulation was detected after NMDA treatment.

Both IL-6 receptors were also expressed at protein level after treatments, but major changes between treatment groups were not observed with ICC. ICC is not a quantitative method, but it seems that Hyper-IL-6 and Hyper-IL-6+KA may upregulate the protein expression of IL-6R. Although, more replicates and results from repeated experiments would be needed to study this

more. It would be also interesting to quantify the fluorescent signal from IL-6 receptor stainings, but it requires more replicates and images per well. Moreover, it would be beneficial to investigate the protein expression levels of IL-6 receptors after treatments using WB analysis. For example, Islam et al. (2009) demonstrated with mouse NSC cultures using WB analysis that Hyper-IL-6 treatment increase protein expression of gp130, but not IL-6R which was undetected also in control conditions and after cytokine treatment. Additionally, they showed that neurons responded more effectively to Hyper-IL-6 than IL-6 treatments (Islam et al. 2009) which is logical if NSC did not express IL-6R.

Taken together, this study indicated that IL-6, Hyper-IL-6 and KA treatments can modulate the gene expression levels of IL-6 receptors on functionally maturated hPSC-derived cortical neural cultures. However, more research is needed since findings from gene or protein expression changes in IL-6 receptors in human neural cultures after IL-6 or Hyper-IL-6 treatments have not been found.

6.4 Effects of IL-6, Hyper-IL-6 & KA treatments on the cell viability of hPSC-derived neural cultures

Cell viability was investigated after cytokine and KA treatments with ICC and LIVE/DEAD assay, which indicated that the treatments did not cause major differences in the viability of hPSC-derived neuronal networks in comparison to controls. According to ICC staining, treated neuronal networks showed similar staining pattern in comparison to controls. However, differences in neuronal networks or astrocytes between the treatment groups might be possible. For example, Islam et al. (2009) reported that IL-6 and especially Hyper-IL-6 treatments increased protein expression levels of β-Tub and GFAP on mouse NSCs. Additionally, increased astrocytic expression has been observed in hiPSC-derived neural aggregates after IL-6 treatment, indicating that IL-6 has a role in astrogliosis (Zuiki et al. 2017). For future studies, it would be interesting to further investigate the effects of treatments to gene or protein expression levels of neuronal and astrocytic markers.

Similarly with the results of ICC, fluorescence-based LIVE/DEAD assay showed that IL-6, Hyper-IL-6 and KA treatments were not cytotoxic for the cells. In our experiments, we used 100 ng/ml IL-6 or Hyper-IL-6, and 5 μM KA. It is known that high KA doses can cause neuronal death (Zheng et al. 2011), thus it was essential to study that the used KA dose did not cause excessive cell death

because its purpose was to induce seizure-like activity. However, after treatments most of the cells were viable but also dead cells were observed at low levels in all groups. Significant differences between control and treated groups were not detected in live nor dead cells. In line with our cell viability results, Hagman et al. (2019) showed with the same LIVE/DEAD assay that IL-6 did not affect the viability of hESC-derived NPCs. Additionally, Islam et al. (2009) showed also that IL-6 or Hyper-IL-6 treatments did not cause apoptosis in mouse NSCs, which was detected measuring protein expression of apoptotic markers (caspase-3 and cleaved caspase-3) with WB. Similar effects were observed after IL-6 treatment in hiPSC-derived neural aggregates, when protein expression of cleaved caspase-3 was investigated with WB (Zuiki et al. 2017).

Moreover, Hagman et al. (2019) reported that secretion of inflammatory factors VEGF and IL-10 was detected after IL-6 treatment on hESC-derived NPCs cultures. It is known that VEGF has neuroprotective effects and IL-10 can regulate both pro- and anti-inflammatory functions (Hagman et al. 2019). Additionally, anti-convulsive effects have been suggested for IL-10 but its role in epilepsy is not clear (Li et al. 2011). In further studies, it could be beneficial to investigate if IL-6, Hyper-IL-6 and KA induce secretion of pro- or anti-inflammatory factors, or neuroprotective or neurotoxic factors.

Currently, it seems that effects of IL-6 or Hyper-IL-6 exposure on the cell viability of functionally maturated hPSC-derived neurons is less studied. Most of the studies have used rodents or rodent neurons, and both neuroprotective (Ali et al. 2000, Hakkoum et al. 2007, Leibinger et al. 2016, Leibinger et al. 2019, Liu et al. 2011, Ma et al. 2015, Xia et al. 2015) and neurotoxic (Conroy et al. 2004, Kalueff et al. 2004, Samland et al. 2003) effects have been reported. Here, results indicated that IL-6, Hyper-IL-6 and KA treatments were not cytotoxic with used concentrations and exposure times. However, more detailed research is needed if the neuroprotective or neurotoxic effects of IL-6 or Hyper-IL-6 on human neurons are to be determined and clarified.

6.5 Effects of IL-6, Hyper-IL-6 & KA treatments on the functionality of hPSC-derived neural cultures

When functionally mature neuronal network activity was achieved after five-week culture, cultures were pre-treated with IL-6 or Hyper-IL-6 and seizure-like activity was induced with KA, which is

a commonly used chemoconvulsant agent (De Sarro et al. 2004, Lehtimäki et al. 2003, Penkowa et al. 2001, Samland et al. 2003, Zheng et al. 2011). The aim was to investigate the effects of cytokine treatment alone and in combination with KA on the activity of human neural cultures using MEA measurements. Previously, the effects of exogenous IL-6 (100 ng/ml for 3, 24 or 48 hours) exposure on the functionality of rodent sensory neurons on MEAs have been reported (Black et al. 2018), but it seems that the effects of IL-6 on the activity of hPSC-derived neurons are less studied. For example, studies where the effects of IL-6 or Hyper-IL-6 on the functionality of hPSC-derived neurons were investigated with MEAs were not found. Neither studies related to epilepsy, where hPSC-derived neurons were treated with these cytokines and seizure-like functionality was induced e.g. with chemoconvulsant agent KA were not found.

In general, MEA results indicated that the spike and burst rates of IL-6 or Hyper-IL-6 treated cultures followed similar trend with controls, whereas cultures treated with cytokines and KA followed similar trend with cultures treated only with KA. Results indicated that IL-6 or Hyper-IL-6 treatments did not cause dramatic change in the spike or burst rates acutely or during 48 hours. However, minor changes were detected such as that Hyper-IL-6 treatment slightly decreased the burst rate compared to IL-6 treatment or controls at 24-hour time point, and both cytokine treatments caused little decrease in the burst rates after 48 hours. Moreover, the spike rate of IL-6 treated cultures was also slightly increased after 24 hours. Interestingly, Black et al. (2018) reported also that IL-6 treatment (100 ng/ml for 3, 24 and 48 hours) increased spiking activity in mouse sensory neurons on MEAs.

Here, results showed that KA induction alone and combined with cytokines disrupted the activity of neuronal networks. After KA induction, the spike rate decreased statistically significantly during 24 hours and it disorganized the bursts similarly as Hyvärinen et al. (2019b) described recently with KA treated hPSC-derived networks. Although, according to the spike and burst rates it seems that IL-6 or Hyper-IL-6 treatment did not affect much to the activity changes caused by KA since significant changes were not detected between IL-6/Hyper-IL-6+KA and KA only treated cultures. Based on these results, pro- or anti-convulsive properties for IL-6 is not possible to state.

Moreover, results showed that at the same time point when KA was added to some well, change in the spike and burst rate was also observed in the control cultures, although only the same volume of culture medium was added to them. Similarly, Hyvärinen et al. (2019a) showed that the spike and burst rate can change in control cultures when small volume of medium was added and other cultures were treated with different compounds. These results indicate that MEAs are very sensitive and even the control cultures are not fully stable during measurements (Black et al. 2018, Hyvärinen et al. 2019a).

Several *in vivo* rodent studies have reported that IL-6 has effect on seizures (De Sarro et al. 2004, Fukuda et al. 2009, Kalueff et al. 2004, Lehtimäki et al. 2003, Penkowa et al. 2001, Samland et al. 2003). Moreover, many *in vitro* study with rodent neurons have investigated the effects of IL-6 on the neuronal functionality (Black et al. 2018, Ma et al. 2015, Orellana et al. 2005, Xia et al. 2015), as described earlier in this work. However, it seems that there is a lack of functionality studies where the effects of IL-6 on hPSC-derived neuronal networks are investigated. In general, it is challenging to compare our results but also other studies together since each research has different cell sources, experimental designs, treatment concentrations, culture and treatment times, as well as functionality assays and data analysis. Here, results indicated that IL-6 or Hyper-IL-6 treatments do not have major effects to the activity of neurons when two parameters, the spike and burst rates, were analysed from the enormous amount of data from MEA measurements. Still, there are multiple other parameters from MEA data which can be studied to achieve more detailed information about the effects of IL-6 and Hyper-IL-6 on the control networks as well as KA induced networks. Additionally, it might be that the used concentration (100 ng/ml) for IL-6 and Hyper-IL-6 was too low, and a higher concentration can possibly cause clearer effects. The concentration used here is quite common in many rodent studies as reported earlier, for example, Black et al. (2018) used the same concentration for rodent sensory neurons on MEAs (10 000 cells/well), but it may not be enough to high density hiPSC-derived neurons on MEAs (80 000 cells/well).

Taken together, effects of IL-6, Hyper-IL-6 and KA treatments on the activity of functionally maturated hiPSC-derived neural cultures were studied with multiwell-MEAs, which were very useful for these experiments with a long culture time and high sample number. Major changes in

the activity of neuronal networks were not detected after cytokine treatments, but KA exposure alone and together with cytokines disturbed the activity of neuronal networks. However, the effects of IL-6 on the functionality of hPSC-derived neuronal networks is less studied and more knowledge is needed with human neurons.

In addition to MEA measurements, also the expression of synaptic proteins was confirmed in each treatment group since they are essential for the functionality of neuronal networks. Co-localization of pre- and post-synaptic proteins was detected on neurons in each treatment group. Moreover, it seemed that IL-6 and IL-6+KA treatment potentially increased the synaptic staining, but fluorescence signal was not quantified in these experiments. In fact, rodent *in vitro* and *in vivo* studies have reported that IL-6 can regulate synaptic functions such as synaptic transmission and plasticity (Gruol 2015). For example, Wei et al. (2012) reported an increase in excitatory synapses and a decrease in inhibitory synapses in IL-6 over-expressing mice leading to imbalance between excitatory and inhibitory synaptic transmission. Moreover, Vereyken et al. (2007) reported that chronic IL-6 treatment in developing rat hippocampal neuron cultures and IL-6 over-expressing mice can reduce protein expression of Group-II metabotropic receptors (mGluR2/3) and L-type Ca^{2+} channels affecting altered functionality of neurons (Vereyken et al. 2007). For further studies, it would be beneficial to study more the effects of IL-6 or Hyper-IL-6 on the expression of synaptic proteins. Moreover, it would be interesting to study if change in excitatory and inhibitory synapses happen after treatments, since also in epilepsy, imbalance between excitatory and inhibitory neurotransmission cause abnormal brain functionality (Patel et al. 2019).

7 Conclusion

The aim of this master's thesis was to study the effects of IL-6 and Hyper-IL-6 treatments on the characteristics and functionality of hPSC-derived cortical neural cultures. Additionally, the effect of KA as potentiating factor of seizure-like activity was studied after IL-6 or Hyper-IL-6 treatments. Gene and protein expression analysis indicated that hPSC-derived neural cultures express both IL-6 receptors IL-6R and gp130. The gene expression levels of gp130 were higher in comparison to the expression of IL-6R, but protein expression results were controversial. Moreover, results indicated that IL-6, Hyper-IL-6 and KA treatments can modulate the gene expression levels of both receptors. Additionally, the cell viability assay indicated that neural cultures had good cell viability after five-week culture and treatments were not cytotoxic. MEA measurements showed that the spontaneous neuronal network activity developed and enhanced during the neuronal maturation. The effects of IL-6, Hyper-IL-6 and KA treatments on the activity of functionally maturated neuronal networks was investigated with MEAs by studying the spike and burst rates. MEA results showed that KA induction disrupted the activity of neuronal networks. Moreover, MEA results indicated that IL-6 and Hyper-IL-6 treated cultures had relatively similar activity with controls whereas cytokine treatments combined with KA induction caused similar trend in the activity than KA alone. All in all, this study indicated that hPSC-derived neural cultures together with MEA technology are promising tools for *in vitro* epilepsy modelling and HTP pharmacology testing. In the future, more research is needed about the effects of IL-6 on the functionality of healthy and epileptic hiPSC-derived neuronal networks to better understand its role in seizures.

References

Alapirtti, T., Rinta, S., Hulkkonen, J., Mäkinen, R., Keränen, T. & Peltola, J. (2009). Interleukin-6, interleukin-1 receptor antagonist and interleukin-1beta production in patients with focal epilepsy: A video-EEG study. Journal of the Neurological Sciences, 280, 94–97.

Alberts, B., Johnson, A., Lewis, J., Morgan, D., Raff, M., Roberts, K. & Walter, P. (2015). Molecular Biology of the Cell. Garland Science: New York and Abingdon, UK, 6th edition, 621–637.

Ali, C., Nicole, O., Docagne, F., Lesne, S., MacKenzie, E. T., Nouvelot, A., Buisson, A. & Vivien, D. (2000). Ischemia-induced interleukin-6 as a potential endogenous neuroprotective cytokine against NMDA receptor-mediated excitotoxicity in the brain. Journal of Cerebral Blood Flow & Metabolism, 20(6), 956–66.

Avior, Y., Sagi, I. & Benvenisty, N. (2016). Pluripotent stem cells in disease modelling and drug discovery. Nature Reviews Molecular Cell Biology, 17(3), 170–82.

Becher, B., Spath, S. & Goverman, J. (2017). Cytokine networks in neuroinflammation. Nature Reviews Immunology, 17(1), 49–59.

Black, B. J., Atmaramani, R., Kumaraju, R., Plagens, S., Romero-Ortega, M., Dussor, G., Price, T. J., Campbell, Z. T. & Pancrazio, J. J. (2018). Adult mouse sensory neurons on microelectrode arrays exhibit increased spontaneous and stimulus-evoked activity in the presence of interleukin-6. Journal of Neurophysiology, 120(3), 1374–1385.

Budday, S., Steinmann, P. & Kuhl, E. (2015). Physical biology of human brain development. Frontiers in Cellular Neuroscience, 9, 257.

Burry, R. W. (2000). Specificity controls for immunocytochemical methods. The Journal of Histochemistry and Cytochemistry, 48(2), 163–6.

Burry, R. W. (2011). Controls for immunocytochemistry: an update. The Journal of Histochemistry and Cytochemistry, 59(1), 6–12.

Campbell, I. L., Erta, M., Lim, S. L., Frausto, R., May, U., Rose-John, S., Scheller, J. & Hidalgo, J. (2014). Trans-signaling is a dominant mechanism for the pathogenic actions of interleukin-6 in the brain. The Journal of Neuroscience, 34(7), 2503–2513.

Carpenter, A. E., Jones, T. R., Lamprecht, M. R., Clarke, C., Kang, I. H., Friman, O., Guertin, D. A., Chang, J. H., Lindquist, R. A., Moffat, J., Golland, P. & Sabatini, D. M. (2016). CellProfiler: image analysis software for identifying and quantifying cell phenotypes. Genome Biology, 7(10), R100.

Carpenter, M. K., Inokuma, M. S., Denham, J., Mujtaba, T., Chiu, C. P. & Rao, M. S. (2001). Enrichment of neurons and neural precursors from human embryonic stem cells. Experimental Neurology, 172, 383–97.

Chalaris, A., Garbers, C., Rabe, B., Rose-John, S. & Scheller, J. (2011). The soluble Interleukin 6 receptor: generation and role in inflammation and cancer. European Journal of Cell Biology, 90(6–7), 484–494.

Chambers, S. M., Fasano, C. A., Papapetrou, E. P., Tomishima, M., Sadelain, M. & Studer, L. (2009). Highly efficient neural conversion of human ES and iPS cells by dual inhibition of SMAD signaling. Nature Biotechnology, 27(3), 275–280.

Como, C. N., Pearce, C. M., Cohrs, R. J. & Baird, N. L. (2018). Interleukin-6 and type 1 interferons inhibit varicella zoster virus replication in human neurons. Virology, 522, 13–18.

Conroy, S. M., Nguyen, V., Quina, L. A., Blakely-Gonzales, P., Ur, C., Netzeband, J. G., Prieto, A. L. & Gruol, D. L. (2004). Interleukin-6 produces neuronal loss in developing cerebellar granule neuron cultures. Journal of Neuroimmunology, 155(1-2), 43–54.

D'Arcangelo, G., Tancredi, V., Onofri, F., D'Antuono, M., Giovedì, S. & Benfenati, F. (2000). Interleukin-6 inhibits neurotransmitter release and the spread of excitation in the rat cerebral cortex. European Journal of Neuroscience, 12(4), 1241–52.

De Luca, G., Di Giorgio, R. M., Macaione, S., Calpona, P. R., Costantino, S., Di Paola, E. D., De Sarro, A., Ciliberto, G. & De Sarro, G. (2004). Susceptibility to audiogenic seizure and neurotransmitter amino acid levels in different brain areas of IL-6-deficient mice. Pharmacology Biochemistry & Behavior, 78, 75–81.

De Sarro, G., Russo, E., Ferreri, G., Giuseppe, B., Flocco, M. A., Di Paola, E. D. & De Sarro, A. (2004). Seizure susceptibility to various convulsant stimuli of knockout interleukin-6 mice. Pharmacology Biochemistry & Behavior, 77, 761–6.

Devinsky, O., Vezzani, A., O'Brien, T. J., Jette, N., Scheffer, I. E., de Curtis, M & Perucca, P. (2018) Epilepsy. Nature Reviews Disease Primers, 3(4), 18024.

DiSabato, D. J., Quan, N. & Godbout, J. P. (2016). Neuroinflammation: the devil is in the details. Journal of Neurochemistry, 139(Suppl 2), 136–153.

Erta, M., Quintana, A. & Hidalgo, J. (2012). Interleukin-6, a major cytokine in the central nervous system. International Journal of Biological Sciences, 8(9), 1254–66.

Faingold, C. L. & Blumenfeld, H. (2014). Chapter 1 - Introduction to Neuronal Networks of the Brain. Neuronal Networks in Brain Function, CNS Disorders, and Therapeutics, Academic Press, San Diego, CA: Elsevier Science, p. 1–10.

Fischer, M., Goldschmitt, J., Peschel, C., Kallen, K. J., Brakenhoff, J. P. J., Wollmer, A., Grötzinger, J. & Rose-John, S. (1997). A designer cytokine with high activity on human hematopoietic progenitor cells. Nature Biotechnology 15, 142–145.

Fisher, R. S., Acevedo, C., Arzimanoglou, A., Bogacz, A., Cross, J. H., Elger, C. E., Engel, J. Jr., Forsgren, L., French, J. A., Glynn, M., Hesdorffer, D. C., Lee, B. I., Mathern, G. W., Moshé, S. L., Perucca, E., Scheffer, I. E., Tomson, T., Watanabe, M. & Wiebe, S. (2014). ILAE Official Report: A practical clinical definition of epilepsy. Epilepsia, 55, 475–482.

Fisher, R. S., Cross, J. H., French, J. A., Higurashi, N., Hirsch, E., Jansen, F. E., Lagae, L., Moshé, S. L., Peltola, J., Roulet Perez, E., Scheffer, I. E. & Zuberi, S. M. (2017). Operational classification of seizure types by the International League Against Epilepsy: Position Paper of the ILAE Commission for Classification and Terminology. Epilepsia, 58(4), 522–530.

Fukuda, M., Morimoto, T., Suzuki, Y., Shinonaga, C. & Ishida, Y. (2007). Interleukin-6 attenuates hyperthermia-induced seizures in developing rats. Brain & Development, 29, 644–8.

Gelfman, S., Wang, Q., Lu, Y. F., Hall, D, Bostick, C. D., Dhindsa, R., Halvorsen, M., McSweeney, K. M., Cotterill, E., Edinburgh, T, Beaumont, M. A, Frankel, W. N., Petrovski, S., Allen, A. S., Boland, M. J., Goldstein, D. B. & Eglen, S. J. (2018). meaRtools: An R package for the analysis of neuronal networks recorded on microelectrode arrays. PLoS Computational Biology, 14(10), e1006506.

Grainger, A. I., King, M. C., Nagel, D. A., Parri, H. R., Coleman, M. D. & Hill, E. J. (2018). In vitro Models for Seizure-Liability Testing Using Induced Pluripotent Stem Cells. Frontiers in Neuroscience, 12, 590.

Grienberger, C. & Konnerth, A. (2012). Imaging calcium in neurons. Neuron, 73(5), 862–85.

Gruol D. L. (2015). IL-6 regulation of synaptic function in the CNS. Neuropharmacology, 96(Pt A), 42–54.

Gruol, D. L., Puro, A., Hao, C., Blakely, P., Janneke, E. & Vo, K. (2011). Neuroadaptive changes in cerebellar neurons induced by chronic exposure to IL-6. Journal of Neuroimmunology, 239(1-2), 28–36.

Hagman, S., Mäkinen, A., Ylä-Outinen, L., Huhtala, H., Elovaara, I. & Narkilahti, S. (2019). Effects of inflammatory cytokines IFN-γ, TNF-α and IL-6 on the viability and functionality of human pluripotent stem cell-derived neural cells. Journal of Neuroimmunology, 331, 36–45.

Hakkoum, D., Stoppini, L. & Muller D. (2007). Interleukin-6 promotes sprouting and functional recovery in lesioned organotypic hippocampal slice cultures. Journal of Neurochemistry, 100(3), 747–57.

Hampel, H., Haslinger, A., Scheloske, M., Padberg, F., Fischer, P., Unger, J., Teipel, S., Neumann, M., Rosenberg, C., Oshida, R., Hulette, C., Pongratz, D., Ewers, M., Kretzschmar, H. & Möller, H. J. (2005). Pattern of interleukin-6 receptor complex immunoreactivity between cortical regions

of rapid autopsy normal and Alzheimer's disease brain. European archives of psychiatry and clinical neuroscience, 255, 269–78.

Hattori, Y., Naito, Y., Tsugawa, Y., Nonaka, S., Wake, H., Nagasawa, T., Kawaguchi, A. & Miyata, T. (2020). Transient microglial absence assists postmigratory cortical neurons in proper differentiation. Nature Communications, 11, 1631.

Heikkilä, T. J., Ylä-Outinen, L., Tanskanen, J. M., Lappalainen, R. S., Skottman, H., Suuronen, R., Mikkonen, J. E., Hyttinen, J. A. & Narkilahti, S. (2009). Human embryonic stem cell-derived neuronal cells form spontaneously active neuronal networks in vitro. Experimental Neurology, 218(1), 109–16.

Hodge, D. R., Hurt, E. M. & Farrar, W. L. (2005). The role of IL-6 and STAT3 in inflammation and cancer. European Journal of Cancer, 41(16), 2502–12.

Hong, Y. J. & Do, J. T. (2019). Neural Lineage Differentiation From Pluripotent Stem Cells to Mimic Human Brain Tissues. Frontiers in Bioengineering and Biotechnology, 7, 400.

Hongisto, H., Ilmarinen, T., Vattulainen, M., Mikhailova, A. & Skottman, H. (2017). Xeno- and feeder-free differentiation of human pluripotent stem cells to two distinct ocular epithelial cell types using simple modifications of one method. Stem Cell Research & Therapy, 8(1), 291.

Hyvärinen, T., Hagman, S., Ristola, M., Sukki, L., Veijula, K., Kreutzer, J., Kallio, P. & Narkilahti, S. (2019a). Co-stimulation with IL-1β and TNF-α induces an inflammatory reactive astrocyte phenotype with neurosupportive characteristics in a human pluripotent stem cell model system. Scientific Reports, 9(1), 16944.

Hyvärinen, T., Hyysalo, A., Kapucu, F. E., Aarnos, L., Vinogradov, A., Eglen, S. J., Ylä-Outinen, L. & Narkilahti, S. (2019b). Functional characterization of human pluripotent stem cell-derived cortical networks differentiated on laminin-521 substrate: comparison to rat cortical cultures. Scientific Reports, 9(1), 17125.

Hyysalo, A, Ristola, M., Mäkinen, M. E., Häyrynen, S., Nykter, M. & Narkilahti, S. (2017). Laminin α5 substrates promote survival, network formation and functional development of human pluripotent stem cell-derived neurons in vitro. Stem Cell Research, 24, 118–127.

Islam, O., Gong, X., Rose-John, S. & Heese, K. (2009). Interleukin-6 and neural stem cells: more than gliogenesis. Molecular Biology of the Cell, 20(1), 188–199.

Kalueff, A.V., Lehtimäki, K.A., Ylinen, A., Honkaniemi, J. & Peltola, J., (2004). Intranasal administration of human IL-6 increases the severity of chemically induced seizures in rats. Neuroscience Letters, 365, 106–110.

Kaur, S., Bansal, Y., Kumar, R. & Bansal, G. A panoramic review of IL-6: Structure, pathophysiological roles and inhibitors. (2020). Bioorganic & Medicinal Chemistry, 28(5), 115327.

Kiamehr, M., Klettner, A., Richert, E., Koskela, A., Koistinen, A., Skottman, H., Kaarniranta, K., Aalto-Setälä, K. & Juuti-Uusitalo, K. (2019). Compromised Barrier Function in Human Induced Pluripotent Stem-Cell-Derived Retinal Pigment Epithelial Cells from Type 2 Diabetic Patients. International Journal of Molecular Sciences, 20(15).

Lappalainen, R. S., Salomäki, M., Ylä-Outinen, L., Heikkilä, T. J., Hyttinen, J. A., Pihlajamäki, H., Suuronen, R., Skottman, H. & Narkilahti, S. (2010). Similarly derived and cultured hESC lines show variation in their developmental potential towards neuronal cells in long-term culture. Regenerative Medicine, 5(5), 749–62.

Lehtimäki, K. A., Liimatainen, S., Peltola, J. & Arvio M. (2011). The serum level of interleukin-6 in patients with intellectual disability and refractory epilepsy. Epilepsy Research, 95,184–187.

Lehtimäki, K. A., Peltola, J., Koskikallio, E., Keränen, T. & Honkaniemi, J. (2003). Expression of cytokines and cytokine receptors in the rat brain after kainic acid-induced seizures. Molecular Brain Research, 110(2), 253–60.

Leibinger, M., Andreadaki, A., Gobrecht, P., Levin, E., Diekmann, H. & Fischer, D. (2016). Boosting Central Nervous System Axon Regeneration by Circumventing Limitations of Natural Cytokine Signaling. Molecular Therapy, 24(10), 1712–1725.

Leibinger, M., Zeitler, C, Gobrecht, P., Andreadaki, A. & Fischer, D. (2019). Transneuronal delivery of designer-cytokine enables functional recovery after complete spinal cord injury. BioRxiv, Cold Spring Harbor, Nov 14.

Li, G., Bauer, S., Nowak, M., Norwood, B., Tackenberg, B., Rosenow, F., Knake, S., Oertel, W. H. & Hamer, H. M. (2011). Cytokines and epilepsy. Seizure, 20(3), 249–56.

Liimatainen, S., Fallah, M., Kharazmi, E., Peltola, M. & Peltola J. (2009). Interleukin-6 levels are increased in temporal lobe epilepsy but not in extra-temporal lobe epilepsy. Journal of Neurology. 256(5), 796–802.

Liu, T., Zhang, L., Joo, D. & Sun, S. C. (2017). NF-κB signaling in inflammation. Signal Transduction and Targeted Therapy, 2, e17023.

Liu, Y., Beyer, A. & Aebersold, R. (2016). On the Dependency of Cellular Protein Levels on mRNA Abundance. Cell, 21, 165(3), 535–50.

Liu, Z. 1., Qiu, Y. H., Li, B., Ma, S. H. & Peng, Y. P. (2011). Neuroprotection of interleukin-6 against NMDA-induced apoptosis and its signal-transduction mechanisms. Neurotoxicity Research, 19(3), 484–95.

Luo, Y. & Zheng, S. G. (2016). Hall of Fame among Pro-inflammatory Cytokines: Interleukin-6 Gene and Its Transcriptional Regulation Mechanisms. Frontiers in Immunology, 7, 604.

Ma, S. H., Zhuang, Q. X., Shen, W. X., Peng, Y. P. & Qiu, Y. H. (2015). Interleukin-6 reduces NMDAR-mediated cytosolic Ca^{2+} overload and neuronal death via JAK/CaN signaling. Cell Calcium, 58(3), 286–95.

Mayer, M., Arrizabalaga, O., Lieb, F., Ciba, M., Ritter, S. & Thielemann, C. (2018). Electrophysiological investigation of human embryonic stem cell derived neurospheres using a novel spike detection algorithm. Biosensors & Bioelectronics, 100, 462–468.

McCaughey-Chapman, A. & Connor, B. (2018). Human Cortical Neuron Generation Using Cell Reprogramming: A Review of Recent Advances. Stem Cells and Development, 27(24).

Nam, Y. & Wheeler, B. C. (2011). In vitro microelectrode array technology and neural recordings. Critical Reviews in Biomedical Engineering, 39(1), 4561.

Nelson, T. E., Netzeband, J. G. & Gruol, D. L. (2004). Chronic interleukin-6 exposure alters metabotropic glutamate receptor-activated calcium signalling in cerebellar Purkinje neurons. European Journal of Neuroscience, 20(9), 2387–400.

Nelson, T. E., Ur, C. L. & Gruol, D. L. (2002). Chronic interleukin-6 exposure alters electrophysiological properties and calcium signaling in developing cerebellar Purkinje neurons in culture. Journal of Neurophysiology, 88, 475–486.

Obien, M. E., Deligkaris, K., Bullmann, T., Bakkum, D. J. & Frey, U. (2015). Revealing neuronal function through microelectrode array recordings. Frontiers in Neuroscience, 8, 423.

Odawara, A., Katoh, H., Matsuda, N. & Suzuki, I. (2016). Physiological maturation and drug responses of human induced pluripotent stem cell-derived cortical neuronal networks in long-term culture. Scientific Reports, 6, 26181.

Orellana, D. I., Quintanilla, R. A., Gonzalez-Billault, C. & Maccioni RB. (2005). Role of the JAKs/STATs pathway in the intracellular calcium changes induced by interleukin-6 in hippocampal neurons. Neurotoxicity Research, 8(3,4), 295–304.

Paavilainen, T., Pelkonen, A., Mäkinen, M.E., Peltola, M., Huhtala, H., Fayuk, D. & Narkilahti, S. (2018). Effect of prolonged differentiation on functional maturation of human pluripotent stem cell-derived neuronal cultures. Stem Cell Research, 29(27), 151–161.

Pasquale, V., Martinoia, S. & Chiappalone, M. (2010). A self-adapting approach for the detection of bursts and network bursts in neuronal cultures. Journal of Computational Neuroscience, 29(1-2), 213–229.

Patel, D. C., Tewari, B. P., Chaunsali, L & Sontheimer, H. (2019). Neuron–glia interactions in the pathophysiology of epilepsy. Nature Reviews Neuroscience, 20, 282–297.

Peltola, J., Palmio, J., Korhonen, L., Suhonen, J., Miettinen, A., Hurme, M., Lindholm, D. & Keränen, T. (2000). Interleukin-6 and interleukin-1 receptor antagonist in cerebrospinal fluid from patients with recent tonic-clonic seizures. Epilepsy Research, 41(3), 205–11.

Penkowa, M., Molinero, A., Carrasco, J. & Hidalgo, J. (2001). Interleukin-6 deficiency reduces the brain inflammatory response and increases oxidative stress and neurodegeneration after kainic acid-induced seizures. Neuroscience, 102(4), 805–18.

Pieraut, S., Lucas, O., Sangari, S., Sar, C., Boudes, M., Bouffi, C., Noel, D. & Scamps F. (2011). An autocrine neuronal interleukin-6 loop mediates chloride accumulation and NKCC1 phosphorylation in axotomized sensory neurons. Journal of Neuroscience, 31(38), 13516–26.

Reubinoff, B. E., Itsykson, P., Turetsky, T., Pera, M. F., Reinhartz, E., Itzik, A. & Ben-Hur, T. (2001). Neural progenitors from human embryonic stem cells. Nature Biotechnology, 19, 1134–40.

Ropelle, E. R., Flores, M. B., Cintra, D. E., Rocha, G. Z., Pauli, J. R., Morari, J., de Souza, C. T., Moraes, J. C., Prada, P. O., Guadagnini, D., Marin, R. M., Oliveira, A. G., Augusto, T. M., Carvalho, H. F., Velloso, L. A., Saad, M. J. & Carvalheira, J. B. (2010). IL-6 and IL-10 anti-inflammatory activity links exercise to hypothalamic insulin and leptin sensitivity through IKKbeta and ER stress inhibition. PLoS Biology, 8(8), e1000465.

Rose-John, S. (2017). The Soluble Interleukin 6 Receptor: Advanced Therapeutic Options in Inflammation. Clinical Pharmacology & Therapeutics, 102(4), 591–598.

Rose-John, S. (2018). Interleukin-6 Family Cytokines. Cold Spring Harbor Perspectives in Biology, 10(2), a028415.

Rothaug M., Becker-Pauly C. & Rose-John S. (2016). The role of interleukin-6 signaling in nervous tissue. Biochimica et Biophysica Acta, 1863, 1218–27.

Ryynänen, T., Pelkonen, A., Grigoras, K., Ylivaara, O., Hyvärinen, T., Ahopelto, J., Prunnila, M., Narkilahti, S. & Lekkala, J. (2019). Microelectrode Array With Transparent ALD TiN Electrodes. Frontiers in Neuroscience, 13, 226.

Ryynänen, T., Toivanen, M., Salminen, T., Ylä-Outinen, L., Narkilahti, S. & Lekkala, J. (2018). Ion Beam Assisted E-Beam Deposited TiN Microelectrodes-Applied to Neuronal Cell Culture Medium Evaluation. Frontiers in Neuroscience, 12, 882.

Samland, H., Huitron-Resendiz, S., Masliah, E., Criado, J., Henriksen, S. J. & Campbell, I. L. (2003). Profound increase in sensitivity to glutamatergic- but not cholinergic agonist-induced seizures in transgenic mice with astrocyte production of IL-6. Journal of Neuroscience Research, 73(2), 17687.

Sandoe, J. & Eggan, K. (2013). Opportunities and challenges of pluripotent stem cell neurodegenerative disease models. Nature Neuroscience, 16(7), 780–9.

Scheffer, I. E, Berkovic, S., Capovilla, G., Connolly, M. B., French, J., Guilhoto, L., Hirsch, E., Jain, S., Mathern, G. W., Moshé, S. L., Nordli, D. R., Perucca, E., Tomson, T., Wiebe, S., Zhang,

Y. H. & Zuberi, S. M. (2017). ILAE classification of the epilepsies: Position paper of the ILAE Commission for Classification and Terminology. Epilepsia, 58(4), 512–521.

Scheller, J., Chalaris, A., Schmidt-Arras, D. & Rose-John, S. (2011). The pro- and anti-inflammatory properties of the cytokine interleukin-6. Biochimica Biophysica Acta,1813(5), 878–88.

Scheller, J. & Rose-John, S. (2006). Interleukin-6 and its receptor: from bench to bedside. Medical Microbiology and Immunology, 195, 173–183.

Shi, Y., Inoue, H., Wu, J. C. & Yamanaka, S. (2017). Induced pluripotent stem cell technology: a decade of progress. Nature Review Drug Discovery, 16(2), 115–130.

Shi, Y., Kirwan, P., Smith, J., Robinson, H. P. & Livesey, F. J. (2012). Human cerebral cortex development from pluripotent stem cells to functional excitatory synapses. Nature Neuroscience, 15(3), 477–86.

Skottman, H. (2010). Derivation and characterization of three new human embryonic stem cell lines in Finland. In Vitro Cellular & Developmental Biology - Animal, 46(3), 206–209.

Sulistio, Y. A., Lee, H. K., Jung, S. J. & Heese, K. (2018). Interleukin-6-Mediated Induced Pluripotent Stem Cell (iPSC)-Derived Neural Differentiation. Molecular Neurobiology, 55(4), 3513–3522.

Sun, T. & Hevner, R. F. (2014). Growth and folding of the mammalian cerebral cortex: from molecules to malformations. Nature Reviews Neuroscience, 15(4), 217–232.

Takahashi, K., Tanabe, K., Ohnuki, M., Narita, M., Ichisaka, T., Tomoda, K. & Yamanaka, S. (2007). Induction of pluripotent stem cells from adult human fibroblasts by defined factors. Cell 131, 861–872.

Takahashi, K. & Yamanaka, S. (2006). Induction of pluripotent stem cells from mouse embryonic and adult fibroblast cultures by defined factors. Cell, 126, 663–676.

Takahashi, K. & Yamanaka, S. (2016). A decade of transcription factor-mediated reprogramming to pluripotency. Nature Reviews Molecular Cell Biology, 17(3), 183-93.

Thomas C. A., Springer P. A., Loeb G. E., Berwald-Netter Y. & Okum L. M. (1972). A miniature microelectrode array to monitor the bioelectric activity of cultured cells. Experimental Cell Research, 74, 61–66.

Thomson, J. A., Itskovitz-Eldor, J., Shapiro, S. S., Waknitz, M. A., Swiergiel, J. J., Marshall, V. S. & Jones, J. M. (1998). Embryonic stem cell lines derived from human blastocysts. Science, 282, 1145–7.

Toivonen, S., Ojala, M., Hyysalo, A., Ilmarinen, T., Rajala, K., Pekkanen-Mattila, M., Äänismaa, R., Lundin, K., Palgi, J., Weltner, J., Trokovic, R., Silvennoinen, O., Skottman, H., Narkilahti, S.,

Aalto-Setälä, K. & Otonkoski, T. (2013). Comparative analysis of targeted differentiation of human induced pluripotent stem cells (hiPSCs) and human embryonic stem cells reveals variability associated with incomplete transgene silencing in retrovirally derived hiPSC lines. Stem Cells Translational Medicine, 2(2), 83–93.

Tukker, A., van Kleef, R., Wijnolts, F., de Groot, A., & Westerink, R. (2020). Towards animal-free neurotoxicity screening: Applicability of hiPSC-derived neuronal models for in vitro seizure liability assessment. ALTEX - Alternatives to Animal Experimentation, 37(1), 121-135.

Vereyken, E. J., Bajova, H., Chow, S., de Graan, P. N. & Gruol, D. L. (2007). Chronic interleukin-6 alters the level of synaptic proteins in hippocampus in culture and in vivo. European Journal of Neuroscience, 25(12), 3605–16.

Vezzani, A., Balosso, S. & Ravizza, T. The role of cytokines in the pathophysiology of epilepsy. (2008). Brain, Behavior, and Immunity, 22(6), 797–803.

Vezzani, A., Balosso, S. & Ravizza, T. (2019). Neuroinflammatory pathways as treatment targets and biomarkers in epilepsy. Nature Reviews Neurology, 15, 459–472.

Vezzani, A., French, J., Bartfai, T. & Baram, T. Z. (2011). The role of inflammation in epilepsy. Nature Reviews Neurology, 7, 31–40.

Vezzani, A., Lang, B. & Aronica, E. (2016). Immunity and inflammation in Epilepsy. Cold Spring Harbor Perspectives in Medicine, 6, a022699.

Vogel, C. & Marcotte, E. M. (2012). Insights into the regulation of protein abundance from proteomic and transcriptomic analyses. Nature Reviews Genetics, 13(4), 227–232.

Vollenweider, F., Herrmann, M., Otten, U. & Nitsch, C. (2003). Interleukin-6 receptor expression and localization after transient global ischemia in gerbil hippocampus. Neuroscience Letter, 341, 49–52.

Wei, H., Chadman, K. K., McCloskey, D. P., Sheikh, A. M., Malik, M., Brown, W. T. & Li, X. (2012). Brain IL-6 elevation causes neuronal circuitry imbalances and mediates autism-like behaviors. Biochimica et Biophysica Acta, 1822(6), 831-42.

Xia, W., Peng, G. Y., Sheng, J. T., Zhu, F. F., Guo, J. F. & Chen, W. Q. (2015). Neuroprotective effect of interleukin-6 regulation of voltage-gated Na^+ channels of cortical neurons is time- and dose-dependent. Neural regeneration research, 10(4), 610–617.

Xu, X. H. & Zhong, Z. (2013). Disease modeling and drug screening for neurological diseases using human induced pluripotent stem cells. Acta Pharmacologica Sinica, 34(6), 755–764.

Ylä-Outinen, L., Heikkilä, J., Skottman, H., Suuronen, R., Äänismaa, R. & Narkilahti, S. (2010). Human cell-based micro electrode array platform for studying neurotoxicity. Frontiers in Neuroengineering, 3, 111.

Ylä-Outinen, L., Tanskanen, J. M. A., Kapucu, F. E., Hyysalo, A., Hyttinen, J. A. K. & Narkilahti, S. (2019). Advances in Human Stem Cell-Derived Neuronal Cell Culturing and Analysis. Advanced in Neurobiology, 22, 299-329.

Yu, J., Vodyanik, M. A., Smuga-Otto, K., Antosiewicz-Bourget, J., Frane, J. L., Tian, S., Nie, J., Jonsdottir, G. A., Ruotti, V., Stewart, R., Slukvin, I. I. & Thomson, J. A. (2007). Induced pluripotent stem cell lines derived from human somatic cells. Science, 318, 1917–1920.

Zhang, S. C., Wernig, M., Duncan, I. D., Brüstle, O. & Thomson, J. A. (2001). In vitro differentiation of transplantable neural precursors from human embryonic stem cells. Nature Biotechnology, 19, 1129–1133.

Zheng, X. Y., Zhang, H. L., Luo, Q. & Zhu, J. (2011). Kainic acid-induced neurodegenerative model: potentials and limitations. Journal of Biomedicine and Biotechnology, 2011, 457079.

Zuiki, M., Chiyonobu, T., Yoshida, M., Maeda, H., Yamashita, S., Kidowaki, S., Hasegawa, T., Gotoh, H., Nomura, T., Ono, K., Hosoi, H. & Morimoto, M. (2017). Luteolin attenuates interleukin-6-mediated astrogliosis in human iPSC-derived neural aggregates: A candidate preventive substance for maternal immune activation-induced abnormalities. Neuroscience Letters, 653, 296–301.

Appendices

Antibody optimization and validation

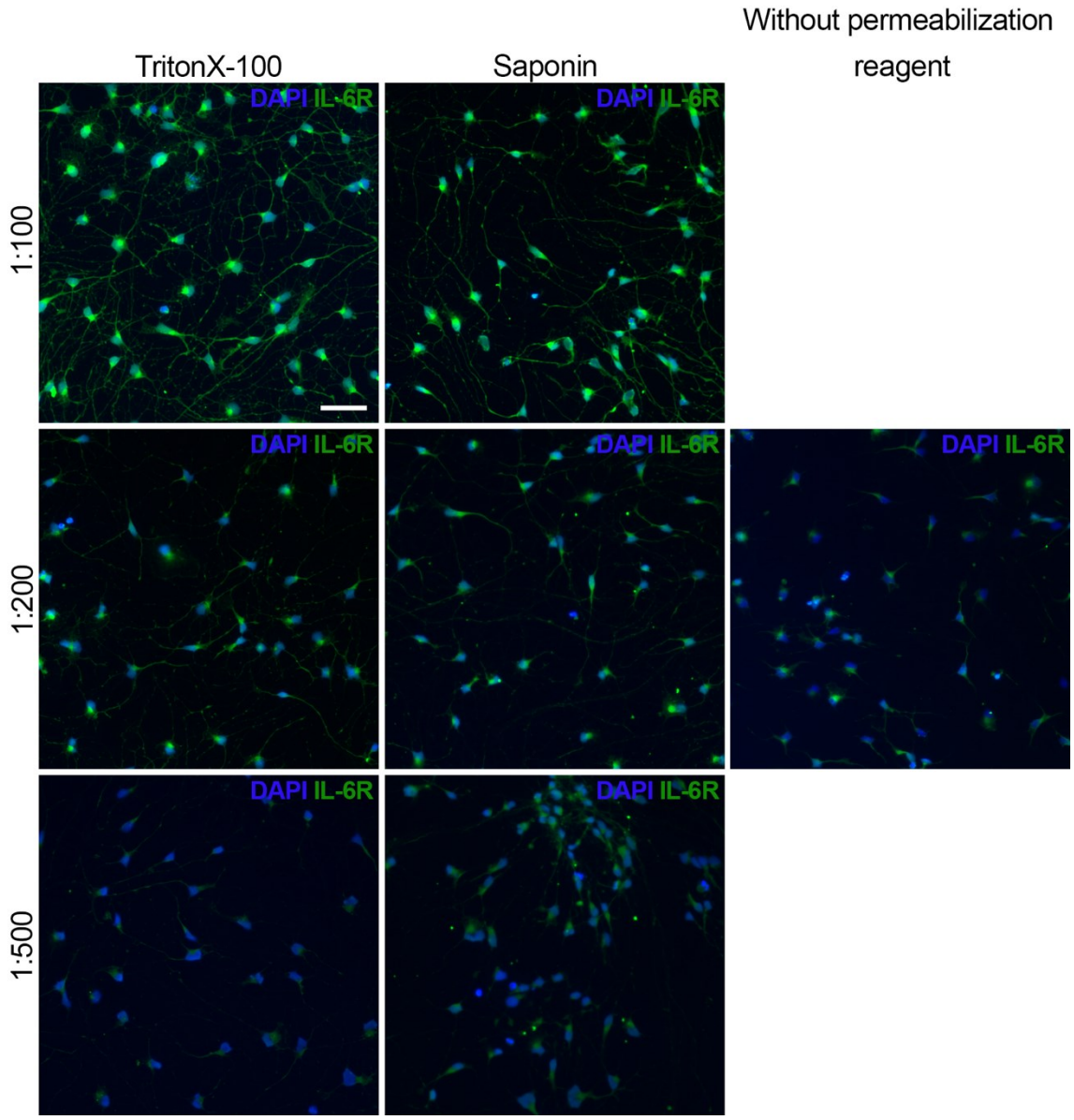

Appendix 1. ICC optimization of anti-IL-6R (Abcam). hESC-derived cortical neurons were stained with anti-IL-6R antibody (1:100, 1:200 and 1:500) after one week culture using TritonX-100 or saponin as a permeabilization reagent. Staining without both permeabilization reagents was also tested. Based on these results, 1:200 dilution with TritonX-100 was chosen for the following stainings. DAPI stained nuclei blue. The scale bar is 50 μm in all images.

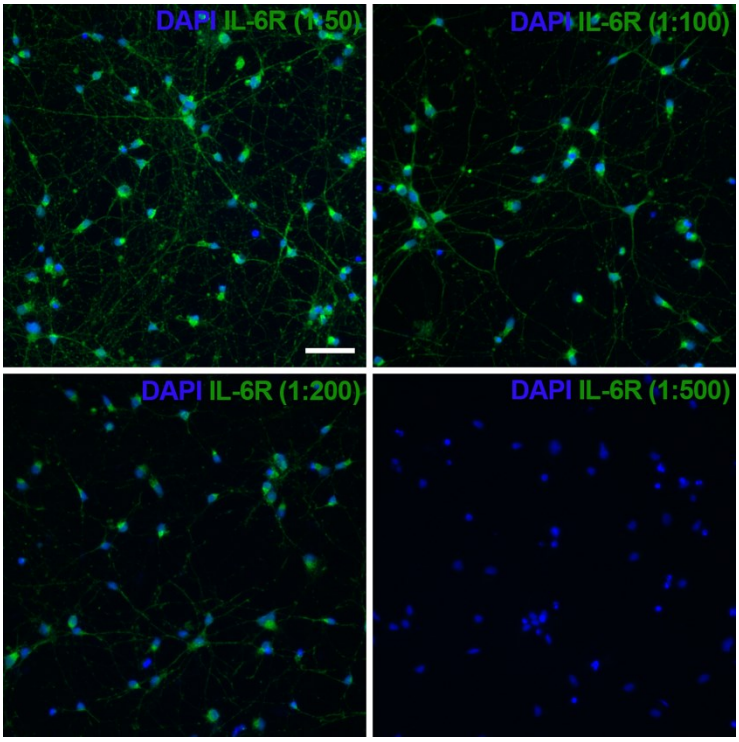

Appendix 2. ICC optimization of anti-IL-6R (R&D Systems). hiPSC-derived cortical neurons were stained with anti-IL-6R antibody (1:50, 1:100, 1:200 and 1:500) after two-week culture with normal ICC protocol (TritonX-100 as a permeabilization reagent). 1:200 dilution was considered as optimal for the following stainings. DAPI stained nuclei blue. The scale bar is 50 μm in all images.

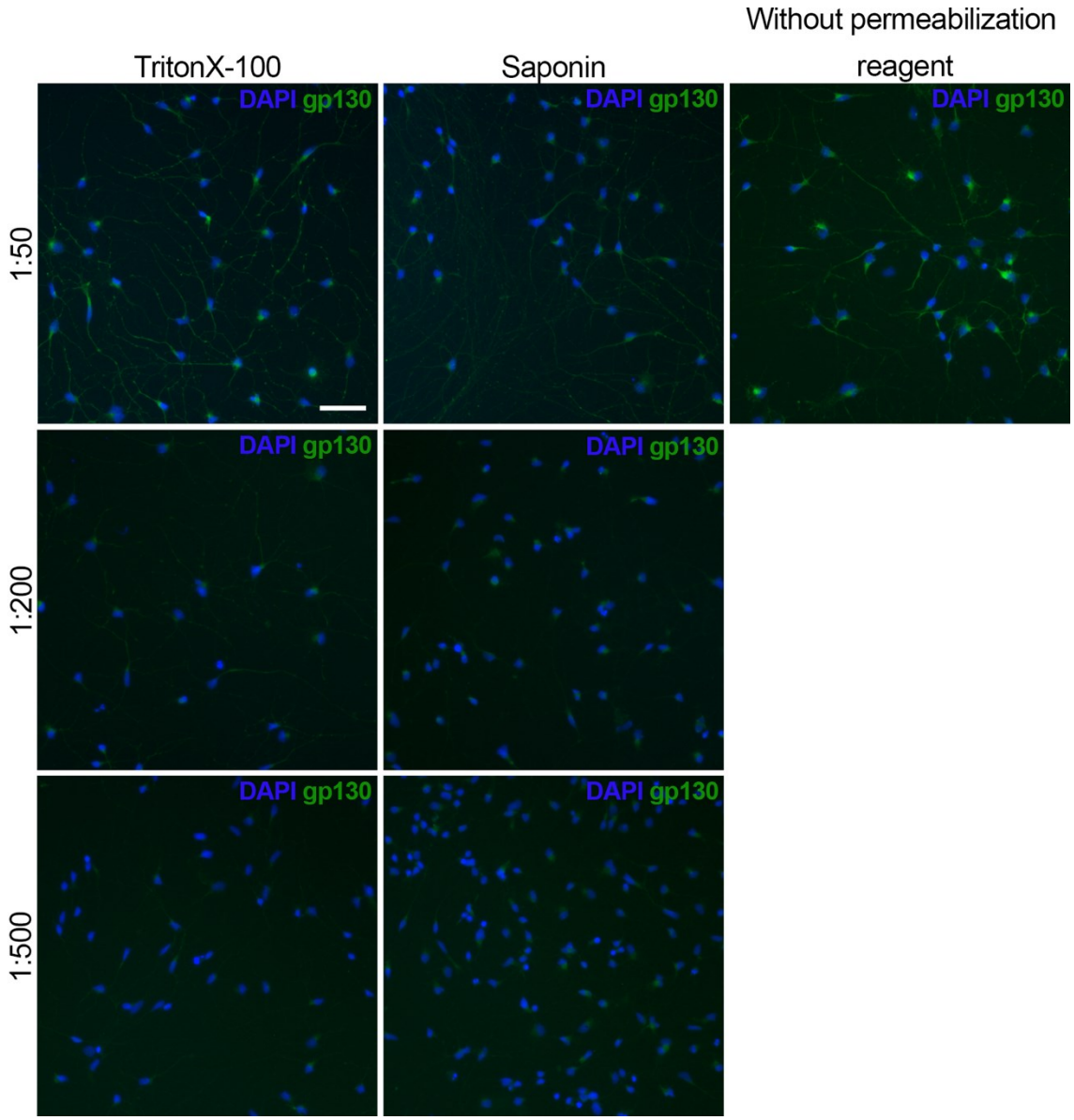

Appendix 3. ICC optimization of anti-gp130 (Santa Cruz). hESC-derived cortical neurons were stained with anti-gp130 antibody (1:50, 1:200 and 1:500) after one week culture using TritonX-100 or saponin as a permeabilization reagent. Staining without both permeabilization reagents was also tested. The most optimal staining was achieved with 1:50 dilution and TritonX-100. DAPI stained nuclei blue. The scale bar is 50 μm in all images.

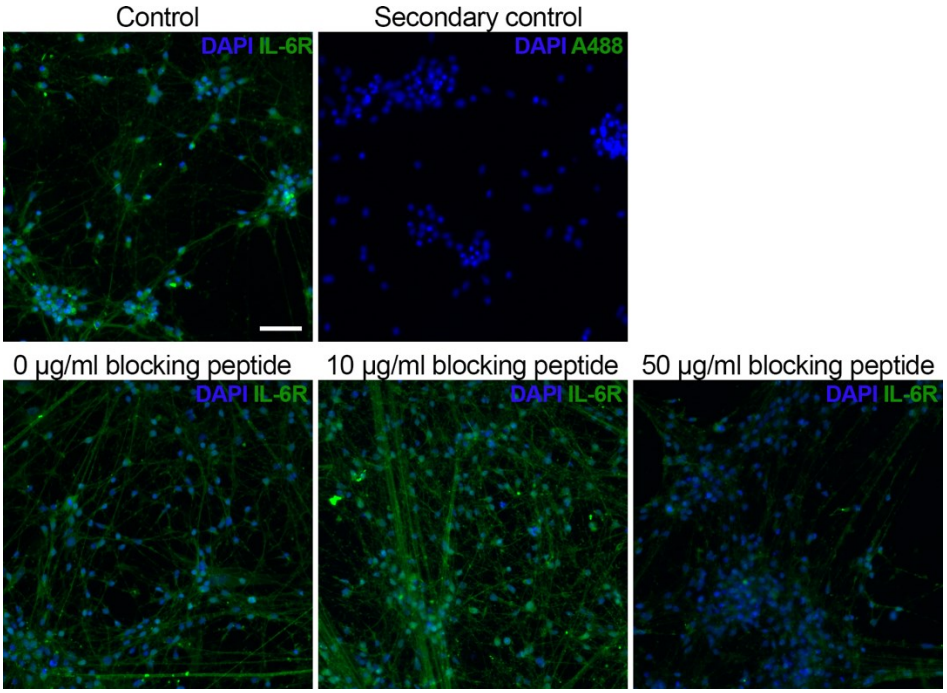

Appendix 4. Peptide blocking test for anti-IL-6R antibody (Abcam). hESC-derived neurons were stained with IL-6R (1:200) and different concentrations of IL-6R blocking peptide after five-week culture. Secondary control shows that secondary antibody is not detected without primary antibody. DAPI stained nuclei blue. The scale bar is 50 µm in all images.

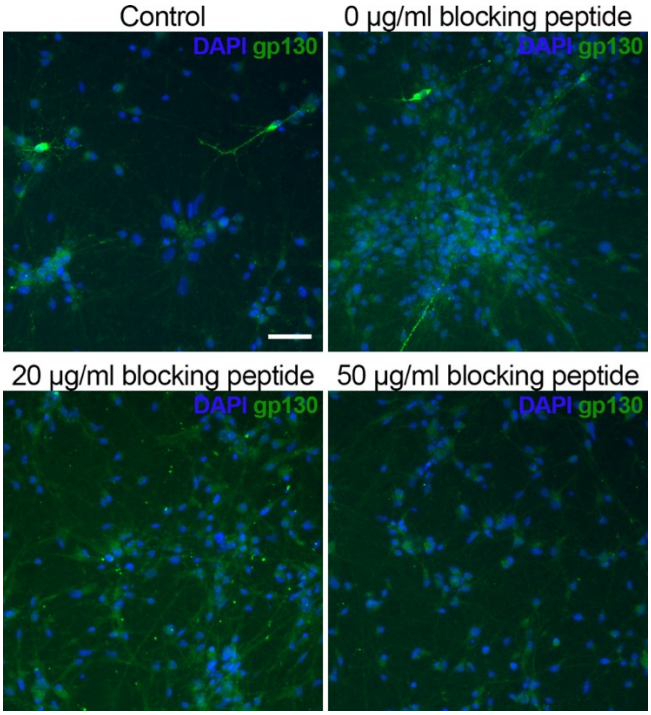

Appendix 5. Peptide blocking test for anti-gp130 antibody (Santa Cruz). hiPSC-derived neurons were stained with gp130 (1:50) and different concentrations of gp130 blocking peptide after five-week culture. DAPI stained nuclei blue. The scale bar is 50 µm in all images.